Monitoring RNA restructuring and translation in real time using a human cell-free extract system

By

MATTIE O'SULLIVAN

DISSERTATION

Submitted in partial satisfaction of the requirements for the degree of

DOCTOR OF PHILOSOPHY

in

Biochemistry, Molecular, Cellular and Developmental Biology

in the

OFFICE OF GRADUATE STUDIES

of the

UNIVERSITY OF CALIFORNIA

DAVIS

Approved:

Christopher Fraser, Chair

Ted Powers

Bruce Draper

Committee in Charge

2021

ABSTRACT

Here I adapted a fluorescent-based helicase assay to monitor RNA restructuring in a high-fidelity translation system using HeLa cell free extracts. In Chapter 1, I describe the method of how to successfully make large quantities of robust translation competent cell-free extracts from HeLa S3 cells, a mammalian suspension cell line. These extracts form the foundation for the remaining work outlined in this dissertation. In Chapter 2 I address how I redesigned the method to demonstrate the physiological implications of these RNA restructuring events. I discuss both engineering of the dual-assay mRNA reporter, and optimization of assay conditions for recapitulating faithful translational regulation and RNA restructuring in the cell free extracts. Moreover, I explore the contribution of the eIF4F complex to the unwinding activity, greatly extending previous work from our lab using a purified reconstituted system. Chapter 3 outlines the method by which I generated factor-dependent stable cell lines, using Invitrogen's Flp-in™ T-REx™ system, and adapt these cell lines to liquid suspension culture to produce large scale factor-dependent extracts. I applied this tool to modulate the amount of eIF4F complex components and associated factors to aim to understand the residual unwinding activity observed in my RNA restructuring assay.

The work outlined in this dissertation underscores the feasibility of monitoring *in vitro* real-time RNA restructuring dynamics. Additionally, I believe my system could serve to screen potential therapeutic agents to identify inhibitors of RNA restructuring.

ACKNOWLEDGMENTS

First and foremost, I am extremely grateful to my supervisor, Chris Fraser, whose mentorship was invaluable to me. Your compassionate guidance helped me through the most difficult times in graduate school. I feel so fortunate to have had the opportunity to work with you.

My sincere thanks must also go to the members of the Fraser lab. Particularly, Nancy Villa, Kateryna Feoktistova, Brian Avanzino, and Masaaki Sokabe. I appreciate the kindness and patience you offered to my countless random questions more than I can express. You all have inspired me to be more conscientious in everything I do.

To my committee members, Ted Powers and Bruce Draper, thank you for generously giving me your time to offer me valuable comments toward improving my work. Your approachable and kindhearted nature made it a pleasure to work with both of you. I would also like to distinguish Lionel Sanz and Frédéric Chédin for their many helpful conversations throughout my time in Davis.

To my past mentors, David Brow, Scott Langevin, Rondi Butler, Karl Kelsey, Thomas Cotter, Tommie McCarthy, David Sheehan, Justin McCarthy, Kellie Dean, and Sinéad Kerins, you were instrumental in my successful admission to graduate school. I wouldn’t have been able to do this without your help.

To my wonderful friends, Alison Deshong, Anastasia Berg, Shannon Owens, Prema Karunanithi, Rebecka Sepela, Hannah Petrek, Lauren Mitchell, and again, Lionel Sanz, I cannot thank you enough for your friendship and providing much needed distractions throughout the years. You all deserve extraordinary appreciation for always

being there when I needed you; through the hard times, celebratory times, just to eat lunch, or watch pointless reality television.

To Royce, thank you for teaching me to find humor in every situation; you have provided so much love and joy to my life. To Arlie, thank you for being best boy in the whole world. To Zuko, your mischievous tendencies become more endearing every day, eating the Christmas lights in particular.

Finally, I would not have achieved any of this without my family. It is hard to put into words how thankful I am for you. Mom, Dad, Eileen, and Liam, you have all been my role models throughout my life; without your endless support none of this would have been possible. I'd like to give special recognition to my grandparents for raising such selfless and caring parents. This thesis is as much an attribute to all of them and their excellence.

TABLE OF CONTENTS

INTRODUCTION

RNA helicases drive the remodeling of ribonucleoprotein complexes (RNPs) at all stages of gene expression. The precise spatial and temporal regulation of their activity is fundamental for various downstream cellular events. Importantly, dysregulation can lead to defects in these events, resulting in disease. Despite the indisputable importance of RNA helicases, our understanding of the molecular details of their function and regulation remains vague, this is partially due to the limitations of current techniques. RNA structure can be analyzed by employing ribonucleases that specifically target single- or double-stranded regions of RNAs, and chemical reagents that covalently modify the RNA base [1-5]. However, the need for tools to gain mechanistic insight into the regulation of RNA structures in real time is apparent.

The fluorescent-based RNA helicase assay is a unique tool that was pioneered by my lab to monitor the RNA-dependent DEAD-box helicase, eIF4A, an essential factor in translation initiation for unwinding RNA secondary structures in the 5' UTR of mRNAs [6-8]. However, this was characterized using a reconstituted system that used purified proteins and short mRNA templates. A concern of this approach is that one can miss a lot of regulation in the cell, or redundancy between components, by just studying a portion of the factors involved. Thus, precise kinetic analysis of helicase activity will require using an active translation system that will not only recapitulate the true physiological implications of the events but will be in compliance with examining immediate kinetic changes in the pathway. Accordingly, my goal was to adapt the fluorescent molecular

beacon assay to monitor RNA duplex separation in true cellular conditions using HeLa cell free extracts [9, 10]. The fluorescent-based helicase assay in combination with cell-free extract offers a unique method of characterizing the role of specific RNA structures in a true cellular environment. Importantly, by incorporating a bioluminescent luciferase gene to the mRNA reporter, one can visualize the changes in overall protein abundance, in parallel. In Chapter 1, I describe a method to successfully make large quantities of robust translation competent cell-free extracts from HeLa S3 cells, a mammalian suspension cell line. These extracts form the foundation for the remaining work outlined in this dissertation.

Chapter 2 addresses how I redesigned the fluorescent helicase assay to demonstrate the physiological implications of these RNA restructuring events. I discuss both engineering of the dual-assay mRNA reporter, and optimization of assay conditions for recapitulating faithful translational regulation and RNA restructuring in the cell free extracts. To characterize RNA restructuring activity in cell-free extracts, I ultimately focused on using a relatively straight-forward and physiologically relevant full-length mRNA reporter (Figure 2.20). I first verified that the restructuring activity is an ATP-driven process. Next, I targeted the eIF4F complex using inhibitors to extend previous work from our reconstituted system [6, 7]. Here I found the restructuring activity to be sensitive to inhibitors of the complex. Moreover, we could successfully dissect mechanistic differences in the function of the m7GTP cap and poly (A) tail in our assay. Unexpectedly, I observed an apparent baseline helicase activity that is insensitive to eIF4F dependent inhibitors, indicating robust eIF4F independent helicase activity. Since it has been

documented that predicted RNA structure is a lot less prevalent *in vivo* [5], one hypothesis is that the residual unwinding could be due to other helicases that may or may not be associated with the eIF4F complex. Additionally, I unexpectedly discover overall disparity between the observed change in unwinding rate compared to the observed change in translation; whereby inhibitors appear to impact the translation of mRNA dramatically over time with only a modest change in helicase activity. The future challenge will be to try to understand these events we observe in our assays.

Chapter 3 outlines the method by which I generated factor-dependent stable cell lines, using Invitrogen's Flp-in™ T-REx™ system, as previously shown [11]. I successfully modified this approach by using an RNAi system involving optimized targeting [12], and a fluorescent read-out of RNAi expression [13] to easily track transcription of our gene. Furthermore, I was able to adapt these cell lines to liquid suspension culture to produce large scale factor-dependent extracts. Here, I applied this tool to stably deplete factors hypothesized to be involved in our RNA restructuring assay. The goal was to verify the importance of identified factors by adding back purified recombinant proteins in wild-type, or mutant forms to more precisely understand their role. I first targeted the eIF4F complex and associated factors to aim to understand the residual unwinding activity observed in our restructuring assay. I characterized eIF4B and eIF4G depletion lines that displayed ~70-80% reduction in protein. However, unexpectedly these extracts did not demonstrate an increased dependence on the factor in my translation assays. It is possible that with optimized translation conditions, these experiments could reveal increased dependency as expected. In the future, another possibility for factor-depletion of factors thought to be

involved in RNA restructuring is to adapt the auxin-inducible degron system [14] for rapid and controlled protein depletion.

Going forward it would be interesting to expand the use of the molecular beacon reporter to reconstitute different regulatory events stemming from RNA restructuring by using a relevant RNA substrate (i.e. non-coding RNAs or pre-mRNAs etc). Of particular interest is determining how all mRNAs in the cell compete with one another for translational machinery through their efficiency in recruitment to the cap-binding complex, eIF4F, and the 40S subunit. The regulatory elements within the 5' and 3' UTR play critical roles in driving differential rates of protein synthesis [15, 16] but no direct evidence has been obtained to demonstrate the mechanism of these processes. This system lends itself to characterizing the regulation that is harbored in the untranslated regions of mRNAs.

Overall, the information generated from this assay will not only help to describe how helicases remodel nucleic acid secondary structure, but also examine the effects of accessory factors or drugs to evaluate regulatory interactions and perform drug candidate screening. Taken together my work should serve as an important tool to help answer these fundamental questions in the future.

References

[1] Ehresmann C, Baudin F, Mougel M, Romby P, Ebel JP, Ehresmann B. Probing the structure of RNAs in solution. Nucleic Acids Res. 1987;15:9109-28.
[2] Leamy KA, Assmann SM, Mathews DH, Bevilacqua PC. Bridging the gap between in vitro and in vivo RNA folding. Q Rev Biophys. 2016;49:e10.
[3] Leamy KA, Yennawar NH, Bevilacqua PC. Cooperative RNA Folding under Cellular Conditions Arises From Both Tertiary Structure Stabilization and Secondary Structure Destabilization. Biochemistry. 2017;56:3422-33.
[4] Zaug AJ, Cech TR. Analysis of the structure of Tetrahymena nuclear RNAs in vivo: telomerase RNA, the self-splicing rRNA intron, and U2 snRNA. Rna. 1995;1:363-74.
[5] Rouskin S, Zubradt M, Washietl S, Kellis M, Weissman JS. Genome-wide probing of RNA structure reveals active unfolding of mRNA structures in vivo. Nature. 2014;505:701-5.
[6] Özeş AR, Feoktistova K, Avanzino BC, Fraser CS. Duplex unwinding and ATPase activities of the DEAD-box helicase eIF4A are coupled by eIF4G and eIF4B. J Mol Biol. 2011;412:674-87.
[7] Feoktistova K, Tuvshintogs E, Do A, Fraser CS. Human eIF4E promotes mRNA restructuring by stimulating eIF4A helicase activity. Proceedings of the National Academy of Sciences. 2013;110:13339-44.
[8] Avanzino BC, Fuchs G, Fraser CS. Cellular cap-binding protein, eIF4E, promotes picornavirus genome restructuring and translation. Proceedings of the National Academy of Sciences. 2017;114:9611-6.
[9] Bergamini G, Preiss T, Hentze MW. Picornavirus IRESes and the poly(A) tail jointly promote cap-independent translation in a mammalian cell-free system. Rna. 2000;6:1781-90.
[10] Thoma C, Ostareck-Lederer A, Hentze MW. A poly(A) tail-responsive in vitro system for cap- or IRES-driven translation from HeLa cells. Methods Mol Biol. 2004;257:171-80.
[11] Rakotondrafara AM, Hentze MW. An efficient factor-depleted mammalian in vitro translation system. Nat Protoc. 2011;6:563-71.
[12] Fang W, Bartel DP. The Menu of Features that Define Primary MicroRNAs and Enable De Novo Design of MicroRNA Genes. Mol Cell. 2015;60:131-45.
[13] Santagata S, Mendillo ML, Tang YC, Subramanian A, Perley CC, Roche SP, et al. Tight coordination of protein translation and HSF1 activation supports the anabolic malignant state. Science. 2013;341:1238303.
[14] Li S, Prasanna X, Salo VT, Vattulainen I, Ikonen E. An efficient auxin-inducible degron system with low basal degradation in human cells. Nature Methods. 2019;16:866-9.
[15] Lasko P. mRNA localization and translational control in Drosophila oogenesis. Cold Spring Harb Perspect Biol. 2012;4:a012294.
[16] Gebauer F, Preiss T, Hentze MW. From cis-regulatory elements to complex RNPs and back. Cold Spring Harb Perspect Biol. 2012;4:a012245.

CHAPTER 1

Development of translation competent mammalian cell-free extracts to monitor RNA duplex unwinding activities

This chapter contains unpublished work and was written by me with editing by Dr. Christopher Fraser. All of the experiments were performed by me.

Abstract

Real time analysis using purified reconstituted systems provide useful insight to the kinetic activities of specific proteins. However, one concern is that important regulation apparent in cells can be missed by only studying a portion of the factors involved. Obtaining precise kinetic analysis of RNA restructuring will therefore require the use of a high fidelity translation system that will not only recapitulate the true physiological implications of the events but will be in compliance with examining immediate kinetic changes in the pathway. Here, I describe the method of how to successfully make large quantities of robust translation-competent cell-free extracts from HeLa S3 cells, a mammalian suspension cell line. Importantly, this system displays high fidelity of translation with regard to synergistic activation of translation by the m7G cap and poly(A) tail. These extracts form the foundation for the remaining work outlined in this dissertation.

Introduction

In vitro translation systems have been widely used to enable cell-free protein synthesis and to investigate the mechanisms of translation. In contrast to *in vivo* systems that typically require hours or days to see effects, cell-free extracts: a) provide the core cellular machinery, b) enable investigation of the earliest steps in real time, c) study translation independently of transcription, and d) allow direct manipulation of protein and RNA levels to help further elucidate molecular underpinnings of regulatory events. Initial *in vitro* studies of translation were performed in extracts derived from rabbit reticulocytes and wheat germ [1, 2]. However, the contribution of the poly(A) tail to cap-dependent translation could not be easily recapitulated in these extracts. The first *in vitro* translation system that could recapitulate the synergism between the cap structure and the poly(A) tail was derived from Saccharomyces cerevisiae [3]. To date, several *in vitro* translation systems that recapitulate this synergy have been reported, including extracts derived from Drosophila melanogaster embryos [4], HeLa cells [5, 6], rabbit reticulocytes [7], and Krebs II ascites cells [8]. Here, I describe an adapted cell-free translation system based on HeLa cell extracts [5, 6], which displays a strong poly(A) tail contribution to the cap-dependent translation. Potential barriers of using cell-free extracts are that some kinetic assays cannot be adapted for use in such a complex environment, and that it is often difficult to generate enough extract to perform robust analysis from tissue culture plates. HeLa S3 cells are a clonal derivative of the parent HeLa line which have been adapted to grow in suspension (spinner) culture. This mammalian suspension cell line offers a viable solution to overcoming the bottleneck in the field. These cells can be grown in multiple two-liter flasks to generate large quantities of lysate, enabling truly robust biochemical analysis of

the pathway. In this chapter I discuss the process of generating the translation competent cell-free extracts. A schematic overview of the method is outlined in Figure 1.1.

Preparation and Maintenance of HeLa (S3) Suspension Cells for Lysate Generation

Planning and Preparation

- *Ensure all the following materials needed for the duration of the lysate preparation are available*

Cell Culture Media

- Corning® Dulbecco's Modification of Eagle's Medium (DMEM) supplemented with 5% Newborn Calf Serum (NCS) and Penicillin-Streptomycin solution (PS)
- One lysate prep from 2-liters of cells corresponds to ~3-mL of lysate per prep. I will usually make 6-8 preps of lysate during the duration of the cells growth ~16-liters of media.
- I usually prepare the media as is needed
- Only use HyClone™ Newborn Calf Serum (Cytiva: SH30118.03) for the cell media

CO_2 Incubator

- Ensure there are enough available stir plates inside the incubator for growing cells. Two stir plates should be sufficient for what I will outline going forward.
- Incubator should be kept at 37°C with 5% CO_2. Stocking up on two or three CO_2 tanks should ensure the incubator doesn't run out of CO_2 during the duration of the prep (assuming ~3 week use of incubator).
- Always maintain a sterile tray of water inside the incubator for humidity.

Spinner Flasks

- Prepare each flask in advance with back-up flasks of each in case of contamination i.e., two 100-mL, two 250-mL, two 1-liter, four 3-liter
- Ensure all reusable spinner flasks have been cleaned thoroughly prior to use
- Cleaning Protocol:
    a. Fill with 10% glacial acetic acid and soak overnight at RT
    b. Disassemble the magnetic spinner and scrub all parts of the flask to get rid of cellular debris. Use a volumetric flask brush set aside specifically for cleaning these flasks.
    c. Five full rinses with deionized water
    d. Five full rinses with milli-Q water
    e. Autoclave for ~30 min on a liquid cycle partially filled with water
    f. Autoclave for ~30 min on a dry cycle
    g. Cover top of flask with aluminum foil and keep in a closed environment to prevent dust entering the flask

List of Materials Needed

Special Reagents and Equipment

- Corning® Dulbecco's Modification of Eagle's Medium (Product Number: 10-013-CV)
- HyClone™ Newborn Calf Serum (Cytiva: SH30118.03)
- Corning® Penicillin-Streptomycin solution (Product Number: 30-002-CI)

- Gibco™ Fetal Bovine Serum (Catalog number: 10437028)
- Hybri-Max™, sterile-filtered Dimethyl sulfoxide (Sigma Aldrich, D2650)
- HyClone™ Trypan Blue Solution (Cytiva SV30084.01)
- Corning® PBS (Phosphate Buffered Saline)
- cOmplete™, Mini, EDTA-free Protease Inhibitor Cocktail
- 6mm shearing probe: Omni 2000
- Bellco Glass reusable glass spinner flasks; two 100-mL, two 250-mL, two 1-liter, four 3-liter
- CO_2 incubator capable of storing at least two stir plates and at least two 3-liter spinner flasks
- An extra stir-plate specifically for counting cells kept near the sterile laminar flow cabinet
- Hemocytometer or a cell counter

Materials for nuclease treatment

- Thermo Scientific™Micrococcal Nuclease Solution 150U/µL
- 0.2M ethylene glycol tetraacetic acid (EGTA) at pH 8.0
- 100mM calcium chloride ($CaCl_2$)
- Micrococcal nuclease buffer:
    1. 20mM Tris-HCl at pH 7.6
    2. 50mM sodium chloride (NaCl)
    3. 50% glycerol

Sterile Laminar Flow Cabinet

- Serological pipettes: 5-mL, 10-mL, 25-mL
- Pipettes: 1-mL, 200-µL, 20-µL, 2-µL
- Pipette gun
- Filter pipette tips: 1-mL, 200-µL, 20-µL, 2-µL
- 1.5-mL and 5-mL microfuge tubes

Outside of Sterile Laminar Flow Cabinet

- Serological pipettes: 5-mL, 10-mL, 25-mL
- Pipettes: 1-mL, 200-µL, 20-µL, 2-µL
- Pipette gun
- Filter pipette tips: 1-mL, 200-µL, 20-µL, 2-µL
- 1.5-mL microfuge tubes

Important Notes Before Beginning

- To reduce contamination, aim to use one side of the flask for aerating and one side for pouring media in and out. I usually will use side to the right of the volume marks for pouring as it allows me to monitor the volume.
- It is best to start expanding the cells as quickly as possible as the larger flasks seem to provide a better environment for their overall health and growth.
- Depending on how quickly you would like to have the cells up and running, and on the availability of frozen cell stocks; prepare one or two flasks. I have had success with starting the cells in both the 250mL flask and the 100mL flask.

- Usually, I will prepare one of each flask to increase my chances of success. If both flasks look healthy in the following days, I will then combine the cells.
- I always fill flasks with media prior to adding cells in case there are any contaminants in the flasks, such as residual acid causing the media to turn yellow.

Thawing HeLa S3 Cells

1. Set up the following materials in the sterile laminar flow cabinet:
    a. Cell media (DMEM, 5% NCS, 1X Pen Strep) warmed to 37°C
    b. Appropriate flasks for growing cells: 100mL and/or 250mL
    c. 1mL pipette with 1mL filter pipette tips
    d. Pipette gun with 5mL and 25mL serological pipettes
- To ensure that the flasks do not have any residual acid or contaminants, fill the flasks with the appropriate volume of media. It is best to fill the smaller flasks using 25mL pipettes to try to reduce contamination
    e. 250mL flask requires a minimum of 150mL to spin the cells
    f. 100mL flask requires a minimum of 50mL to spin the cells
2. I aim to achieve a final cell density of 0.5*10^6 cells/mL when thawing the HeLa S3 cells (The parent cells are frozen at a density of 25 million cells/mL).
3. Typically, I will start both a 100mL flask and a 250mL flask with the goal of combining them the following day, assuming they both are healthy.
4. To thaw, I first ensure the tube is closed tightly after removing from the liquid nitrogen tank. Then, I warm the tube of cells in a water bath until there is a small

amount of ice remaining (~1-2 minutes), checking frequently to ensure they do not thaw completely.

5. I ensure the tube is sterilized before bringing it into the sterile laminar flow cabinet. Using the 1mL pipette, I transfer the cells into the media of the appropriate flask. I'll often add some more media from that same flask back into the tube and mix before ejecting the liquid back into the flask to ensure I collect as many cells as possible.
6. Once the flasks have been inoculated with cells, it is important to put the cells spinning (~70 rpm) in a 37°C incubator with 5% CO_2. Always keep a clean tray of water in the incubator to provide the appropriate amount of humidity for the cells.
7. Leave the cells to incubate overnight before checking their density.

HeLa S3 Cell Expansion and Maintenance

1. The following morning, I would expect the cells to be at > 70% viability, but I don't anticipate them to have fully doubled that quickly.
2. If both flasks of cells look healthy, I will pour the cells from the 100mL flask (50mL) into the 250mL flask (150mL) and then leave for another night to grow.
3. The following day I would expect the cells to have doubled, and to split the cells with a target cell density of > 0.3*10^6 cells/mL into a 1L flask. Again, cell viability should be > 70%.
4. I continue the process of checking the cells daily and splitting to 0.3*10^6 cells/mL until they reach a volume of 1-liter in the 1-liter flask. From here, I transfer all the cells into a 3-liter flask, but with maximum volume of 2-liters. Finally, I will

incorporate a second 3-liter flask with final volume of 2-liters, with the end goal of having a total of two 3-liter flasks with 4-liters of cells.

5. Once the cells reach this point, I feel comfortable splitting the cells back to a density of 0.15*10^6 cells/mL and expect a doubling rate of 24-hours.
6. While it is not necessary to check the cells daily at this point, I will try to not let them exceed a density of 1*10^6 cells/mL during the process.

Counting of Suspension Cells

- Suspension cells settle fast so if the spinning flask is not very close to the hood, install a plug-in spin plate next to the hood, and stir the flask for 1-minute before counting.
- Additionally, I recommend setting up the hood for counting in advance, so the process is as quick as possible.
- Remove 1-2mL cells using a 5mL serological pipette and place into a 5mL tube.
- Re-suspend these cells thoroughly ~ 15 times using a 1mL pipette.
- Immediately take 10µL of cells and mix with 10µL of HyClone™ Trypan Blue Solution in a microfuge tube, thoroughly but not aggressively ~ 30 times. Then load the mix onto a slide for counting.
- Density and viability of the cells can be checked using a hemocytometer or a cell counter
- Cell viability can be low at the beginning in smaller flasks, but usually >80%.
- Low viability may be improved by spiking flask with 1-2% FBS or letting cells to settle for 1 minute and pouring off some of the top layer (dead cells).

Freezing of HeLa S3 Cells

1. HeLa S3 cells are frozen at 25*10^6 cells/mL in 90% Gibco™ Fetal Bovine Serum +10% Hybri-Max™, sterile-filtered Dimethyl sulfoxide (DMSO).
2. Cells should be in a healthy phase of growth (~0.5*10^6 cells/mL) with high viability (>95%) prior to freezing
3. To maintain sterility the cells are concentrated in 50mL falcon tubes ~500rcf, 5-minutes at a time.
4. I recommend setting up the hood in advance with everything needed, so the process is as quick as possible.
5. The cryo tubes should be labelled with the following: Cell Type, Media, Cell Density, Initials, Date, and any other relevant notes.
6. Once concentrated in cryo tubes, keep the vials of cells in a Styrofoam container at -20˚C freezer for ~2 hours, then move to -80˚C freezer overnight.
7. Move vials to liquid nitrogen storage for long-term storage following day. Take note of the location of cells.

Materials for freezing cells

- Styrofoam container to hold cryo tubes
- Cryo tubes
- 50-mL falcon tubes
- Alcohol resistant permanent marker

Harvest and Lysis of HeLa S3 Cells for Lysate Generation

Preparation for Harvesting HeLa S3 Cells

1. On the day of harvest, cell viability should be >90% and cell density is between 0.25-0.35*10^6 cells/mL
2. Ensure have appropriate reagents for preparing lysates before harvesting
3. 1-hour before desired harvest:
    a. Measure the density and viability of cells and make a note
    b. Set aside ~3-hours for the entire duration of the preparation
    c. Add 1-2% Gibco™ Fetal Bovine Serum to one flask of 2-liters of cells

Preparation During FBS incubation (1-hour)

4. Once the cells are centrifuged, it is important to keep everything as cold as possible for the duration of the lysate prep.
5. Gather one large bin of ice to keep 1-liter flasks cool, one bin of ice to fit ~3 microfuge racks, and one normal sized bucket of ice for keeping smaller tubes during the prep
6. Rinse two 1-liter super-speed centrifuge bottles with sealing closure. Leave to dry upside down on paper towels prior to spinning cells
7. Reserve (if necessary) and pre-cool centrifuges to 4°C:
    a. Floor centrifuge using a high capacity (1-liter) rotor (e.g. SLC-600)
    b. Benchtop centrifuge for 15-mL falcon tubes
    c. Benchtop centrifuge for 1.5-mL microfuge

8. Run the shearing probe of the tissue homogenizer in 70% ethanol, followed by Milli-Q. Dry the probe and leave covered by a paper towel to keep clean prior to use on the cells.
9. Label two empty 15-mL tubes “PBS wash” and “Lysate supernatant” and keep on ice for later
10. Keep ~50-mL of Corning® PBS (Phosphate Buffered Saline) on ice
11. Make 10mL of lysis buffer and keep on ice:
    a. 10mM HEPES at pH 7.5
    b. 10mM potassium acetate
    c. 0.5mM magnesium acetate
    d. 5mM DTT
    e. 1 mini protease inhibitor tablet (for 10mL)
12. Fill 200-mL of bleach into a large (4-liter) beaker to sterilize the media decanted from the centrifuged cells
13. Gather several 10-mL serological pipettes and a pipette gun for removing the media from cells during the lower volume wash steps
14. Keep a 1-mL pipette with filter tips aside, and ~8 microfuge tubes on ice for collecting the lysate later

Preparation for Nuclease Treatment (if necessary)

1. Make an 18ºC water bath for micrococcal nuclease treatment of extract
2. Keep the following reagents on ice:
    a. 0.2M ethylene glycol tetraacetic acid (EGTA) at pH 8.0

b. 100mM calcium chloride ($CaCl_2$)

c. 150U/µL micrococcal nuclease (Thermo Scientific™)

d. Micrococcal nuclease buffer:

   i. 20mM Tris-HCl at pH 7.6

   ii. 50mM sodium chloride (NaCl)

   iii. 50% glycerol

Preparation for Aliquoting Lysate (ideally done at this stage too)

1. Put ~80 microfuge tubes (open) into 2-3 microfuge racks on a bed of ice. Once racks are filled, cover with aluminum foil to keep dust out. I put this bin of ice in the freezer, if possible, too.
2. Set up repeat pipettor with tip to dispense 50 µL
3. Prepare a box for storing lysate labeled with: Date, Initials, Nuclease treatment status, and Concentration (OD)
4. Gather a dewar full of liquid nitrogen for rapid freezing once prep has completed

Pelleting and Washing Cells

1. Stand the two 1-liter capacity centrifuge flasks in the sterile laminar flow cabinet
2. After the 1-hour incubation of FBS, bring the flask into the sterile hood and pour the cells into the centrifuge flasks, taking care to not exceed the capacity of the centrifuge flask
3. Ensure both flasks have an equal volume for balance in the centrifuge
4. Spin the cells in the pre-cooled floor centrifuge at 700-rcf for 10-minutes

5. Immediately transfer the flasks to the bin of ice once the cells are pelleted
6. Decant the media slowly into the 4-liter container with bleach to a final concentration of 10% bleach
7. Add ~10mL of PBS to the cells in the flask to re-suspend and combine both pellets. Transfer the cells and PBS mix to the 15-mL tube labeled “PBS Wash”
8. Spin the cells in a pre-cooled tabletop centrifuge at 700-rcf for 5-minutes with an appropriate balance
9. Remove the PBS and re-suspend the cells in a fresh 10-mL of PBS, then repeat the spin in the pre-cooled tabletop centrifuge at 700-rcf for 5-minutes.
10. Repeat that step once more for a total of three PBS washes

Cell Lysis

1. After the final wash, usually I expect to have a 1-2-mL pellet of cells from the initial 2-liters of cells.
2. Add lysis buffer as compared to the mass of the cell pellet. Typically, I will add twice the volume of cold lysis buffer to the volume of pelleted cells.
3. Let the lysis buffer incubate with the cells on ice for ~5-minutes
4. Shear cells using the tissue homogenizer (speed setting #1) for 20-seconds, followed by a 10-second break on ice. Repeat this for a total of 3 rounds.
5. Once the cells are lysed, split the lysate into the 8 pre-cooled microfuge tubes
6. Spin these microfuge tubes at 13,000-rcf for 5-minutes in the pre-cooled tabletop centrifuge.

7. Once the lysate has been centrifuged, pool the supernatant into the 15-mL tube labeled “Lysate Supernatant”. Be very careful not to draw up any pellet!
8. Note the total volume of the supernatant and measure the A280nm of the lysate, using the lysis buffer as a blank. Expected A280 ~30-50mg/mL. Take note of the concentration of lysate to put on the box the lysate will be stored in later.

Nuclease Treatment

For the purpose of this dissertation, I removed the endogenous mRNAs by treatment of the extracts with micrococcal-nuclease to study the effects of our reporter without conflating our results with competition from other mRNAs. However, it is optional to exclude this step. Moreover, In the future, it will be of interest to re-visit my work in the presence of endogenous mRNAs to study the true physiological preservation of the extract.

1. Typically, I will dilute the micrococcal nuclease stock (150U/ µL) to 30U/ µL (total volume of ~30-µL should be sufficient) right before I add it to the cells. I do not keep this dilution after each preparation; therefore, I make a small volume every time.
2. Add 1mM $CaCl_2$ and 150U of micrococcal nuclease to the lysate supernatant.
3. Ensure complete mixing by inverting the tube of lysate three times.
4. Incubate the reaction in the 18ºC water bath for 20 minutes.
5. Add 2mM EGTA pH at 8.0 to stop the reaction. Again, invert the tube three times.
6. Keep the lysate on ice after the nuclease treatment is complete.

Lysate Freezing and Storage

1. Draw up ~1-mL of lysate into the repeat pipettor at a time
2. Aliquot 50 µL of the lysate into each microfuge tube (on ice).
3. Once all of the lysate has been aliquoted into the pre-cooled microfuge tubes, close each cap and put into the liquid nitrogen dewar for flash freezing
4. After flash freezing each tube, add all of the frozen lysate to the prepared storage box and put into the -80°C freezer for long term storage
5. Never freeze thaw the lysate for experiments

Testing Translatability of Cell-Free Extracts

It is critical to verify that the cell-free extracts undergo faithful translational regulation prior to applying the extracts to monitor cellular activities. A detailed account of this process and all-important considerations necessary are outlined in Chapter 2.

Additional Protocols for Cell-Free Extracts

Pre-Treatment of HeLa S3 Cells

In addition to generating serum-activated cells, the cells can be treated with inhibitors to measure the effects of cellular inhibition downstream in our assays. To this end, I tested Torin, the potent and selective ATP-competitive inhibitor of mTOR (mammalian target of rapamycin) kinase [9]. Based on previous data, I decided to treat cells with 250 nM Torin, 2-hours before harvesting. In tandem, I grew non-serum-activated cells as a control. Both lysates were harvested as outlined in our above protocol.

Accordingly, I tested the lysates' ability to translate mRNAs with varying levels of structure in the 5′UTR; ten CAA repeats (unstructured) or a 25.1 kcal/mol hairpin at the +4 position (structured). The structured hairpin sequence was as follows: CCACCACGGCCGATATCACGGCCGTGGTGG). Interestingly, both the unstructured and structured messages showed a decrease in activity in response to the Torin treatment (Figure 1.2). However, it will be important to repeat this experiment given my more recent optimization of the lysate preparation and translation protocols (outlined in Chapter 2) to ensure the data is reproducible and accurate.

Fractionation of Cell-Free Extracts

The cell-free extract can be fractionated by ultracentrifugation as a means of assessing specific activities, and/or as a means of determining the dependence of specific mRNAs upon their presence [10]. Ultracentrifugation allows rapid separation of ribosomes and ribosome-associated proteins. Associated factors can be removed by "washing" ribosomes in high salt and can be further divided into district subfractions by differential ammonium sulfate precipitation [11, 12]. Reconstitution of a functional translation system from these various fractions, comprising distinct populations of initiation factors, can therefore be controlled at will. An overview of the method of ribosome depletion is depicted in Figure 1.3*A*.

Preparation before Ultracentrifugation of Lysate

1. Pre-cool Beckman Coulter TLA-100 Fixed-Angle Rotor at 4°C

2. Pre-cool Beckman 11x34mm tubes on ice. These tubes hold 1-1.2mL; this volume is required to prevent tubes from caving in.
3. Importantly, aliquot the lysate into two tubes evenly

Preparation of Benchtop Ultracentrifuge

1. Settings: 20' 4C 100,000rpm. The acceleration and deceleration should be set to 1 (fastest) for getting up to 100,000rpm
2. The Beckman Coulter TLA-100 Fixed-Angle Rotor clips in: push on silver button in middle
3. The ultracentrifuge will also let to you adjust time etc during the run

Post-Fractionation; Ribosome-Depleted Extract

1. Carry the rotor carefully back to lab
2. Take out tubes carefully with a tweezers and place on ice
3. The lipid layer is expected on top, and the ribosome pellet is at the bottom
4. For ribosome depleted extract, take up the middle two thirds of the supernatant ~700uL, but be modest, don't try to get near top or bottom layer

Preparation of Ribosome Pellet

1. Resuspending the ribosome pellet is at least a 1-hour process.
2. It is important to carry out this procedure slowly on ice and ensure no bubbles to prevent oxidation of the ribosome pellet
3. Use lysis buffer (1/10th of total volume) to re-suspend

Confirmation of Ribosome Depletion

The levels of key translation factors pre- and post-ribosome depletion should be assessed by western blot, as indicated in Figure 1.3*B*. Antibodies used are outlined in Table 1.

Factor Depletion

Stable cell lines are considered a powerful model for expressing specific protein products on a production scale and have wide utility in molecular biology. I have applied this tool to stably deplete factors hypothesized to be involved in our RNA re-structuring assay i.e., each member of the eIF4F complex. Stable depletion of these components in lysate provides a more targeted approach to asking questions about specific factors in the pathway. Following verification of factor depletion, I successfully adapted these cell lines to liquid suspension culture to produce large-scale factor-dependent extracts. The aim is to apply these extracts to study kinetic deficiencies in the pathway. Furthermore, by titrating back in recombinant forms of the complex in wild type or mutant forms, it is possible to reveal the precise role each factor has in directing RNA re-structuring and translation. In Chapter 3 I have discussed my method of depleting factors from cells in detail. Please refer to that chapter for more information.

Future Directions

Cell-free extracts are a powerful tool for recapitulating the true physiological implications of events and are in compliance with examining immediate kinetic changes in the pathway. Here, I describe the detailed method of how to successfully make large quantities of robust translation competent cell-free extracts from HeLa S3 cells, a mammalian suspension cell line.

Applying these extracts to our assays allowed the opportunity to ask outstanding questions about translation in the context of RNA restructuring, but there are plenty of questions remaining. Firstly, understanding more about translation and restructuring in the presence of endogenous mRNAs (untreated extract). Secondly, capitalizing on the ribosome fractionation protocol to a) isolate and characterize fractions possessing unwinding activities, and b) to add back recombinant factors to restore their activities e.g. high salt washed ribosomes. Thirdly, taking advantage of pre-treatment of the extracts with Torin-1, enabled me to investigate the downstream effects of this drug in terms of how certain mRNAs are targeted such as unstructured and structured messages. While my preliminary experiment (Figure 1.2) suggested no change in inhibition preference; it would be interesting to follow up this work with my optimized translation and RNA restructuring conditions. Additionally, in combination with more physiologically relevant unstructured and structured target mRNAs.

Taken together this work should serve as an important tool to help answer these fundamental questions in the future.

References

[1] Jackson RJ, Hunt T. Preparation and use of nuclease-treated rabbit reticulocyte lysates for the translation of eukaryotic messenger RNA. Methods Enzymol. 1983;96:50-74.
[2] Both GW, Banerjee AK, Shatkin AJ. Methylation-dependent translation of viral messenger RNAs in vitro. Proc Natl Acad Sci U S A. 1975;72:1189-93.
[3] Iizuka N, Najita L, Franzusoff A, Sarnow P. Cap-dependent and cap-independent translation by internal initiation of mRNAs in cell extracts prepared from Saccharomyces cerevisiae. Mol Cell Biol. 1994;14:7322-30.
[4] Gebauer F, Corona DF, Preiss T, Becker PB, Hentze MW. Translational control of dosage compensation in Drosophila by Sex-lethal: cooperative silencing via the 5' and 3' UTRs of msl-2 mRNA is independent of the poly(A) tail. Embo j. 1999;18:6146-54.
[5] Bergamini G, Preiss T, Hentze MW. Picornavirus IRESes and the poly(A) tail jointly promote cap-independent translation in a mammalian cell-free system. Rna. 2000;6:1781-90.
[6] Thoma C, Ostareck-Lederer A, Hentze MW. A poly(A) tail-responsive in vitro system for cap- or IRES-driven translation from HeLa cells. Methods Mol Biol. 2004;257:171-80.
[7] Michel YM, Poncet D, Piron M, Kean KM, Borman AM. Cap-Poly(A) synergy in mammalian cell-free extracts. Investigation of the requirements for poly(A)-mediated stimulation of translation initiation. J Biol Chem. 2000;275:32268-76.
[8] Svitkin YV, Imataka H, Khaleghpour K, Kahvejian A, Liebig HD, Sonenberg N. Poly(A)-binding protein interaction with eIF4G stimulates picornavirus IRES-dependent translation. RNA (New York, NY). 2001;7:1743-52.
[9] Liu Q, Chang JW, Wang J, Kang SA, Thoreen CC, Markhard A, et al. Discovery of 1-(4-(4-propionylpiperazin-1-yl)-3-(trifluoromethyl)phenyl)-9-(quinolin-3-yl)benzo[h][1,6]naphthyridin-2(1H)-one as a highly potent, selective mammalian target of rapamycin (mTOR) inhibitor for the treatment of cancer. J Med Chem. 2010;53:7146-55.
[10] Rau M, Ohlmann T, Pain VM, Morley SJ. A fractionated reticulocyte lysate system for studies on protein synthesis initiation factors. Methods Mol Biol. 1998;77:211-26.
[11] Morley SJ, Dever TE, Etchison D, Traugh JA. Phosphorylation of eIF-4F by protein kinase C or multipotential S6 kinase stimulates protein synthesis at initiation. J Biol Chem. 1991;266:4669-72.
[12] Morley SJ, Hershey JW. A fractionated reticulocyte lysate retains high efficiency for protein synthesis. Biochimie. 1990;72:259-64.

CHAPTER 2

Engineering of an mRNA reporter to study RNA restructuring and protein synthesis in mammalian cell-free extracts

This chapter contains unpublished work and was written by me with editing by Dr. Christopher Fraser. All of the experiments were performed by me.

Abstract

Previous work using the fluorescent strand displacement assay has highlighted the roles of particular factors in unwinding secondary structures. However, this was characterized using reconstituted proteins and short mRNA templates. Accordingly, my goal was to adapt this assay to monitor duplexes in true cellular conditions using cell-free extracts. I discussed the generation of our cell-free extracts from HeLa cells in Chapter 1. Here, I address how I redesigned and optimized our method to demonstrate the physiological implications of these RNA restructuring events. Specifically, I incorporated a bioluminescent luciferase gene to the mRNA reporter to enable visualization of changes in overall protein abundance, in parallel. Moreover, the assay conditions were revised to ensure optimal functionality in translation prior to measuring RNA restructuring.

Introduction

The fluorescent-based helicase assay is a unique tool that was pioneered by my lab to monitor the RNA helicase, eIF4A, an essential factor in translation initiation for unwinding RNA secondary structures in the 5'-UTR of mRNAs [1-4]. The reconstitution of the kinetic events in the first round of translation can be achieved by using just a subset of purified protein factors. However, the concern with real-time kinetic assays, such as the fluorescent-based helicase assay is that one can miss a lot of regulation in the cell by just studying a portion of the factors involved.

To overcome the limitations of purified reconstituted systems, I have adapted the fluorescent strand displacement assay to now monitor the melting of duplexes in real time using a translation competent cell-free extract system generated from HeLa cells [3, 5, 6]. In contrast to *in vivo* systems that typically require hours or days to see effects, cell-free extracts: a) provide the core cellular machinery, b) enable investigation of the earliest steps in real time, c) study translation independently of transcription, and d) allow direct manipulation of protein and RNA levels to help further elucidate molecular underpinnings of regulatory events. The potential barriers of using cell-free extracts are that some kinetic assays cannot be adapted for use in such a complex mixture and it can be difficult to generate enough extract to perform robust analysis using culture plates. HeLa S3 cells, a mammalian suspension cell line offers a viable solution to overcoming this bottleneck in the field. As discussed in Chapter 1, these cells can be grown in multiple 2-liter flasks to generate large quantities of lysate, enabling truly robust biochemical analysis of the pathway. While the mammalian nature of these cells increases the likelihood of recapitulating faithful mammalian cellular regulation, it is imperative to verify this.

Accordingly, I have incorporated a luciferase gene, NanoLuc (Nluc) [7] into the RNA reporter to study the downstream effects on protein synthesis. This design provides the added benefit of enabling the study of more regulatory events in the context of protein synthesis. Luciferase reporters are generally limited in their capacity to provide extensive mechanistic insight into the translation pathway, but in parallel with the fluorescent-based helicase assay it is a very powerful tool.

In this chapter, I discuss engineering of the dual-assay mRNA reporter and optimization of assay conditions for recapitulating faithful translational regulation and RNA restructuring in cell-free extracts. An overview of the system is outlined in Figure 2.1.

Development of the Dual-Assay Reporter mRNA

Plasmid Design

The mRNA template was engineered to include several key elements separated by carefully chosen restriction sites. This modular nature of the mRNA template allows ease of manipulation for cloning (Figure 2.2). The following features were considered in the design of my reporter:

1. T7 RNA polymerase promoter binding side for generating mRNA template [8-10]
2. Restriction sites to incorporate unique sequences in the 5′UTR and 3′UTR and sites for annealing fluorescent beacons (5′-end Cy3 labeled RNA reporter strand, and 3′ -end BHQ labeled RNA reporter strand) at adjacent positions anywhere along the template [1]
3. A bioluminescent luciferase gene to report downstream translation activity.

This backbone can be synthesized by a gene synthesis company such as GenScript. The features of interest can be cloned in by ligating digested inserts to the vector or via annealed oligos.

During the reporter template synthesis by PCR, a poly (T) tail modification can be added at the 3′ end of the reverse primer to form a poly (A) tail during transcription; characterized by addition of greater than 50 sequential adenylate nucleotides. Post-RNA synthesis, a 7-methylguanylate structure (m7G cap) can be added to the 5′ end of the mRNA. This cap protects the mature mRNA from degradation and serves a role in efficient translation together with the poly (A) tail.

Luciferase Reporter Gene

Luciferases are proteins that catalyze emission of light from the enzymatic conversion of a supplemented substrate. The two key requirements for the production of bioluminescence, are the enzyme responsible for catalyzing the reaction and producing light (luciferase) and the substrate for this enzyme (luciferin) [11]. There is a wide dynamic range by the emission of light from this variety of engineered luciferase (Luc) genes from beetles and marine organisms that are expressed after exogenous addition of their respective luciferin substrates. The bioluminescent genes available to me in the lab were: Renilla luciferase (RLuc), Firefly (FLuc), and Nano luciferase (NLuc) [12]. FLuc reacts with D-luciferin in the presence of adenosine triphosphate (ATP), molecular oxygen, and magnesium to produce light. RLuc only requires coelenterazine and oxygen to produce light. Bioluminescence from NLuc occurs when the optimized substrate called furimazine

reacts with NLuc in the presence of molecular oxygen, yielding furimamide and luminescence output.

Rluc was the default choice by the lab due to the intermediate luminescence sensitivity offered by the enzyme. However, I found the signal of Rluc too weak to parse out the details needed for validating the cell-free extract system, while maintaining the RNA concentration at a physiologically relevant level. To determine which reporter gene was best to use in my assay, I generated all three reporter constructs (Rluc, Fluc, Nluc) to measure side by side. Fluc displayed an even lower signal than the Rluc, and Nluc gave a signal that was beyond the linear range of the plate reader to accurately measure. To overcome the limitation of the excessive Nluc signal, I adapted the luciferase platform of Nluc to work in combination with the Rluc substrate, coelenterazine. This adaptation enabled my constructs to emit higher luminescence than Rluc alone, while still operating within an appropriate linear range of signal (Figure 2.3).

Design of Fluorescent Duplex Substrates

The fluorescent reporter RNA oligonucleotides are chemically synthesized, modified, and HPLC-purified by Integrated DNA Technologies (IDT). The reporter strand is modified with cyanine 3 (Cy3) on its 5′-end, and the quenching strand is modified with a spectrally paired black hole quencher (BHQ) on its 3′-end. There are options for fluorescent beacon length and sequence. To establish a duplex substrate that is suitable for use in a cell-free extract environment, I screened three fluorescent duplexes previously characterized to have a thermal stability close to −24 kcal/mol [1] shown in Table 2. I discuss how I established which fluorescent beacon would be appropriate for my assay in the results section of this chapter “Selection of Fluorescent RNA Reporter”.

Moreover, the beacon annealing sites can be inserted via annealed oligos at any position along the length of the loading template, taking advantage of the restriction sites in the template as described in Plasmid Design (Figure 2.2).

RNA Synthesis and Purification

DNA Preparation

Transcription templates consist of phenol extracted products from a PCR of the luciferase-reporter DNA. Briefly, the DNA template is amplified by PCR with appropriate primers from a pUC57 plasmid. The forward primer encodes the T7 promoter required to initiate transcription. T7. The reverse primer anneals to the end of the desired mRNA template and is generated in the presence or absence of a 50 nt poly-A region at the 3′-end, which is above the minimal length required for efficient PABP binding [13]. PCR templates are purified by phenol-chloroform extraction followed by ethanol precipitation. The PCR product is verified to be free of aberrant bands by agarose gel electrophoresis.

In vitro Transcription

The loading strand is generated using published methods for in vitro transcription reactions with minor modifications [8-10]. The RNA is transcribed with T7 polymerase and purified by phenol-chloroform extraction followed by ethanol precipitation with ammonium acetate. For each 500µL reaction, 7µg of DNA template is incubated with 8 mM ATP, 8 mM GTP, 8 mM CTP, 8 mM UTP, 0.4 mg/mL T7 RNA polymerase in transcription buffer (40 mM Tris/HCl, pH 8.1, 0.01% Triton X-100, 60 mM magnesium chloride, 1 mM spermidine, 5 mM DTT). Incubations are carried out at 37°C for 1-4 h. Following

transcription, the RNA product is directly extracted by phenol-chloroform treatment and precipitated by ethanol and ammonium acetate. Additionally, free nucleotides are removed from the RNA using Sephadex G25 resin (GE Healthcare). This step is critical for clean RNA (Figure 2.4). ATP, GTP, CTP and UTP were purchased from Sigma-Aldrich, and all were stored at −20°C in H_2O at pH 7.5.

Purification Analysis

To assess RNA integrity and purity of the transcription product, 1µg of RNA is denatured in 50% (vol/vol) formamide at 70°C for 10 min and separated by electrophoresis on an 8% (wt/vol) denaturing urea-polyacrylamide gel. (Figure 2.4)

Vaccinia Capping Enzyme System

The mRNA can be capped at the 5′-end by the vaccinia virus guanylyltransferase [14] using a Vaccinia capping system according to the manufacturer's guidelines (New England Biolabs). We successfully generated our own functional Vaccinia capping proteins by expressing them recombinantly using baculovirus expression in SF9 insect cells. The lab generated enzymes produced mRNA capped to the same extent as commercial enzyme, as assayed by protein synthesis (Figure 2.5).

Testing Translatability in Cell-Free Extracts

Translation Assay Protocol

Reaction Components

- 0.8mM ATP-Mg
- 0.1mM GTP-Mg
- 50µM Spermidine
- 16mM HEPES, pH=7.5
- 60 µM amino acid mix
- 1X salt buffer (90 mM potassium acetate, 45 mM potassium chloride, 2 mM magnesium acetate)
- 20mM creatine phosphate
- 40µg creatine phosphokinase
- 0.4 U/µl Promega RNasin® Ribonuclease Inhibitor
- Promega Renilla Luciferase Assay System
- 40% HeLa cell free extract (nuclease treated or untreated)
- 500nM mRNA diluted in a 1X buffer (see below)
- Protein diluted in a 1X buffer (see below)

mRNA and any supplemental proteins are diluted in the following buffer:

- 20mM Tris-Acetate pH 7.5.
- 2mM Mg-Acetate pH 7.5.
- 0.2mM DTT.
- 100mM KCl.

- 10% glycerol.

Important Storage Information

- Protein stocks are kept at -80°C, once diluted they are not re-frozen.
- mRNA kept >1µM at -20°C for less than 1 year, or -80°C for longer.
- The Renilla Luciferase Assay buffer needs to be at room temperature for measuring.
- Aliquot mRNA and protein stocks. Freeze thawing >3 times is not recommended.
- HeLa extract aliquots kept at -80°C. Never freeze thaw.
- Store the Renilla Luciferase Assay substrate in a light protective box at -20°C. Keep the Renilla Luciferase Assay substrate at -20°C until needed.
- All other reagents are kept at -20°C and thawed on ice if needed.

Reaction Calculations

- Luciferase translation assays are carried out in a 70 µL (3.5 X individual reactions) volume for measuring triplicate reads (20 µL each). The final reaction contains the components outlined in “Reaction Components” above.
- It is important in advance to determine the number of reactions needed, and then calculate the amount of each reagent. *Always do the calculations for extra reactions to ensure there is enough mix for the experiment. I use an Excel spreadsheet for these calculations.

- Example: for testing four experimental conditions in triplicate: 3.5 X 4 = 14. Here, I would set up a 17-reaction master mix to be sure there is enough reagent for the experiment. Refer to Table 4 to visualize the reaction set up calculations.
- It is not recommended to set up less than a 6X master mix as volumes will be too small.

Method

1. Always re-check concentrations of mRNA and protein before diluting them to the working concentration.
2. Add any supplemental proteins or inhibitors to each reaction tube first and keep on ice: 3.5 X individual reaction volume (2µL) = 7µL per tube.
3. Assemble the translation master mix (calculated in advance). Thaw the lysate on ice to add last. Do not add the mRNA with the master mix. Each tube should contain 56 µL of master mix and 7µL of protein/inhibitor (or buffer).
4. Pre-incubate lysate, translation mix and any supplemental proteins or inhibitors for 10-minutes at 30°C.
5. After pre-incubation, add 500nM of mRNA (7µL per tube) for a final concentration of 50nM. Mix well and incubate at 30°C for 30 minutes.
6. In the last few minutes, take the Renilla Luciferase Assay substrate from the -20°C and mix 1 µL:100 µL with the Renilla Luciferase Assay buffer for every individual 20µL reaction.
7. When translation is complete, spin down the tubes for a few seconds

8. Following centrifugation, the 70 µL reaction is split into three individual 20 µL volumes before adding the Promega Renilla Luciferase substrate buffer mix.
9. After mixing, 100 µL is then immediately transferred to a 96-well OptiPlate (Perkin-Elmer).
10. Luminescence is measured for 10 s by using a Victor X5 Multilabel Plate Reader (Perkin-Elmer).

Data Analysis

Counts per second obtained for each translation reaction are normalized to basal nonspecific levels of luciferase translation taken from reactions lacking mRNA. The data are presented as normalized luciferase (LUC) translation. Luciferase translation is quantified as the mean of at least three independent experiments ± SEM.

Summary of Changes to Protocol

- A temperature of 30°C was selected to accommodate temperature sensitivity of the fluorophores.
- The translation conditions were adjusted to ensure high-fidelity initiation codon selection [8]. See Table 3 and 4.
- mRNA reporter concentration of 50nM was selected (Figure 2.6*A*).
- A pre-incubation step was incorporated for the lysate for 10 minutes at 30°C prior to initiating the assay (Figure 2.6*B*).

Validation of High-Fidelity Extracts

It is critical that the cell-free extracts are verified to translate the mRNA reporter linearly, for at least 30-minutes. (Figure 2.7*A*). For monitoring RNA restructuring in parallel, it is also important to verify that annealing the beacons to the mRNA reporter does not cause a significant defect in translation. (Figure 2.8).

To determine the fidelity of the cell-free extract, I tested a known *in vivo* hallmark of translation: the synergy between the 5′-cap and 3′-poly (A) tail. *In vivo* translation studies have demonstrated that the poly (A) and cap interact synergistically to stimulate translation initiation in yeast, tobacco protoplasts, and mammalian cells [15, 16]. This can also be recapitulated *in vitro* [17-21]. I investigated this by priming my mRNA reporter construct with different combinations of the cap and poly (A) modifications to the mRNA and carried out translation assays in Hela lysates, comparing the level of luciferase generated between each reporter (Figure 2.7*B*). The data argue that these extracts support robust cap and pA-dependent translation, in line with *in-vivo* studies. These results demonstrated that my HeLa extracts exhibit authentic translation control and are thus a suitable model system for studying translation regulation.

Monitoring Unwinding in Cell-free Extracts

Overview

A schematic overview of the assay is outlined in Figure 2.4. Briefly, an unmodified mRNA loading strand is engineered with sites to anneal a cyanine 3 (Cy3) labeled RNA oligo, and a spectrally paired black hole quencher (BHQ) labeled RNA oligo (IDT). I find that, when the two reporters are annealed 1 nt apart, the Cy3 fluorescence is efficiently quenched by proximal BHQ, resulting in a low fluorescence state. The unwinding reaction

is initiated by cell-free extract. As a helicase unwinds the loading strand, the enzyme displaces the Cy3- modified reporter, thus separating it from the BHQ-modified reporter. Cy3-strand separation is detected in real time as an increase in the total fluorescence of the reporter strand. As detailed in the Data Analysis section, the change in Cy3 fluorescence is then manually converted to fraction of duplex unwound. The observed initial rate of each unwinding reaction is then calculated by using the initial linear portion of the time course.

Duplex Annealing

The RNA substrate used for unwinding reactions is created by annealing the fluorescent reporters (Cy3 and BHQ) to the mRNA template. The reporters and RNA template are mixed to a final concentration of 500 nM in unwinding buffer [20 mM Tris-acetate at pH 7.5, 2 mM magnesium acetate, 100 mM potassium acetate, and 0.2 mM dithiothreitol (DTT)]. The annealing reaction is placed at 80 °C and slow-cooled to room temperature for ~1-2 h by removing the heating block and letting it cool on the bench. Thereafter, the product is incubated on ice for 10 min. The final annealed RNA substrate is diluted to 250 nM using 1X unwinding buffer.

Fluorescence Optimization

The unwinding reactions are performed in a 50-µL cuvette (Starna) by using a Fluorolog-3 spectrofluorometer (Horiba). It is important to optimize the fluorescent signal to minimize photobleaching in the cell-free extract. Through optimization of the fluorometer conditions using the following methods, I could achieve 50-fold greater R^2 from 0.7256 to 0.982 (Figure 2.10).

Cuvette Position

Primarily, care should be taken to minimize variance in fluorescence intensity due to changes in the cuvette position in the holder of the fluorometer. It is important to ensure reproducible cuvette placement in the fluorometer holder. Putting some tape on the edge of the cuvette can help bolster the cuvette in position. Additionally, I find that placing the cuvette such that it is pressed against the bottom right corner gives us the highest signal.

Fluorometer Settings

The excitation and emission wavelengths will depend on the fluorophore-quencher pair. By conducting an emission spectrum analysis in our fluorometer, I determined the Cy3 fluorophore operated best between excitation λ= 545 nm and emission λ= 575 nm. Moreover, I optimized the width of the entrance slits to 3nm, and the exit slit to 25nm. For my cell-free extract, fluorometer, and fluorophores these settings gave the most robust signal with least amount of photobleaching and noise in the data.

Unwinding Reactions

The unwinding reactions were based on the previously described method [2] with modifications for the cell-free extracts listed below. It is essential to calibrate the maximum possible fluorescence signal of the RNA reporter strand. A mock unwinding assay reaction mixture is prepared that contains all of the reaction components at the appropriate concentration and temperature in the absence of the BHQ-modified oligonucleotide (Cy3-modified oligonucleotide, loading mRNA template, ATP, cell-free

extract). The maximum fluorescence reading also serves as a useful guide to determine how much Cy3 photobleaching occurs over time (Figure 2.11*A*). To measure unwinding activity, I combine the annealed RNA substrate (50nM), 2mM ATP in our 1X reaction buffer. The baseline fluorescence is monitored for at least 100 seconds to verify substrate annealing and the absence of extraneous RNase activity (Figure 2.11*B*). The background fluorescence is generally 10-50% of the maximum fluorescence. Here, unlike previous work, the reaction is initiated with pre-incubated cell-free extract and any other accessory proteins. The pre-incubation conditions for the extract were 10-minutes at 30°C. The assay is not initiated with ATP since there is likely residual ATP present in the extract already. The assay measures the total fluorescence as a function of time. The unwinding profile of cell-free extracts reaches a maximum fluorescence in ~6–8 min (Figure 2.11*C*). Please note that, to ensure reproducibility, the unwinding assay should be repeated at least three times.

Data Analysis

The data are analyzed as previously described with minor modifications [2]. Primarily, I modified the collection of data points (S1) to automatically remove any noise from the lamp intensity (R1) using the formula S1/R1 to generate our fluorescence curves over time. To quantify the unwinding activity, the fraction of duplex unwound at each time point must be calculated. This quantification is made possible by calibrating the assay using the maximum fluorescence and the baseline fluorescence immediately after addition of cell-free extract. The baseline fluorescence is subtracted from the values for each time point and from the maximum fluorescence (Figure 2.11*C*). The maximum

fluorescence of the 24-nt Cy3-modified reporter (50 nM) is measured in the presence of 50 nM loading RNA strand, 40% cell-free extract, and 2 mM ATP·Mg-acetate in 1X unwinding buffer. Upon RNA annealing, I observe the quenching of Cy3 fluorescence by BHQ to be typically in the range of 70% to 90%.

The fraction of duplex unwound for each time point is obtained by simply dividing the baseline-corrected fluorescence values at each time point by the corrected maximum fluorescence value (Figure 2.12*A*): fraction of duplex unwound = (baseline-corrected fluorescence)/(baseline-corrected maximum fluorescence). The data can be quantified by fitting a linear regression line to the initial portion of the fraction of duplex unwound versus time (Figure 2.12*B*) and converted to fraction unwound per minute (Figure 2.12*C*). Alternatively, the fraction of duplex unwound versus time can be fit to single-or double-exponential equations to obtain rate constants for this process. All data were plotted and analyzed by both Microsoft Excel and GraphPad Prism software.

Summary of Changes to Protocol

1. The reactions are carried out at 30 °C, as the luciferase assays are also carried out at this temperature.
2. In my hands, the Cy3 fluorophore operated best between excitation λ = 545 nm and emission λ = 575 nm. Moreover, I optimized the width of the entrance slits to 3nm, and the exit slit to 25nm for best signal.

3. I modified the collection of data points (S1) to automatically remove any noise from the lamp intensity (R1) using the formula S1/R1 prior to generating the unwinding curves.
4. A competitor DNA strand is not included in the assay since the cell-free extracts contain potent DNase activity rendering the strand ineffective.
5. To measure the baseline unwinding activity, I combine 50nM annealed RNA substrate and 2mM adenosine triphosphate-magnesium acetate (ATP-MgAce) in our 1X reaction buffer.
6. The unwinding reaction is initiated with pre-incubated cell-free extract and any other accessory proteins. The assay is not initiated with ATP since there is likely residual ATP present in the extract already.
7. The pre-incubation conditions for the extract were 10-minutes at 30°C.

Further Characterization of the mRNA Reporter

Selection of Fluorescent RNA Reporters

To first establish a duplex substrate that is suitable for use in this assay in a cell-free extract environment, I screened three fluorescent duplexes previously characterized to have a thermal stability close to −24 kcal/mol [1] shown in Table 2. I engineered these beacons to anneal 40nts downstream of the 5′ end of the RNA to allow for efficient protein loading. Based on the results of my screen (Figure 2.13*A*), I chose to focus on the 12nt CY3 beacon as it demonstrated the most robust unwinding activity and was unwound in an ATP dependent manner (Figure 2.13*B*).

It is worth noting that the final RNA concentration in the assay was 25nM. Moreover, this data was collected prior to further optimization of the assay conditions as described in this chapter.

Position of Duplex Substrates for Monitoring RNA Restructuring

I shifted the position of the 12nt beacon to the middle of the luciferase (501nts from the 5′ end) to measure how this beacon responded. I first confirmed this position did not disrupt the ability of the Nluc gene to translate (Figure 2.14). Unexpectedly, the beacon at position 501nts unwound in a similar manner to the upstream beacon (40nts from the 5′ end), and surprisingly, was modestly stimulated by the ribosome transit elongation inhibitor, cycloheximide (Figure 2.15). I determined one possibility was that the 12nt beacon was reporting on events that correspond to another regulatory event in the cell lysate such as an RNAi pathway. To test this, I supplemented the assay with a dominant negative eIF4A (eIF4A R362Q), a potent inhibitor of the key translational helicase. The

unwinding defect was inconsequential to the 12nt CY3 beacon (Figure 2.16*A*). However, in the context of the newly optimized conditions, I re-visited the 24nt CY3 beacon, and found that I could now measure robust unwinding signal and observed changes in a manner I expect for translational regulation (Figure 2.16*B*). Nevertheless, from my initial data prior to optimization, I determined to discontinue working with the 12nt CY3 beacon as it did not appear at the time to respond to translational regulation as expected. While this is an interesting phenomenon, it was beyond the scope of the project, but might be in interesting area of exploration for future research.

Going forward I focused only on RNA restructuring with the 24nt beacon in the 5′UTR of the mRNA reporter (40nts). Unfortunately, when I engineered the 24nt beacon to the middle of the Nluc gene (position 501nt) it disrupted the luciferase protein such that translation could not be measured. I also attempted to measure the 24nt beacon in the 3′UTR position, but the addition of this sequence caused a disruption to the synergistic translation of the cap and poly (A) mRNA reporter (observed in Figure 2.7), which could not be explained (Figure 2.17). It would be interesting to follow up with this data to test if it's possible to monitor unwinding in the 3′UTR region as it would provide some context to RNA restructuring throughout the entire length of the mRNA.

Design of Sequence in the 5' UTR

Initially, I focused on generating secondary structure in the 5′-UTR because it correlates with large changes in the rates of translation. Accordingly, I hypothesized this would result in drastic changes in my re-structuring assay. 5′-UTR secondary structures have been determined to be particularly prevalent among mRNAs encoding transcription

factors, proto-oncogenes, growth factors, and proteins poorly translated under normal conditions. These intricate structures provide an additional layer of translational control of gene expression by regulating cap-dependent translation initiation through occluding the m7G cap from the cap-binding complex eIF4F, or by preventing eIF4F from fully binding to the mRNA [22-24]. When secondary structure is located further away from the m7G cap, it may also reduce the rate of scanning by the 48S complex. While it is possible to computationally predict, at least approximately, secondary structures in the 5′-UTR of mRNAs, we still understand very little about the degree to which individual mRNAs possess secondary structure in cells. Despite significant effort to understand how individual functional mRNA structures can regulate translation, the precise mechanistic of cap-recognition by the eIF4F complex and how secondary structure regulates the recruitment of this complex to mRNA is yet to be established [25].

To begin to understand the nature of this regulation, I decided to apply my assays to test 5′-UTR with varying levels of structure. I modeled my experiments on previous work showing that a hairpin structure of modest stability (–25 kcal/mol) can modulate translation of reporter genes by up to 50-fold by only varying the position of a stable hairpin relative to the 5′ m7G cap as little as 9 nucleotides [26]. Initially, I designed my constructs to include a –25.1 kcal/mol hairpin at the previously published positions; +1, +4, and +10 nucleotides from the cap structure (Figure. 2.18*A*). The hairpin sequence was as follows: CCACCACGGCCGATATCACGGCCGTGGTGG. The mRNAs also contained a 50-nt poly (A) tail. Then, I measured their activity in the presence or absence of the cap structure and compared these structured templates to equivalent unstructured templates (CAA repeats). The data showed that the stem-loop structure inhibited

uncapped translation at each position along the 5′-UTR (Figure. 2.18*B*). However, the stem-loop located at 10-nt in the presence of the cap demonstrated a stimulatory effect equivalent to the unstructured template. Whereas closer to the cap (1-nt and 4-nt) could not overcome the energy barrier to stimulate translation to the same degree. Since the RNA restructuring capacity of these stem-loop hairpin reporters were measured prior to optimizing the conditions of my system, the data is considered incomplete to report here.

Given the complex nature of optimizing the restructuring system, I determined that to simplify the results of my experiments, I would initially characterize my system using a more physiologically relevant unstructured sequence, human β-globin 5′- untranslated regions (UTR); see sequence in “Plasmid Sequences” under MOS54.

Design of Sequence in the 3′ UTR

3′-untranslated regions (3′-UTRs) are the noncoding parts of mRNAs. The sequence space occupied by 3′-UTRs has substantially expanded during the evolution of higher organisms and correlates with cellular complexity of organisms [27, 28]. 3′-UTRs are best known to regulate mRNA-based processes such as: polyadenylation, localization, translation efficiency, and mRNA stability. The relative contributions of these different regulatory mechanisms remain poorly understood as the readouts for testing 3′-UTR functions don’t go far beyond measuring the regulation of protein abundance by luciferase reporter assays. The fluorescence-based helicase assay in parallel with the luciferase assay (dual assay reporter system) offers a unique approach to providing insight into 3′- sequence-directed processes.

To investigate the validity of this approach, I first decided to design a 3′-UTR of random sequence to serve as a control by including 500bps of additional random

sequence from the pUC57 vector which was used to clone the mRNA template. In contrast to an mRNA with no 3′-UTR, the luciferase activity generated from this construct showed a 92% decrease in signal (Figure. 2.19). To determine if this was due to the length of the 3′-UTR, I generated constructs with 3′-UTRs of shorter lengths (350 and 250 nts) from the pUC57 vector. Interestingly, the luciferase signal did increase with the decreasing size of the 3′-UTR as shown in (Figure. 2.19). Moreover, with the goal of investigating miRNA regulatory sequences, I tested a 3′-UTR with six target sites to a miRNA (miR-21) highly expressed in HeLa S3 cells, the source of the cell lysates. Surprisingly, this did not show a decrease in the level of luciferase activity, as I would have expected.

From this data, I determined that to simplify the results of the experiments initially, I would characterize my system using a minimal (100 nt) 3′-UTR of random sequence from the pUC57 vector.

Characterizing RNA Restructuring in Cell-Free Extracts

Dual-Assay mRNA Reporter

I had set out to determine the most reproducible reporter construct for characterizing my system. While I investigated the various features outlined above, I predominantly focused on validating the fluorescence-based helicase assay in cell-free extracts using a simple, but physiologically relevant full-length mRNA reporter (Figure 2.20). The reporter contains an m7GTP cap, a globin 5′-UTR, followed by sites for the beacons with attached fluorescent moieties (24 nt Cy3 and 19 nt BHQ), a NanoLuc gene, 100-nt of random pUC57 sequence from our cloning vector as the 3′-UTR, and a 50 nt poly (A) tail.

RNA duplex unwinding in nuclease-treated cell-free extracts is ATP dependent.

To examine the degree of energy-dependent unwinding in cell-free extracts, I measured unwinding in the presence of a non-hydrolysable ATP analogue, adenosine 5′-(β,γ-imido) triphosphate (AMP-PNP). The data indicate that unwinding is clearly arrested in the presence of 10mM AMP-PNP suggesting that this event is a predominantly ATP driven process (Figure 2.21). This suggests that the unwinding kinetics (observed as a change in total fluorescence) is not due to protein binding to the duplex substrate, which would be expected to occur in the presence of AMP-PNP. Consistent with this data, protein synthesis was also found to be inhibited (Figure. 2.21*D*).

RNA duplex unwinding in nuclease-treated cell-free extracts is eIF4A-dependent.

As mentioned, eIF4A is a prototypical member of the DEAD box family of RNA helicases and plays a critical role in translation, through its incorporation into eIF4F.

To establish that the RNA re-structuring I see in my assay is eIF4A-dependent, I used a well-characterized small molecule, hippuristanol [29], to specifically inhibit eIF4A helicase activity in the cell-free extract. As outlined in Figure. 2.22*A*, hippuristanol functions by allosterically binding eIF4A and locking it in a closed (inactive) conformation [29-32], preventing both free eIF4A and eIF4F-bound eIF4A from interacting with RNA [33]. Its binding site is not conserved among other DEAD-box RNA helicases, making it a selective eIF4A inhibitor [30]. To measure the effectiveness of hippuristanol I used the equivalent concentration of the inhibitor solvent (DMSO) for a control. The maximum concentration of hippuristanol I could use was 3 μM in 0.3% DMSO, without the DMSO control having an inhibitory effect on protein synthesis itself (Figure 2.22*E*). Addition of 3 μM hippuristanol resulted in a 35.5% inhibition (p = 0.00742) in the initial rate of duplex unwinding for helicase reactions (Figure 2.22*B-D*). I confirmed the effectiveness of the inhibitor in my cell-free extracts by monitoring translation (Figure 2.22*E*).

Next, I took advantage of a eIF4A mutant (eIF4A R362Q) which is known to exhibit a dominant negative effect on translation. As shown in Figure 2.22*F*, this mutant is thought to function by becoming incorporated into eIF4F but then cannot readily exchange, rendering the complex inactive [34]. In support of my hippuristanol data, this mutant exhibited a dose response dependent inhibition of unwinding, with the highest

concentration of 6μM causing a 36% decrease (p = 0.003201) in the initial rate of duplex unwinding (Figure 2.22*G-I*). Thus, I established that the eIF4A R362Q mutant can efficiently inhibit translation in my luciferase assay (Figure 2.22*J*).

RNA duplex unwinding in nuclease-treated cell-free extracts is eIF4E-dependent.

Human eukaryotic translation initiation factor 4E (eIF4E) binds to the mRNA cap structure and interacts with eIF4G, which serves as a scaffold protein for the assembly of eIF4E and eIF4A to form the eIF4F complex. The eIF4E component of eIF4F is generally considered to be the rate-limiting factor in translation initiation [35]. I decided to investigate the effect of inhibiting eIF4E to rigorously characterize the role of the eIF4F complex in my RNA restructuring assay. It has been shown that substitution of a non-aromatic amino acid for Trp-73 disrupts the ability of eIF4E to interact with eIF4G and 4E-BPs, resulting in a dominant-negative mutant [36, 37]. Thus, I generated the mutant, eIF4E W73L to test in my unwinding assay; mechanism depicted in Figure 2.23*A*. In agreement with my data for eIF4A inhibition, this mutant showed a dose-dependent inhibition of unwinding in my cell-free extracts with the maximum concentration of mutant (2 μM) resulting in a 52% inhibition (p = 0.01411) (Figure 2.23*B-D*). Consistent with these data, eIF4E W73L also inhibited translation in a dose-dependent manner (Figure 2.23*E*).

RNA duplex unwinding in nuclease-treated cell-free extracts is regulated by m7GTP cap but not poly(A) tail.

The synergistic contribution that the poly(A) tail makes to the translation of capped mRNAs (Figure 2.7) is a well-documented phenomenon [14,15]. There has been prior

data supporting that synergy could only be detected after the first-round of translation [27]. However, it has not yet been tested during the early steps of translation. Thus, the mechanistic details of this observation remain unclear. Here, I tested whether we could detect these events in our restructuring assay using the four mRNA constructs outlined previously, with different combinations of cap and poly(A) tail as depicted in Figure 2.24A. The data in Figure 2.24*B-D* shows that the addition of an m7GTP cap provides a significant increase (57% ± SEM, p = 0.000789) in the rate of unwinding while the poly(A) tail does not appear to have a stimulatory effect (9% ± SEM, p = 0.410). By contrast, the luciferase data in Figure 2.7 demonstrates that these cell-free extracts do recapitulate synergy between the m7GTP cap and poly(A) tail.

Discussion of Results

Pervasive RNA structuring has been documented by employing ribonucleases that specifically target single- or double-stranded regions of RNAs, and chemical reagents that covalently modify the RNA base [38]. Existing approaches for evaluating the mechanism of RNA restructuring have been largely limited. The fluorescent-based helicase assay is a unique tool that was pioneered by my lab to monitor the RNA helicase, eIF4A, an essential factor in translation initiation for unwinding RNA secondary structures in the 5' UTR of mRNAs [1]. However, this was characterized using reconstituted proteins and short mRNA templates. Accordingly, my goal was to adapt this assay to monitor duplexes in true cellular conditions using cell free extracts. The fluorescent-based helicase assay in combination with cell-free extract offers a unique method of characterizing the role of specific RNA structures in a true cellular environment [39]. Here, I address how we

redesigned the method to demonstrate the physiological implications of these RNA restructuring events. Specifically, I incorporated a bioluminescent luciferase gene to the mRNA reporter to enable visualization of changes in overall protein abundance, in parallel.

My goal was to first characterize that the unwinding event was an ATP driven process rather than random protein binding. I verified this using the non-hydrolysable ATP analogue (AMP-PNP) which abolished unwinding activity (Figure 2.21). Next, I investigated the role of the RNA helicase, eIF4A, which had been previously studied using a reconstituted system. To do this I supplemented the lysate with a small molecule inhibitor of eIF4AI, hippuristanol [33] and increasing doses of a dominant negative eIF4A mutant (eIF4A R362Q) [34]. The restructuring assay could detect eIF4A inhibition by ~36% by both inhibitors (Figure 2.22*B-D* and *G-I*), however the modifications appeared to have a dramatic inhibitory effect (>90%) on overall protein synthesis (Figure 2.22*E* and *J*).

In support of inhibiting eIF4A, I inhibited another member of the eIF4F complex, eIF4E. This protein binds to the mRNA cap structure and interacts with eIF4G, which serves as a scaffold protein for the assembly of eIF4E and eIF4A to form the eIF4F complex. To inhibit eIF4E, I used a dominant negative eIF4E mutant (eIF4E W73L) which functions by disrupting the ability of eIF4E to interact with eIF4G [36, 37]. In agreement with my data for eIF4A inhibition, this mutant showed a dose-dependent inhibition of unwinding in our cell-free extracts. Curiously, this mutant resulted in a stronger inhibition

of RNA restructuring (52%), and in closer alignment with this data, eIF4E W73L inhibited translation in a dose-dependent manner, with maximal inhibition of ~70% (Figure 2.23). This data raises the question of why the restructuring event was more sensitive to inhibition of eIF4E. One possibility is that the mode of eIF4E inhibition I used prevents the formation of eIF4F on the mRNA. In contrast, eIF4A inhibition is not expected to prevent eIF4F, and possibility even 48S complex formation. It has been shown that the DDX3/ded1p helicase can bind to eIF4G [40]. It is therefore entirely possible that the additional unwinding observed in the eIF4A inhibition experiments is due to DDX3/ded1p or another eIF4G associated helicase. Should eIF4A inhibitors not prevent the formation of the 48S complex, it is also possible that helicases such as DHX29, which binds directly to the 40S subunit [41], may also be responsible for the additional unwinding observed in the eIF4A inhibited experiments compared with the eIF4E inhibited experiments. It is also a possibility that eIF4A R362Q may require multiple recycling events to generate sensitivity to this inhibition, thereby resulting in less inhibition compared to eIF4E inhibition.

To further dissect mechanistic differences in our assay, I examined the role of the m7GTP cap and poly(A) tail modifications. As mentioned, these structures are known to promote synergy of translation over time (Figure 7) [25, 26]. In line with inhibition of eIF4E, the cap binding protein, removal of an m7GTP cap causes a significant increase (57% ± SEM, $p = 0.000789$) in the rate of unwinding while the poly (A) tail does not appear to have a stimulatory effect (9% ± SEM, $p = 0.410$), shown in Figure 2.24. It is interesting that the poly(A) tail did not appear to have an effect. This suggests an alternative model

for inhibition, possibly affecting the recycling step of translation. It would be interesting to study how increasing the length of the poly (A) tail would alter the rates of unwinding and translatability. Also, it is worth acknowledging here the overall disparity between the unwinding effects and translation effects; these inhibitors appeared to impact the translation of mRNA dramatically over time while only modestly altering the helicase activity.

Another clear observation from these data is the clear residual unwinding activity present in each reaction (besides non-hydrolysable ATP analogue). One possibility is that generating the lysate has an artifact of releasing helicases due to the disrupting of the cell architecture. In this case it highlights the limitation of robust unwinding activity in the extracts for use in other experimental work. However, it has been documented that RNA structure is a lot less prevalent *in vivo* [42]. Given we also detect a robust unwinding activity, it is tempting to speculate that alternatively, the residual unwinding in the restructuring assay could be due to other helicases that are dependent and/or independent eIF4F.

Irrespective of the mechanism, this phenomenon underscores that the interpretation of RNA restructuring for translation regulation is more complex than previously thought. The future challenge will be to understand the baseline unwinding activity observed in my assays. As mentioned in the previous chapter, lysate fractionation provides an attractive solution to revealing the helicase responsible for the residual unwinding we observe in the extract. Another possibility to parse out the details of this

mechanism is to apply factor-depleted extracts, which I will discuss more next, in Chapter 3.

Future Directions

In this chapter, I discussed engineering of the dual-assay mRNA reporter and optimization of assay conditions for recapitulating faithful translational regulation and RNA restructuring in the cell free extracts generated from Chapter 1.

I predominantly focused on validating the fluorescence-based helicase assay in cell-free extracts using a simple and physiologically relevant full-length mRNA reporter (Figure 2.20). Going forward it would be interesting to expand the use of my reporter to reconstitute different regulatory events stemming from RNA restructuring by just using different RNA substrates. Of particular interest is understanding how all mRNAs in the cell compete with one another for translational machinery through their efficiency in recruitment to the cap-binding complex, eIF4F, and the 40S subunit. The regulatory elements within the 5' and 3' UTR play critical roles in driving differential rates of protein synthesis [43, 44] but no direct evidence has been obtained to demonstrate the mechanism of these processes. This system lends itself to characterizing the regulation that is harbored in the untranslated regions of mRNAs.

Beyond studying regulatory elements of known mRNAs, another area for future work is to understand the unwinding activities of the 12nt beacon vs the 24nt beacon. This warrants further characterization and may reveal mechanisms by which we can study different RNA helicases in the cell. Moreover, further work is required to monitor different positions of the beacon along the mRNA reporter.

A potential modification to the fluorescent helicase assay itself that could reveal more precise kinetic information is to incorporate rapid mixing technology to reduce the time taken to measure either via stopped-flow or by adapting the cuvette to include a stir bar.

Overall, the information generated from this assay will not only help to describe how helicases remodel nucleic acid secondary structure, but also examine the effects of accessory factors or drugs to evaluate regulatory interactions and perform drug candidate screening. Certain factors of interest include tumor suppressor, PDCD4 and DAP5/p97 for their importance in cancer [45, 46].

References

[1] Özeş AR, Feoktistova K, Avanzino BC, Fraser CS. Duplex unwinding and ATPase activities of the DEAD-box helicase eIF4A are coupled by eIF4G and eIF4B. J Mol Biol. 2011;412:674-87.
[2] Özeş AR, Feoktistova K, Avanzino BC, Baldwin EP, Fraser CS. Real-time fluorescence assays to monitor duplex unwinding and ATPase activities of helicases. Nature Protocols. 2014;9:1645-61.
[3] Avanzino BC, Fuchs G, Fraser CS. Cellular cap-binding protein, eIF4E, promotes picornavirus genome restructuring and translation. Proceedings of the National Academy of Sciences. 2017;114:9611-6.
[4] Feoktistova K, Tuvshintogs E, Do A, Fraser CS. Human eIF4E promotes mRNA restructuring by stimulating eIF4A helicase activity. Proceedings of the National Academy of Sciences. 2013;110:13339-44.
[5] Thoma C, Ostareck-Lederer A, Hentze MW. A poly(A) tail-responsive in vitro system for cap- or IRES-driven translation from HeLa cells. Methods Mol Biol. 2004;257:171-80.
[6] Bergamini G, Preiss T, Hentze MW. Picornavirus IRESes and the poly(A) tail jointly promote cap-independent translation in a mammalian cell-free system. Rna. 2000;6:1781-90.
[7] Hall MP, Unch J, Binkowski BF, Valley MP, Butler BL, Wood MG, et al. Engineered Luciferase Reporter from a Deep Sea Shrimp Utilizing a Novel Imidazopyrazinone Substrate. ACS Chemical Biology. 2012;7:1848-57.
[8] Pleiss JA, Derrick ML, Uhlenbeck OC. T7 RNA polymerase produces 5' end heterogeneity during in vitro transcription from certain templates. RNA (New York, NY). 1998;4:1313-7.
[9] Milligan JF, Groebe DR, Witherell GW, Uhlenbeck OC. Oligoribonucleotide synthesis using T7 RNA polymerase and synthetic DNA templates. Nucleic Acids Res. 1987;15:8783-98.
[10] Nilsen TW, Rio DC, Ares M, Jr. High-yield synthesis of RNA using T7 RNA polymerase and plasmid DNA or oligonucleotide templates. Cold Spring Harb Protoc. 2013;2013.
[11] McCapra F. Chemical mechanisms in bioluminescence. Accounts of Chemical Research. 1976;9:201-8.
[12] Dixon AS, Schwinn MK, Hall MP, Zimmerman K, Otto P, Lubben TH, et al. NanoLuc Complementation Reporter Optimized for Accurate Measurement of Protein Interactions in Cells. ACS Chemical Biology. 2016;11:400-8.
[13] Bernstein P, Peltz SW, Ross J. The poly(A)-poly(A)-binding protein complex is a major determinant of mRNA stability in vitro. Mol Cell Biol. 1989;9:659-70.
[14] Shuman S, Hurwitz J. Mechanism of mRNA capping by vaccinia virus guanylyltransferase: characterization of an enzyme--guanylate intermediate. Proc Natl Acad Sci U S A. 1981;78:187-91.
[15] Gallie DR. The cap and poly(A) tail function synergistically to regulate mRNA translational efficiency. Genes Dev. 1991;5:2108-16.
[16] Gallie DR. A tale of two termini: a functional interaction between the termini of an mRNA is a prerequisite for efficient translation initiation. Gene. 1998;216:1-11.

[17] Tarun SZ, Jr., Sachs AB. A common function for mRNA 5' and 3' ends in translation initiation in yeast. Genes Dev. 1995;9:2997-3007.
[18] Preiss T, Hentze MW. Dual function of the messenger RNA cap structure in poly(A)-tail-promoted translation in yeast. Nature. 1998;392:516-20.
[19] Iizuka N, Najita L, Franzusoff A, Sarnow P. Cap-dependent and cap-independent translation by internal initiation of mRNAs in cell extracts prepared from Saccharomyces cerevisiae. Mol Cell Biol. 1994;14:7322-30.
[20] Gebauer F, Corona DF, Preiss T, Becker PB, Hentze MW. Translational control of dosage compensation in Drosophila by Sex-lethal: cooperative silencing via the 5' and 3' UTRs of msl-2 mRNA is independent of the poly(A) tail. Embo j. 1999;18:6146-54.
[21] Michel YM, Poncet D, Piron M, Kean KM, Borman AM. Cap-Poly(A) synergy in mammalian cell-free extracts. Investigation of the requirements for poly(A)-mediated stimulation of translation initiation. J Biol Chem. 2000;275:32268-76.
[22] Topisirovic I, Svitkin YV, Sonenberg N, Shatkin AJ. Cap and cap-binding proteins in the control of gene expression. Wiley Interdiscip Rev RNA. 2011;2:277-98.
[23] Pichon X, Wilson LA, Stoneley M, Bastide A, King HA, Somers J, et al. RNA binding protein/RNA element interactions and the control of translation. Curr Protein Pept Sci. 2012;13:294-304.
[24] Nuro-Gyina PK, Parvin JD. Roles for SUMO in pre-mRNA processing. Wiley Interdiscip Rev RNA. 2016;7:105-12.
[25] Leppek K, Das R, Barna M. Functional 5' UTR mRNA structures in eukaryotic translation regulation and how to find them. Nat Rev Mol Cell Biol. 2018;19:158-74.
[26] Babendure JR, Babendure JL, Ding J-H, Tsien RY. Control of mammalian translation by mRNA structure near caps. RNA (New York, NY). 2006;12:851-61.
[27] Chen CY, Chen ST, Juan HF, Huang HC. Lengthening of 3'UTR increases with morphological complexity in animal evolution. Bioinformatics. 2012;28:3178-81.
[28] Mayr C. Evolution and Biological Roles of Alternative 3'UTRs. Trends Cell Biol. 2016;26:227-37.
[29] Bordeleau ME, Mori A, Oberer M, Lindqvist L, Chard LS, Higa T, et al. Functional characterization of IRESes by an inhibitor of the RNA helicase eIF4A. Nat Chem Biol. 2006;2:213-20.
[30] Lindqvist L, Oberer M, Reibarkh M, Cencic R, Bordeleau M-E, Vogt E, et al. Selective pharmacological targeting of a DEAD box RNA helicase. PLoS One. 2008;3:e1583-e.
[31] Sun Y, Atas E, Lindqvist LM, Sonenberg N, Pelletier J, Meller A. Single-molecule kinetics of the eukaryotic initiation factor 4AI upon RNA unwinding. Structure. 2014;22:941-8.
[32] Naineni SK, Itoua Maïga R, Cencic R, Putnam AA, Amador LA, Rodriguez AD, et al. A comparative study of small molecules targeting eIF4A. Rna. 2020;26:541-9.
[33] Cencic R, Pelletier J. Hippuristanol - A potent steroid inhibitor of eukaryotic initiation factor 4A. Translation (Austin). 2016;4:e1137381.
[34] Pause A, Méthot N, Svitkin Y, Merrick WC, Sonenberg N. Dominant negative mutants of mammalian translation initiation factor eIF-4A define a critical role for eIF-4F in cap-dependent and cap-independent initiation of translation. Embo j. 1994;13:1205-15.
[35] Duncan R, Milburn SC, Hershey JW. Regulated phosphorylation and low abundance of HeLa cell initiation factor eIF-4F suggest a role in translational control. Heat shock effects on eIF-4F. J Biol Chem. 1987;262:380-8.

[36] Pyronnet S, Imataka H, Gingras AC, Fukunaga R, Hunter T, Sonenberg N. Human eukaryotic translation initiation factor 4G (eIF4G) recruits mnk1 to phosphorylate eIF4E. Embo j. 1999;18:270-9.
[37] Ptushkina M, von der Haar T, Karim MM, Hughes JM, McCarthy JE. Repressor binding to a dorsal regulatory site traps human eIF4E in a high cap-affinity state. Embo j. 1999;18:4068-75.
[38] Ehresmann C, Baudin F, Mougel M, Romby P, Ebel JP, Ehresmann B. Probing the structure of RNAs in solution. Nucleic Acids Res. 1987;15:9109-28.
[39] Tani H, Fujita O, Furuta A, Matsuda Y, Miyata R, Akimitsu N, et al. Real-time monitoring of RNA helicase activity using fluorescence resonance energy transfer in vitro. Biochem Biophys Res Commun. 2010;393:131-6.
[40] Soto-Rifo R, Rubilar PS, Limousin T, de Breyne S, Décimo D, Ohlmann T. DEAD-box protein DDX3 associates with eIF4F to promote translation of selected mRNAs. Embo j. 2012;31:3745-56.
[41] Pisareva VP, Pisarev AV, Komar AA, Hellen CU, Pestova TV. Translation initiation on mammalian mRNAs with structured 5'UTRs requires DExH-box protein DHX29. Cell. 2008;135:1237-50.
[42] Rouskin S, Zubradt M, Washietl S, Kellis M, Weissman JS. Genome-wide probing of RNA structure reveals active unfolding of mRNA structures in vivo. Nature. 2014;505:701-5.
[43] Lasko P. mRNA localization and translational control in Drosophila oogenesis. Cold Spring Harb Perspect Biol. 2012;4:a012294.
[44] Gebauer F, Preiss T, Hentze MW. From cis-regulatory elements to complex RNPs and back. Cold Spring Harb Perspect Biol. 2012;4:a012245.
[45] Ozpolat B, Akar U, Zorrilla-Calancha I, Vivas-Mejia P, Acevedo-Alvarez M, Lopez-Berestein G. Death-associated protein 5 (DAP5/p97/NAT1) contributes to retinoic acid-induced granulocytic differentiation and arsenic trioxide-induced apoptosis in acute promyelocytic leukemia. Apoptosis. 2008;13:915-28.
[46] Matsuhashi S, Manirujjaman M, Hamajima H, Ozaki I. Control Mechanisms of the Tumor Suppressor PDCD4: Expression and Functions. Int J Mol Sci. 2019;20:2304.

CHAPTER 3

Development of factor-depleted HeLa cell-free extracts

This chapter contains unpublished work and was written by me with editing by Dr. Christopher Fraser. All of the experiments were performed by me.

Abstract

This chapter outlines the method by which I generated factor-dependent stable cell lines, using Invitrogen's Flp-in™ T-REx™ system, as previously shown [1]. I successfully modified this approach by using an RNAi system involving optimized targeting [2], and a fluorescent read-out of RNAi expression [3] to track transcription of our gene easily. Furthermore, I was able to adapt these cell lines to liquid suspension culture to produce large-scale factor-depleted extracts

Introduction

Stable cell lines are cells able to express a foreign gene that has been inserted into the cell's genome. These cell lines are considered a powerful system for expressing specific protein products on a production scale and have wide utility in molecular biology. We hypothesized that specific components of the eIF4F complex are required for RNA restructuring in vivo. To test this, I produced stable cell lines expressing shRNAs to reduce the production of individual components, and then tested the activity of lysates derived from these lines using our RNA re-structuring assay. Stable depletion of these components in lysate provides a more targeted approach to asking questions about specific factors in the pathway.

I accomplished this by targeting these factors using shRNAs integrated into inducible stable cell lines generated through Invitrogen's Flp-In™ TREx™ system. The system allows for the generation of stable mammalian cell lines under a tetracycline inducible promoter. This allows tight control over the expression of the gene of interest. This approach has been validated in HeLa cells [1] and I adapted this approach by using an RNAi system; involving optimized targeting [2], and a fluorescent read-out of RNAi expression [3] to easily track transcription. I ultimately check via immunoblotting at different time points following induction for stable depletion of the factor of interest.

Following verification of factor depletion, my goal was to adapt these cell lines to liquid suspension culture to produce large-scale factor-dependent extracts, as outlined in Chapter 1. Extracts enable simple manipulation of mRNA and factors. The aim is to apply

these extracts to study kinetic deficiencies in the pathway. Furthermore, by titrating back in recombinant forms of the complex in wild type or mutant forms, it is possible to reveal the precise role each factor has in directing RNA re-structuring and translation. With this system in place, the same methodology can be applied to generate factor-depleted lysates for any gene of interest. An overview of the system can be found in Figure 3.1.

Experimental Design

Invitrogen's Flp-In™ TREx™ system

These cell lines are created by the integration of a cassette directly into the genome of the cell. This plasmid cassette contains an FRT site that is downstream from the ATG initiation codon of the lacZ-Zeocin fusion protein. This FRT site acts as the binding site for the Flp recombinase that will allow for the stable integration of the gene of interest [4]. Upon transfection of this plasmid, the cells can be selected for by Zeocin and single colonies can be isolated to generate cells with a single integration site in their genome. Once the Flp-in™ T-REx™ host cell line is generated, the gene of interest in the pcDNA5/FRT/TO expression vector can be integrated into the cells. This is done via the Flp recombinase-mediated DNA combination that occurs at the FRT site, which is constitutively expressed in the pOG44 plasmid under the control of the human CMV promoter [4-6]. The pcDNA/FRT/TO plasmid expresses the gene of interest under a tetracycline inducible promoter. It also contains an FRT site and a hygromycin resistance gene in the 5' coding region. Upon successful recombination, the lacZZeocin fusion gene is inactivated and the hygromycin resistance gene will be in frame with the ATG start site. Therefore, cells that have successfully integrated the gene of interest will exhibit resistance to hygromycin and the protein expression can be induced using tetracycline. For more details, see the Flp-In™ T-Rex™ Core Kit manual from Invitrogen.

Construct Design

The parent vector I use for integrating my shRNA target of interest is pcDNA5 FRT/TO. This vector (MOS27 or MOS42; sequences provided in "Plasmid Sequences") has been

adapted to include the following features under the control of the tetracycline inducible promoter:

- ORF: encodes GFP to easily monitor integration of the gene of interest.
- 3′-UTR: encoding flanking features for RNAi targeting; designed to initiate the extraction of the shRNA and deplete my factor of interest [2].
- Optimally placed restriction sites to incorporate the shRNA of interest via unique annealed oligos.

For most of my depletion vectors I used MOS27, however, the flanking restriction sites: HindIII and KpnI were not compatible, which often made cloning difficult. I switched out the KpnI site for BamHI in the vector labelled MOS42. I would recommend re-sequencing this vector as I didn't continue using it once my project shifted away from studying factor depletion.

siRNA Design

The 3′-UTR of the GFP gene integrated into the pcDNA5 FRT/TO vector is designed to form a stem-loop shRNA and target our factor of interest. For best knockdown results, it is recommended to use siRNA designed from previous published work. Otherwise, I have incorporated information given to me by Gabrielle Fuchs (University at Albany) on how to create your own siRNA oligos.

The siDESIGN Center is an advanced, user-friendly siRNA design tool, which significantly improves the likelihood of identifying functional siRNA. For accurate design the program requests a Gene ID number from the NCBI Gene Library. To knockdown a

specific isoform, use the accession number in tandem. It is possible to use their BLAST option or BLAST the individual siRNAs results afterwards. Both options are fine.

The output provides a short summary including information about the transcript you've selected. On the bottom it will display the region targeted, GC content, overall score and whether the siRNA requires a sense modification. If it does, I usually ignore it because it has a hard time determining which strand of the siRNA is the sense/anti-sense strand.

Importantly, identify the nucleotides from the start position and locate this region within the mRNA sequence from transcript targeted (accession number). Count 18 nucleotides down (total length of the targeting sequence is 19), that would be the sense strand. Take the reverse complement for the anti-sense strand. Then add UU to the 3′-end of each strand, those are the siRNA sequences you would get from Dharmacon.

Sense 807 Fwd: ccaagaaguucaugagggaUU

Antisense: ucccucaugaacuucuuggUU

Two capitalized Us on 3′-end are unpaired overhangs in siRNAs. For good siRNAs you want to have a strong 5′-end at the sense strand compared to the as strand. In this example, the sense strand starts with CC, the anti-sense strand with UC, so unwinding should be easier from the 5′-end of the as strand resulting in its incorporation. It is best to identify a couple of potential siRNAs. After, it is recommended to manually blast them again to look more closely at:

- how many transcripts might get targeted
- which transcripts might get targeted

- The likelihood of the transcripts being targeted

Based on the results of that analysis, you can determine which siRNAs to test.

Design and Integration of the shRNA 3'-UTR cassette

Design for efficient siRNA Processing

Once the desired siRNA sequence has been determined and the parent vector is ready, the siRNA sequence will need to be 1) transformed into an shRNA sequence and 2) add additional flanking basal motifs to facilitate efficient factor-depletion. These motifs have been shown to promote siRNA processing from the stem-loop region, enabling de novo design of functional siRNA genes [2]. I have highlighted the motifs employed in the design of my pri shRNA loops (Figure 3.2*A*). Some of these motifs are incorporated into the backbone of the vector and some are incorporated into the oligo design, which will be important to creating new shRNA oligos.

Integration of shRNA to vector

Next, the shRNA sequence will need to be integrated into the vector via annealed oligos. There are several things that are important to include in the design of the annealed oligos to ensure efficient integration. Prior to generating oligos, I plot out the final desired construct to visualize, incorporating the siRNA hairpin and basal motifs. Then I determine which restriction sites I will use to insert the oligos (MOS27; KpnI and HindIII digest, MOS42; BamHI and HindIII digest).

1. Be mindful of the restriction site sticky ends. These will be different for the forward and reverse primers.

2. Basal motifs as indicated in Figure 3.2*A* should always be maintained in their positions.
3. siRNA sequence: the first site (5′-3′) on the forward primer can be inserted exactly as published, the second site on the forward primer is a reverse of the first sequence to form a stem loop. It might be helpful to draw this out to avoid confusion. The reverse primer is simply a reverse complement to the forward primer. Once you're sure the primers will anneal to each other and insert into the vector using the correct sticky ends, then I create the reverse of the "reverse" primer for ordering.
4. Given the oligos will incorporate a duplicate restriction site, it is only recommended to clone the new oligos into the original parent vector (MOS27 or MOS42). I have tried my best to highlight the important sequences and restriction sites needed for oligo design (Figure 3.2*B*-D)
5. A ligase is finally used to incorporate the annealed oligos into the parent vector resulting in an efficient knockdown construct.
6. Finally, check the construct on an agarose to ensure the correct size and send for sequencing to confirm. I've indicated one primer annealing site (PMOS125) for sequencing.

Note: a complete list of constructs generated is provided in Table 5, and siRNA sequences in Table 6.

Development of Stable Factor-Depleted HeLa Cell Lines

Note: Before (or in tandem with) generating stable cell lines it is recommended to transiently transfect the construct of interest to analyze the efficiency of knockdown.

Special Reagents and Equipment

- Corning® Dulbecco's Modification of Eagle's Medium (Product Number: 10-013-CV)
- HyClone™ Newborn Calf Serum (Cytiva: SH30118.03)
- Corning® Penicillin-Streptomycin solution (Product Number: 30-002-CI)
- Gibco™ Fetal Bovine Serum (Catalog number: 10437028)
- Hybri-Max™, sterile-filtered Dimethyl sulfoxide (Sigma Aldrich, D2650)
- HyClone™ Trypan Blue Solution (Cytiva SV30084.01)
- Zeocin® (InvivoGen) 100mg/mL
- Blasticidin (InvivoGen) 10mg/mL
- Hygromycin B Gold (InvivoGen) 100mg/mL
- Corning® PBS (Phosphate Buffered Saline)
- cOmplete™, Mini, EDTA-free Protease Inhibitor Cocktail
- Roche X-tremeGENE™ 9 DNA Transfection Reagent
- Gibco™ Opti-MEM™ Reduced Serum Medium (Catalog number: 31985062)
- Invitrogen™ TRIzol™ Reagent (Catalog number: 15596026)
- pOG44 Flp-Recombinase Expression Vector
- pcDNA™5/FRT/TO Vector
- Hemocytometer or a Bio-Rad cell counter

Preparation for HeLa R19 Stable Transfection

Plasmid Preparation

All plasmid derivatives were verified by sequencing through Quintarabio's sequencing services using a primer designed against the pcDNA5/FRT/TO plasmid. Once verified, each plasmid derivative was transformed into DH5 alpha competent cells and grown overnight at 37 °C in a 6 mL LB culture containing 100 µg/mL Carbenicillin. Both the plasmids containing the gene of interest and the recombinase expression vector (POG44) were then purified using standard Qiagen Miniprep Columns according to the manufacturer's guidelines. The DNA must be completely clean prior to transfection, so all preparation of DNA was done with new miniprep columns as described. It is important to use total DNA volume for transfections between 0.5-5µL. Thus, the mini-preps should ideally be greater than 500ng/ µL for transfection of 1 µg of each vector.

Special note: pOG44 does not express very well. It would be best to prepare this vector by multiple pellets or a maxi prep.

Preparation of HeLa R19 Cells

The stable HeLa cell lines are generated using a HeLa R19 Flp-in™ T-REx™ inducible cells supplied by the lab of Matthias Gromeier [7]. The parent cell line was thawed according to a similar procedure outlined in Chapter 1. By contrast to the HeLa S3 cells, the HeLa R19 cells are an adherent cell line, frozen at a cellular density of ~ $3*10^6$ cells/mL. Once thawed, the cells are centrifuged in ~5mL of DMEM +10% FBS

(D10 media) prior to re-suspending the cells in 10mL of D10 and plating on a T-75 flask. The cells are kept at 37°C with 5% CO_2, and humidity supplied by a water tray in the incubator. After 24 hours, the media is changed to D10 supplemented with 100 µg/mL Zeocin and 10 µg/mL Blasticidin to select for cells containing the Flp-in cassette. Once the plate has reached confluency, the cells were trypsinized using 3 mL of trypsin plus 5 mL of DMEM media (with FBS in the media) to quench the reaction. The cells were then split into a 6-well dish with $0.3*10^6$ cells per well in 3 mL of the D10 media. I always account for a non-transfected control and a pOG44 only control when I calculate how many wells I need.

Stable Transfection of HeLa R19 Cells

Preparation of HeLa R19 Cells for Transfection

1. Before starting, the cells should be 60-70% confluent.
2. In a sterile environment, aliquot enough Opti-MEM media for incubating with DNA in the next section (100 µL per transfection).
3. Prepare a separate mix of Opti-MEM media with 3% FBS in a sterile laminar flow cabinet (1mL per transfection).
4. Remove old media from cells and rinse with PBS.
5. Add 1mL of the Opti-MEM FBS media to the side of each well.
6. Leave sit for 30-minutes.

Preparation of DNA for Transfection

1. Each transfection should contain 1 µg of pOG44, and 1 µg of pcDNA5 FRO/TO vector. This amount may change depending on the size of the gene expressed.
2. For each transfection, 6 µL of X-tremeGENE9 DNA Transfection Reagent (Roche) was diluted in 100 µL of Opti-MEM media. The un-transfected control and a pOG44 only control will still contain reagent mix.
3. Incubate this mix for 10-minutes at room temperature.
4. Aliquot the appropriate amount of DNA in individual tubes specifically for each transfection.
5. Add 106 µL of the Optimem and Xtremegene9 mix to each DNA tube.
6. Incubate this mix for 15-minutes at room temperature.

Transfection of Cells

1. Slowly pipette DNA:lipid complex on to cells drop wise, swirl plates after 2-3 drops
2. Keep in incubator for 4-6hrs
3. Aspirate media and replace with 3mL DMEM (No antibiotics or FBS)
4. Don’t touch for 3 days

Re-plate Cells with Selection Markers

1. Trypsinize cells and re-plate at low density (10-25%) in a 6-well dish using selection medium: D10 media supplemented with 10 µg/mL Blasticidin, and 100 µg/mL Hygromycin. The antibiotics won't work when cells are too confluent.
2. Be careful to fully resuspend cells and break up clumps.

3. Every three days, the media was changed into fresh selection media until colonies appeared.

Selection and Expansion of Stable Cell Lines

1. Cells will begin to die off in 2-3 days. In ~1-2 weeks, nice colonies should become visible.
2. Once the colonies become denser, it may be necessary to trypsinize these cells and place them into a new 6-well plate dish to allow them to grow (otherwise the cells in each colony will become too dense and grow on top of each other.
3. When transfected cells have grown up to 80-90% confluency, wash cells with PBS, Trypsinize, and move them to a T-25 or a T-75 flask.
4. When the cells have recovered and been passaged successfully, perform a Zeocin sensitivity test and tetracycline induction of your gene of interest to test for successful stable cell-line.
5. If this is a new line, you should aim to grow enough cells to freeze them as soon as possible. The freezing protocol is similar to the protocol outlined in Chapter 1, however, since these cells are adherent, they should be frozen at a lower density of ~ $3*10^6$ cells/mL.

Tetracycline Induction Test

Preparation of Stable Cell Lines for Tetracycline Induction

1. Typically, I will grow each test set of cells in 2*15cm cell culture dishes to provide enough cellular material for RNA extraction and western blot.

2. Be careful to plate an even number of cells on each plate to compare the cells later.
3. I will always prepare an extra set of uninduced control set of cells for comparison.
4. It is recommended to conduct a time course of tetracycline induction for new cells to monitor the expression of the gene over time.

Tetracycline Preparation

1. Cells are induced with 0.1-1µg/mL tetracycline.
2. Generate a 0.1µg/µL tetracycline stock but do not dilute lower because it is unstable.
3. Add 10-100µL of 0.1 µg/µL stock for 0.1-1µg/mL.
4. Tetracycline has a 24hr half-life, therefore you will need to add more at a later time for longer time points.

Harvest Tetracycline Induced Stable Cells

1. After 6-72hrs of tetracycline induction, aspirate media, place cells on ice
2. Wash the cells with PBS (~5mL)
3. Remove PBS, re-add 1mL PBS
4. Scrape the cells into PBS
5. Finally, resuspend cells in 3mL PBS in a 5mL test tube and split cells into two 1.5mL microfuge tubes for a) generating lysate for a western blot, and b) conducting an RNA extraction for qPCR analysis.

Analysis of Tetracycline Induced Stable Cells

GFP Analysis of Tetracycline Induced Stable Cells

Since the ORF of my integrated gene encodes GFP it is easy to monitor the integration of the shRNA cassette. Once I have harvested the cells, it is important to ensure that the uninduced and induced cells are equal density for measuring GFP. This can be checked using a cell counter or hemocytometer. Take 10µL of cells resuspended in PBS, and place into one of the wells of a 96-well fluorescence microplate (Perkin-Elmer, OptiPlate-96, Black). I add 90µL of PBS to the well to bring the total volume to 100µL. GFP fluorescence is measured using a Victor X5 Multilabel Plate Reader (Perkin-Elmer). Final results should appear similar to Figure 3.3.

Generating Protein Extracts for Immunoblotting

1. Prepare lysis buffer (20mM HEPES pH 7.5, 50mM KCl, 1mM DTT, 0.5% NP40, 0.5% Triton X-100, and 1X protease Inhibitor cocktail).
2. Spin at 4°C for 2 minutes at 500rcf.
3. Remove PBS from the cells.
4. Re-suspend the cells in 50-500µL of Lysis buffer, depending on the size of pellet
    a. 6-well dish: 30µL, as long as the mix is not too gunky
    b. 10cm plate: 50-100µL
5. Vortex the cells for 10 minutes on and off; 50 seconds on ice, 10 seconds vortex.
6. Spin the cells at 4°C 14000 rpm for 10 minutes.
7. Move the supernatant (lysate) into a new tube.
8. Store lysates at -20°C short term and -80°C long term.

9. Determine the lysate protein concentration using the Bradford Protein Assay before running samples on SDS-PAGE gel for western blot analysis.

Immunoblotting

Equal amounts of lysates were resolved by SDS-PAGE (% depending on size) and transferred onto a nitrocellulose membrane using the Trans-Blot Turbo Transfer System (Bio-Rad). Immunoblots are blocked with 5% (wt/vol) non-fat dry milk for 30 min at room temperature, followed by incubation with primary antibodies diluted in TBST for 1.5 h at room temperature or 4°C overnight. Blots are washed with TBST three times for 10 min, and then incubated for 1 h at room temperature with fluorescently labeled secondary antibodies. Blots are visualized using the Odyssey Infrared Imaging System (Li-Cor). The antibodies and conditions for each western blot varied and are outlined in Table 1.

RNA Extraction for qPCR

1. Spin at 4°C for 2 minutes at 500 rcf.
2. Remove PBS from the cells.
3. In the fume hood, add TRIzol™ Reagent to cells.
    a. 1mL of TRIzol™ to cells from a 10cm plate.
    b. 500µl TRIzol™ reagent to cells from a 60mm plate.
    c. 250µl TRIzol™ to cells from a 6-well plate.
4. Invert tube several times to mix.
5. Can freeze at -20C to store at this point or continue to the next steps.

6. In the fume hood, add 0.2 volumes of Chloroform to each sample. Vortex for 10 seconds until the sample is pink like pepto-bismol.
7. Incubate the mix at room temperature 2-3 minutes.
8. Centrifuge 12,000rcf at 4°C for 15 minutes and remove top aqueous layer, but don't touch white interphase.
9. Add 0.5 volume (of original TRIzol™ volume) isopropanol (100%).
10. Vortex and incubate at room temperature for 10 minutes. Then, spin 12,000rcf for 10 minutes at 4°C.
11. Resuspend in 100µl water. Add 0.1 volume of 3M NaOAc pH 5.2 (20µl) or 0.3 volume of 7.5M NH4OAc. Then add 2.5x volumes of 100% ethanol (prechilled), vortex and precipitate -80°C for 1 hr.
12. Spin at max speed (20,000rcf) for 15 minutes at 4°C.
13. Decant supernatant, resuspend pellet in 500µl of 70% ethanol.
14. Spin 20,000rcf for 5 minutes at 4°C.
15. Decant, leave tube upside down on paper towel to dry pellet.
16. Resuspend pellet in 30µl RNase free water.
17. Measure the absorbance using the Nanodrop. A260/280 for pure RNA is 2.0, for DNA 1.8.
18. For RT-qPCR, the purified RNA must be DNaseI treated prior to cDNA Synthesis by M-MLV reverse transcriptase.

RT-qPCR Primer Design

Exon Selection

The primers for qPCR are designed based off genomic data from the UCSC genome browser. It is important to design the primers over two exons in order to be able to discriminate DNA from RNA in the qPCR run.

1. Select the genome: Human h19.
2. Type the gene of interest into search bar of genome (H19) and wait until they give you suggestion for gene name.
3. Select to design the primers between two exons with mostly no variants in between the exons (should be fine) and covering all alternative transcripts.
4. Take note of the two exon numbers you are using.
5. Click on main gene highlighted with a black outline and view genomic sequence.
6. Make sure the exons are selected, and are shown in upper case while everything else is in lower case.
7. Copy and paste the sequence into a Word document.
8. Find the two exons you are choosing to amplify from on the document by counting.

Primer Design

Using the two exonic sequences from the UCSC genome browser, you will want to design two appropriate qPCR primers. This is done using the program Primer3

1. Copy and paste the first exon sequence (Forward primer) into Primer 3.
2. Click design left primer, unclick design right primer.

3. Make sure Primer size = 20bps, and Primer Tm = 60°C.
4. Submit. Note the Tm to make sure it is within 1-2 °C of the other primer.
5. Take note of the 5'-3' sequence given, this will be the actual primer you will order, not the region in the genome. Shown below is the region is amplified and primer annealing is indicated.
6. Copy and paste the second exon sequence (Reverse primer).
7. Click design right primer, unclick left primer.
8. Use the same parameters as above.
9. The product size range for the primers should be 90-150. Check where primers anneal from the word document with the genomic sequence by deleting the intronic region. This will allow you to figure out the size of the amplification fragment. If the size is greater than 150 redesign using different exons.

qPCR Primer Validation

To ensure that the primers anneal to your DNA you should validate the primers by performing a qPCR standard curve. Set up qPCR reactions to amplify different amounts of the same DNA sample. Efficient primers will result in a proportional dose-response curve.

1. Dilute primers in 100µL of H_2O.
2. Measure 1µL on nano-drop: Take note of A260 reading.
3. Determine molarity using the A260 and the extinction coefficient on data specification sheet.
4. Calculate remaining volume of H_2O to add to dilute the primers to 100µM.

5. If too dilute, reduce to 50uM and make 10uM accordingly but be very careful to take note on the primer stocks.
6. Dilute cDNA or whole genomic DNA 100ng/µL.
7. Measure OD to ensure DNA is at 100ng/uL, and re-dilute to 10ng/µL.
8. Serial dilute the 10ng/µL stock to 1ng/µL, 0.1ng/µL, 0.01ng/µL If using plasmid, will need to use much less DNA: 10pg/µL - 0.01pg/µL.
9. Be sure to incorporate a negative control.
10. Set up triplicates of each reaction (Total volume: 20 µL):
    a. 5µL cDNA or whole genomic DNA (10ng/µL 1ng/µL, 0.1ng/µL, 0.01ng/µL).
    b. 1µL of forward primer (10µM).
    c. 1µL of reverse primer (10µM).
    d. 3µL of H_2O.
    e. 10µL of 2X Biorad SYBR green (light-sensitive).
11. Load the plate and seal with plastic covering. Spin down the plate if possible.
12. Set up qPCR machine to run validation of primers.
13. Some qPCR software have an application to analyze your standard curve from the cycle threshold (Ct) data. It generates the curve and calculates the efficiency of the reaction. Alternatively, see qPCR Data Analysis below.
14. Acceptable ranges are between 90 and 110% with a slope of the curve around -3.3 for an efficiency of 100%. The R^2 of the curve should be > 0.99 to provide a good confidence within the correlation.

Note: A complete list of qPCR primers generated is provided in Table 7.

qPCR to Analyze Factor (RNA) Depletion

1. When measuring the amount of RNA for depleting your gene of interest, it is important to also monitor a control gene in parallel (such as Actin) for a total of four sets of reactions:
    a. the housekeeping gene: control (un-induced) and experimental (tetracycline induced) conditions.
    b. the gene of interest: control (un-induced) and experimental (tetracycline induced) conditions.
2. Always measure qPCR reactions in duplicates (Total volume: 20 µL):
    a. 5µL cDNA or whole genomic DNA (10ng/µL 1ng/µL, 0.1ng/µL, 0.01ng/µL).
    b. 1µL of forward primer 10µM.
    c. 1µL of reverse primer 10µM.
    d. 3µL of H_2O.
    e. 10µL of 2X Bio-Rad SYBR green (light-sensitive).

qPCR Data Analysis

The qPCR output is in terms of the cycle threshold (Ct) which is defined as the number of cycles required for the fluorescent signal to cross the threshold (i.e. exceeds background level). Ct levels are inversely proportional to the amount of target nucleic acid in the sample (i.e. the lower the Ct level the greater the amount of target nucleic acid in the sample).

- Cts < 29 are strong positive reactions indicative of abundant target nucleic acid in the sample.
- Cts of 30-37 are positive reactions indicative of moderate amounts of target nucleic acid.
- Cts of 38-40 are weak reactions indicative of minimal amounts of target nucleic acid.

Output should include qPCR Ct values (raw data) for:

- the housekeeping gene: control and experimental conditions.
- the gene of interest: control and experimental conditions.

1. With the Ct data in hand, you will need to average the replicates prior to quantifying the amount of RNA. Take the average of the Ct values for the housekeeping gene and the gene being tested in the experimental and control conditions, returning 4 values. The 4 values are Gene being Tested Experimental (TE), Gene being Tested Control (TC), Housekeeping Gene Experimental (HE), and Housekeeping Gene Control (HC).
2. Next, calculate the differences between experimental values (TE – HE) and the control values (TC – HC). These are your ΔCt values for the experimental ΔCTE) and control (ΔCTC) conditions, respectively.
3. Then, calculate the difference between the ΔCT values for the experimental and the control conditions (ΔCTE – ΔCTC) to arrive at the double delta Ct value (ΔΔCt).

4. Since all calculations are in logarithm base 2, every time there is twice as much DNA, your Ct values decrease by 1 and will not halve. You need to calculate the value of 2^(-2ΔΔCt) to determine the expression fold change.
5. This value is the fold change of your gene of interest in the test condition, relative to the control condition, which has all been normalized to your housekeeping gene.

Adaptation of Stable Factor-Depleted HeLa R19 Cells to Suspension Culture

HeLa R19 Flp-in T-Rex cell lines are an adherent cell line that are typically grown on plates. Following verification of factor depletion, my goal was to adapt these cell lines to liquid suspension culture to produce large scale factor-dependent extracts, as outlined in Chapter 1. The aim is to apply these extracts to study kinetic deficiencies in the pathway and shed light on the precise role each factor has in directing RNA re-structuring and translation. Due to their nature as adherent cells, the HeLa R19 cell lines tend to have very low survival rates in suspension culture. I have adapted the protocol to successfully grow the HeLa R19 cells in liquid suspension culture.

Adjust Cells to RPMI Media

The adaptation of adherent cells to suspension causes a tendency of the cells to adhere to other cells, resulting in large clumps of aggregated cells. The presence of divalent cation in the DMEM media could facilitate this aggregation of cells. DMEM media contains a high concentration of calcium (1.8 mM) and lower phosphate (1 mM) compared to RPMI media, which contains 0.8 mM calcium and 5 mM phosphate [8]. To mitigate the

aggregation of cells, I first adapted all cells to grow in RPMI media rather than DMEM media.

1. Thaw adherent cell line into DMEM+10% FBS and plate on a T-75 flask.
2. Once cells have adhered (~24 hours), add 100µg/mL Hygromycin and 10µg/mL Blasticidin.
3. Once sufficiently confluent, cells can be split into 4*10cm plates in RPMI+10% FBS + 100µg/mL Hygromycin and 10µg/mL Blasticidin.
4. Once these cells are 90% confluent, split in to 8*15cm plates RPMI+10% FBS + 100µg/mL Hygromycin and 10µg/mL Blasticidin.

Adapt Cells to Suspension Growth

Important Notes

- Keep cells in 10% FBS until reach 500mL.
- 1X Pen strep added in all stages of suspension growth.
- Make sure FBS and NCS are high quality.

Starter Culture Flask Options

- 3*100mL sized flasks (50mL total volume per flask).
- 1*250mL flask with 150mL cells.

*Note: Using 3*100mL may increase your chances of success if cells in one flask die at the beginning*

1. Trypsinize cells from 15cm plates (5mL of trypsin per plate, quench with 7mL of RPMI media).
2. Spin down at 200rcf for 5 minutes.
3. Re-suspend in 40mL RPMI+10% FBS and count cells.
4. Aim to seed cells at 0.4-0.5 million cells /mL in RPMI+10% FBS + 100µg/mL Hygromycin and 10µg/mL Blasticidin. See “Starter Flask Options” to determine which flask to seed cells.

Scaling-up Volume of Adapted Cells

1. After the first 2 days, it is important to spin all cells at 200rcf for 5 minutes and re-suspend all cells in fresh RPMI+10% FBS + 100ug/mL Hygromycin and 10ug/mL Blasticidin.
2. Re-seed at 0.5million/mL in either:
    - 2*250mL flasks with 100mL.
    - 1*1L flask with 300-400mL.
3. Once the cells have doubled, split back to 0.5million/mL. At this point they should be over 500mL, so switch to RPMI 2.5% FBS + NCS 2.5% + 1X Pen Strep + 100µg/mL Hygromycin and 10µg/mL Blasticidin.

Note: Cells grew well in 3% FBS and 2% NCS but were growing poorly in 5% NCS with no FBS supplementations

4. Once at 0.7million/mL split cells 1:2 into a 4L flask, using max 2L. At this time, cells should be preserved by freezing prior to making lysates. See freezing protocol in Chapter 1.

Tetracycline Induction

As before, it is important to maintain an uninduced and an induced flask, ensuring the densities are equal at all times. Moreover, it is important to conduct a tetracycline time course to determine depletion of the gene of interest. To induce cells, add 200uL Tetracycline (0.1µg/mL) every 24hrs to 2L of induced cells for the duration of the time course. When ready to prepare cells for generating lysate, refer to protocols outlined in Chapter 1.

Note: The HeLa R19 cells are larger and more dense than HeLa S3 cells so an increased volume of lysis buffer will be required to achieve a final concentration between 30-50mg/mL.

Preparing Cells for Analysis

1. For downstream analysis, harvest 16 million (live) cells of each flask. It is imperative to count the cells and ensure both flasks are at equal density.
2. Spin at 200rcf for 5min in a 50mL falcon tube.
3. Re-suspend in 2mL PBS (Final concentration = 8 million/mL).
4. Continue as above with adherent cell lines.

shRNA Knockdown Constructs

Here, I applied this tool to stably deplete factors hypothesized to be involved in RNA restructuring in vivo using my RNA restructuring assay i.e., the eIF4F complex and associated factors to rigorously characterize their functional role. The list of successful factor-dependent cell lines generated are outlined in Table 5. In summary, I generated adherent lines targeting eIF4E (MOS28 and MOS29), eIF4B (MOS32), DDX3 (MOS35), eIF4G (MOS33), and adapted the eIF4B and eIF4G targeted lines to suspension culture. In addition, I designed constructs to deplete eIF4AI, eIF4AII, DDX6, and a construct incorporating a generic siRNA scramble sequence as a negative control. The plasmids sequences for constructs generated are supplied in the section “Plasmid Sequences of shRNA Factor-Depletion Vectors”.

Non-targeting siRNA Control

It is important to include a generic siRNA scramble sequence as a negative control for RNAi experiments. Non-targeting siRNAs control for non-specific effects related to siRNA delivery to provide a baseline for target gene silencing. Here, I designed two constructs incorporating negative-control sequences provided by Gabrielle Fuchs. These constructs have not been successfully cloned yet.

Dharmacon negative-control siRNA#3 [30]

sense strand: 5′-AUGUAUUGGCCUGUAUUAGUU

antisense strand: 5′-CUAAUACAGGCCAAUACAUUU

siGL2 luciferase siRNA [31]

sense strand: 5′-UCG AAG UAU UCC GCG UAC GUU-3′

antisense strand: 5′-CGU ACG CGG AAU ACU UCG AUU-3′

Eukaryotic Initiation Factor 4E (eIF4E)

Human eukaryotic translation initiation factor 4E (eIF4E) binds to the mRNA cap structure and interacts with eIF4G, which serves as a scaffold protein for the assembly of eIF4E and eIF4A to form the eIF4F complex. The eIF4E component of eIF4F is generally considered to be the rate limiting factor in translation initiation [9].

Here, I tested integration of two constructs incorporating two different siRNA sequence (MOS28; si4E1 and MOS29; si4E2). After generation of the stable cell lines, I induced expression by 0.1µg/mL tetracycline for 48 hours, confirming successful integration of the construct by GFP analysis. The depletion of protein by each construct was measured by immunoblotting for eIF4E and Actin (Figure 3.4). In the western blot the construct MOS28 (sh4E1) appeared to have modest depletion but it was not clear due to non-specificity of the antibody (Santa Cruz Biotechnologies; sc-9976) whether there was efficient depletion of the protein; only mentioned as a caution for the use of this antibody. I continued investigating this depletion construct using a newer antibody (BD Biosciences; 61029) and fortunately could discern the protein from the immunoblot, however, it only appeared to deplete the protein ~40-60% (Figure 3.5 *A,B*). This result was substantiated by qPCR results of the eIF4E mRNA depletion indicating a ~40% reduction in mRNA at 72-hrs (data not shown). Both cell lines were frozen in liquid nitrogen. Another construct with a third siRNA sequence was generated in tandem (MOS38) but not tested yet.

Eukaryotic Initiation Factor 4G (eIF4G)

The largest component of the mammalian eIF4F complex is the 175 kDa protein eIF4G [10-15]. eIF4G acts as a molecular scaffold that recruits and coordinates the activities of these other initiation components. In addition to stabilizing these interactions, mammalian eIF4G has 2 additional pivotal roles in mRNA recruitment to the ribosome. Through its direct interaction with eIF3, eIF4G helps bridge the eIF4F-mRNA complex and the 43S preinitiation complex (PIC) [16-18]. Additionally, its interaction with the DEAD box helicase eIF4A is required to recruit this helicase to the mRNA, which ultimately functions to unwind secondary structures located in the 5′UTR to facilitate ribosome recruitment and scanning [19, 20].

Here, I tested integration of a construct incorporating a previously verified efficient siRNA sequence (MOS33; si4G31) [21]. After generation of the stable cell lines, I induced expression by 0.1µg/mL tetracycline for 72 hours, confirming successful integration of the construct by GFP analysis. The depletion of protein by each construct was measured by immunoblotting for eIF4G and Actin; it demonstrated 55-80% reduction in eIF4G (Figure 3.6). The adherent cell line was both frozen and adapted to suspension culture. Following a tetracycline induction time-course (6-72 hrs), eIF4G was re-analyzed by western blot and displayed a maximum ~80% reduction in protein (Figure 3.7). This cell line was frozen in liquid nitrogen. The tetracycline induced cells were taken through the lysate generation process for continued testing in my assays. I tested the translatability of the eIF4G depletion lysate in combination with titrations of the recombinant eIF4G$_{557\text{-}1699}$; however, not only did the results not demonstrate any significant changes with the titration of

protein, but the depleted lysate displayed increased luciferase activity compared to the control lysate (Figure 3.8). I would suggest that these data are further explored in the future. Additionally, given these experiments were conducted in a nuclease-treated extract, it would be worth investigating in an untreated extract environment.

Eukaryotic Initiation Factor 4B (eIF4B)

eIF4B is an RNA binding protein involved in the regulation of the initiation stage of protein synthesis. This protein is critical for the recruitment of the mRNA to the ribosome. It helps unwind secondary structures in the mRNA to allow ribosome scanning, via enhancing the duplex unwinding activity of the DEAD box helicase eIF4A [20, 22].

Here, I tested integration of a construct incorporating siRNA sequence from my siDESIGN protocol (MOS32; si4B1). After generation of the stable cell lines, I induced expression by 0.1µg/mL tetracycline for 72 hours, confirming successful integration of the construct by GFP analysis. The depletion of protein by each construct was measured by immunoblotting for eIF4B and Actin; it demonstrated 60-80% reduction in eIF4B (Figure 3.6). The adherent cell line was both frozen and adapted to suspension culture. Following a tetracycline induction time-course, 6-72eIF4B was re-analyzed by western blot and displayed a maximum ~70% reduction in protein (Figure 3.9). This cell line was frozen in liquid nitrogen. The tetracycline induced cells were taken through the lysate generation process for continued testing in my assays. I tested the translatability of the eIF4B depletion lysate in combination with an mRNA reporter containing a CDC25C 5′UTR, a sequence that has shown to be sensitive to eIF4B levels [23]. Unexpectedly the results did not demonstrate any significant changes to a control lysate, even when

supplemented with recombinant eIF4B [19] (75nM - 1200nM) as shown in Figure 3.10. However, it is important to note that these experiments were conducted in a nuclease-treated extract and it would be worth testing in an untreated extract environment.

DEAD-box RNA Helicase 3 (DDX3)

DDX3 and its essential yeast homolog, Ded1, have ATP-dependent RNA helicase activity [24]. Among the reported roles for Ded1 in yeast, the most compelling evidence exists for a direct role in translation initiation. In particular, Ded1 is present in the cytoplasm and is required for translation *in vitro* [25] and *in vivo* [26]. Ded1 also interacts genetically with several translation initiation factors, including the well-known DEAD box RNA helicase eIF4A and the cap-binding protein eIF4E [25, 27, 28]. Additional studies have led to the model that Ded1 is required, in addition to eIF4A, for unwinding RNA during scanning for the translation initiation codon [29].

Here I generated two constructs to deplete DDX3 using oligos siDDX3-1 (MOS34) and siDDX3-2 (MOS35). The cell transfections with the MOS35 successfully generated stable lines. Upon measuring the depletion of DDX3 it was discovered that knockdown was not convincing based on the two amounts of protein loaded (Figure 3.11), and therefore should not be considered efficiently depleted. Going forward I would continue with transfections of the alternate construct, MOS34.

Eukaryotic Initiation Factor 4A (eIF4AI and eIF4AII)

eIF4A is the ATP-dependent RNA helicase which is a subunit of the eIF4F complex involved in cap recognition and is required for mRNA binding to ribosome. In the current

model of translation initiation, eIF4A unwinds RNA secondary structures in the 5'UTR of mRNAs which is necessary to allow efficient binding of the small ribosomal subunit, and subsequent scanning for the initiator codon. eIF4A has two isoforms (eIF4AI and eIF4AII) which are highly conserved (~95% amino acid similarity), and thought to be functionally interchangeable [32].

Here I aimed to deplete each isoform by designing unique oligos to deplete each factor. The construct designed for depleting eIF4AI was based on the siRNA sequence provided by Thermo Fisher (seq s4567; si4AI-1) [33]. The clone has been frozen as MOS36 with no further studies.

For eIF4AII, the siRNA sequence was provided by Ambion Silencer (seq s4571; si4AII-1), however, this has not been successfully incorporated into the parent vector yet. The remaining steps for generating eIF4AII depletion vector: ligate parent vector (MOS42) digested with HindIII and BamHI to phosphorylated annealed oligos: PMOS130 and PMOS131).

DEAD-Box Helicase 6 (DDX6)

Given the propensity of the RNA restructuring assay to monitor ATP-dependent winding, I sought to deplete other known helicases in the cell to investigate the effect on our restructuring assay in cell-free extract. DDX6 is a conserved DEAD-box protein (DBP) that plays central roles in cytoplasmic RNA regulation, including processing body (P-body) assembly, mRNA decapping, and translational repression [34].

I chose two siRNA sequences (siDDX6-1 and siDDX6-2), then designed annealed oligos (PMOS111:PMOS112 for siDDX6-1, and PMOS113:PMOS114 for siDDX6-2) to

generate the final vector, however, these have not been successfully incorporated into the parent vector (MOS27) yet.

Future Directions

This chapter outlines the method by which I generated factor-dependent stable cell lines, using Invitrogen's Flp-in™ T-REx™ system, as previously shown [36]. I successfully modified this approach by using an RNAi system involving optimized targeting [37], and a fluorescent read-out of RNAi expression [38] to track transcription of our gene easily. Furthermore, I was able to adapt these cell lines to liquid suspension culture to produce large scale factor-dependent extracts.

Here, I applied this tool to stably deplete factors hypothesized to be involved in our RNA restructuring assay. The goal was to verify the importance of identified factors by adding back purified recombinant proteins in wild-type, or mutant forms to more precisely understand their role.

I first targeted the eIF4F complex and associated factors to aim to understand the residual unwinding activity observed in my restructuring assay. I characterized eIF4B and eIF4G depletion lines which displayed ~70-80% reduction in protein. However, unexpectedly these extracts did not demonstrate an increased dependence on the factor in my translation assays. It is possible that with optimized translation conditions, these experiments could reveal increased dependency as expected. In the future, another possibility for factor-depletion of factors thought to be involved in RNA restructuring is to adapt the auxin-inducible degron system [35] for rapid and controlled protein depletion.

References

[1] Rakotondrafara AM, Hentze MW. An efficient factor-depleted mammalian in vitro translation system. Nat Protoc. 2011;6:563-71.
[2] Fang W, Bartel DP. The Menu of Features that Define Primary MicroRNAs and Enable De Novo Design of MicroRNA Genes. Mol Cell. 2015;60:131-45.
[3] Santagata S, Mendillo ML, Tang YC, Subramanian A, Perley CC, Roche SP, et al. Tight coordination of protein translation and HSF1 activation supports the anabolic malignant state. Science. 2013;341:1238303.
[4] O'Gorman S, Fox DT, Wahl GM. Recombinase-mediated gene activation and site-specific integration in mammalian cells. Science. 1991;251:1351-5.
[5] Broach JR, Guarascio VR, Jayaram M. Recombination within the yeast plasmid 2mu circle is site-specific. Cell. 1982;29:227-34.
[6] Buchholz F, Ringrose L, Angrand PO, Rossi F, Stewart AF. Different thermostabilities of FLP and Cre recombinases: implications for applied site-specific recombination. Nucleic Acids Res. 1996;24:4256-62.
[7] Kaiser C, Dobrikova EY, Bradrick SS, Shveygert M, Herbert JT, Gromeier M. Activation of cap-independent translation by variant eukaryotic initiation factor 4G in vivo. Rna. 2008;14:2170-82.
[8] Wu X, Lin M, Li Y, Zhao X, Yan F. Effects of DMEM and RPMI 1640 on the biological behavior of dog periosteum-derived cells. Cytotechnology. 2009;59:103-11.
[9] Duncan R, Milburn SC, Hershey JW. Regulated phosphorylation and low abundance of HeLa cell initiation factor eIF-4F suggest a role in translational control. Heat shock effects on eIF-4F. J Biol Chem. 1987;262:380-8.
[10] Marcotrigiano J, Gingras AC, Sonenberg N, Burley SK. Cap-dependent translation initiation in eukaryotes is regulated by a molecular mimic of eIF4G. Mol Cell. 1999;3:707-16.
[11] Hentze MW. eIF4G: a multipurpose ribosome adapter? Science. 1997;275:500-1.
[12] Imataka H, Gradi A, Sonenberg N. A newly identified N-terminal amino acid sequence of human eIF4G binds poly(A)-binding protein and functions in poly(A)-dependent translation. Embo j. 1998;17:7480-9.
[13] Keiper BD, Gan W, Rhoads RE. Protein synthesis initiation factor 4G. Int J Biochem Cell Biol. 1999;31:37-41.
[14] Prévôt D, Darlix JL, Ohlmann T. Conducting the initiation of protein synthesis: the role of eIF4G. Biol Cell. 2003;95:141-56.
[15] Yan R, Rychlik W, Etchison D, Rhoads RE. Amino acid sequence of the human protein synthesis initiation factor eIF-4 gamma. J Biol Chem. 1992;267:23226-31.
[16] Villa N, Do A, Hershey JW, Fraser CS. Human eukaryotic initiation factor 4G (eIF4G) protein binds to eIF3c, -d, and -e to promote mRNA recruitment to the ribosome. J Biol Chem. 2013;288:32932-40.
[17] Hinton TM, Coldwell MJ, Carpenter GA, Morley SJ, Pain VM. Functional analysis of individual binding activities of the scaffold protein eIF4G. J Biol Chem. 2007;282:1695-708.
[18] Lamphear BJ, Kirchweger R, Skern T, Rhoads RE. Mapping of functional domains in eukaryotic protein synthesis initiation factor 4G (eIF4G) with picornaviral proteases.

Implications for cap-dependent and cap-independent translational initiation. J Biol Chem. 1995;270:21975-83.
[19] Feoktistova K, Tuvshintogs E, Do A, Fraser CS. Human eIF4E promotes mRNA restructuring by stimulating eIF4A helicase activity. Proceedings of the National Academy of Sciences. 2013;110:13339-44.
[20] Özeş AR, Feoktistova K, Avanzino BC, Fraser CS. Duplex unwinding and ATPase activities of the DEAD-box helicase eIF4A are coupled by eIF4G and eIF4B. J Mol Biol. 2011;412:674-87.
[21] Coldwell MJ, Morley SJ. Specific isoforms of translation initiation factor 4GI show differences in translational activity. Mol Cell Biol. 2006;26:8448-60.
[22] García-García C, Frieda KL, Feoktistova K, Fraser CS, Block SM. RNA BIOCHEMISTRY. Factor-dependent processivity in human eIF4A DEAD-box helicase. Science (New York, NY). 2015;348:1486-8.
[23] Shahbazian D, Parsyan A, Petroulakis E, Topisirovic I, Martineau Y, Gibbs BF, et al. Control of cell survival and proliferation by mammalian eukaryotic initiation factor 4B. Molecular and cellular biology. 2010;30:1478-85.
[24] Iost I, Dreyfus M, Linder P. Ded1p, a DEAD-box protein required for translation initiation in Saccharomyces cerevisiae, is an RNA helicase. J Biol Chem. 1999;274:17677-83.
[25] Chuang RY, Weaver PL, Liu Z, Chang TH. Requirement of the DEAD-Box protein ded1p for messenger RNA translation. Science. 1997;275:1468-71.
[26] Beckham C, Hilliker A, Cziko AM, Noueiry A, Ramaswami M, Parker R. The DEAD-box RNA helicase Ded1p affects and accumulates in Saccharomyces cerevisiae P-bodies. Mol Biol Cell. 2008;19:984-93.
[27] Linder P. Yeast RNA helicases of the DEAD-box family involved in translation initiation. Biol Cell. 2003;95:157-67.
[28] de la Cruz J, Iost I, Kressler D, Linder P. The p20 and Ded1 proteins have antagonistic roles in eIF4E-dependent translation in Saccharomyces cerevisiae. Proc Natl Acad Sci U S A. 1997;94:5201-6.
[29] Marsden S, Nardelli M, Linder P, McCarthy JE. Unwinding single RNA molecules using helicases involved in eukaryotic translation initiation. J Mol Biol. 2006;361:327-35.
[30] Wehner KA, Schütz S, Sarnow P. OGFOD1, a novel modulator of eukaryotic translation initiation factor 2alpha phosphorylation and the cellular response to stress. Mol Cell Biol. 2010;30:2006-16.
[31] Machlin ES, Sarnow P, Sagan SM. Masking the 5' terminal nucleotides of the hepatitis C virus genome by an unconventional microRNA-target RNA complex. Proc Natl Acad Sci U S A. 2011;108:3193-8.
[32] Yoder-Hill J, Pause A, Sonenberg N, Merrick WC. The p46 subunit of eukaryotic initiation factor (eIF)-4F exchanges with eIF-4A. J Biol Chem. 1993;268:5566-73.
[33] Meijer HA, Kong YW, Lu WT, Wilczynska A, Spriggs RV, Robinson SW, et al. Translational repression and eIF4A2 activity are critical for microRNA-mediated gene regulation. Science. 2013;340:82-5.
[34] Huang J-H, Ku W-C, Chen Y-C, Chang Y-L, Chu C-Y. Dual mechanisms regulate the nucleocytoplasmic localization of human DDX6. Scientific Reports. 2017;7:42853.

[35] Li S, Prasanna X, Salo VT, Vattulainen I, Ikonen E. An efficient auxin-inducible degron system with low basal degradation in human cells. Nature Methods. 2019;16:866-9.

Figures Tables and Legends

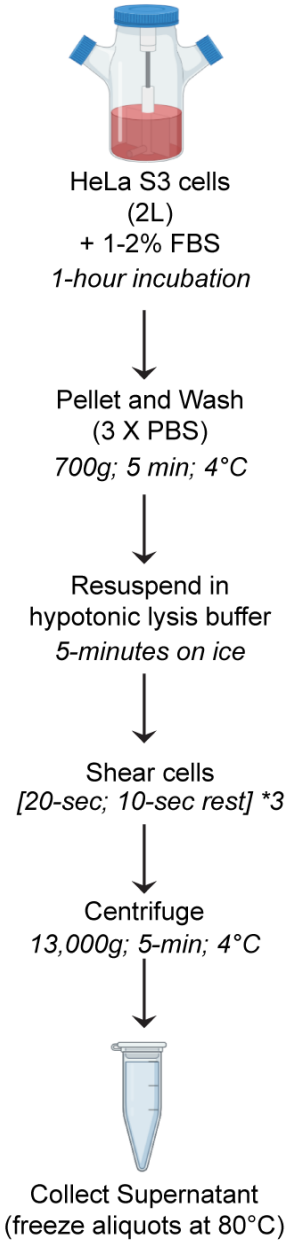

Figure 1.1 Schematic of the Preparation of Translation Competent Extracts from HeLa Cells

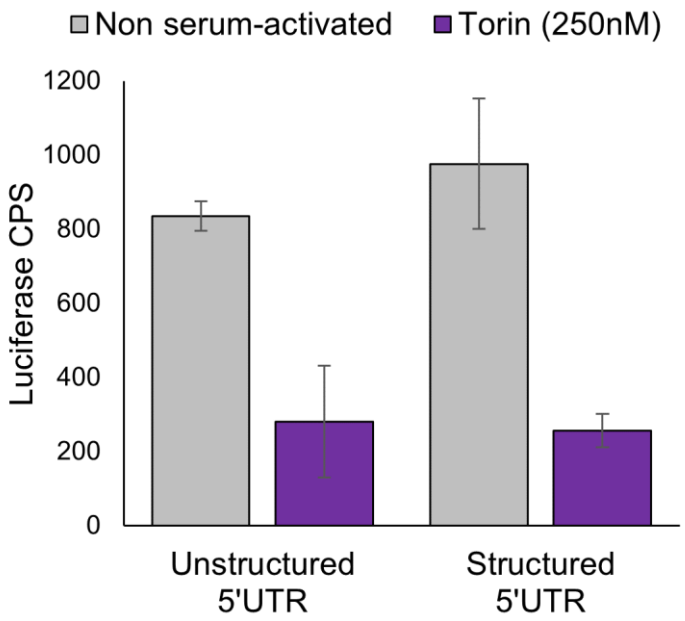

Figure 1.2 Effect of Torin Treatment on mRNAs with varying 5′UTR structure

HeLa S3 suspension cells response to treatment with the mTOR inhibitor Torin. The mRNAs tested contained 5′UTRs with varying levels of structure; unstructured (CAA repeats) or structured (containing a -25.1 kcal/mol hairpin hairpin at the +4 position, CCACCACGGCCGATATCACGGCCGTGGTGG).

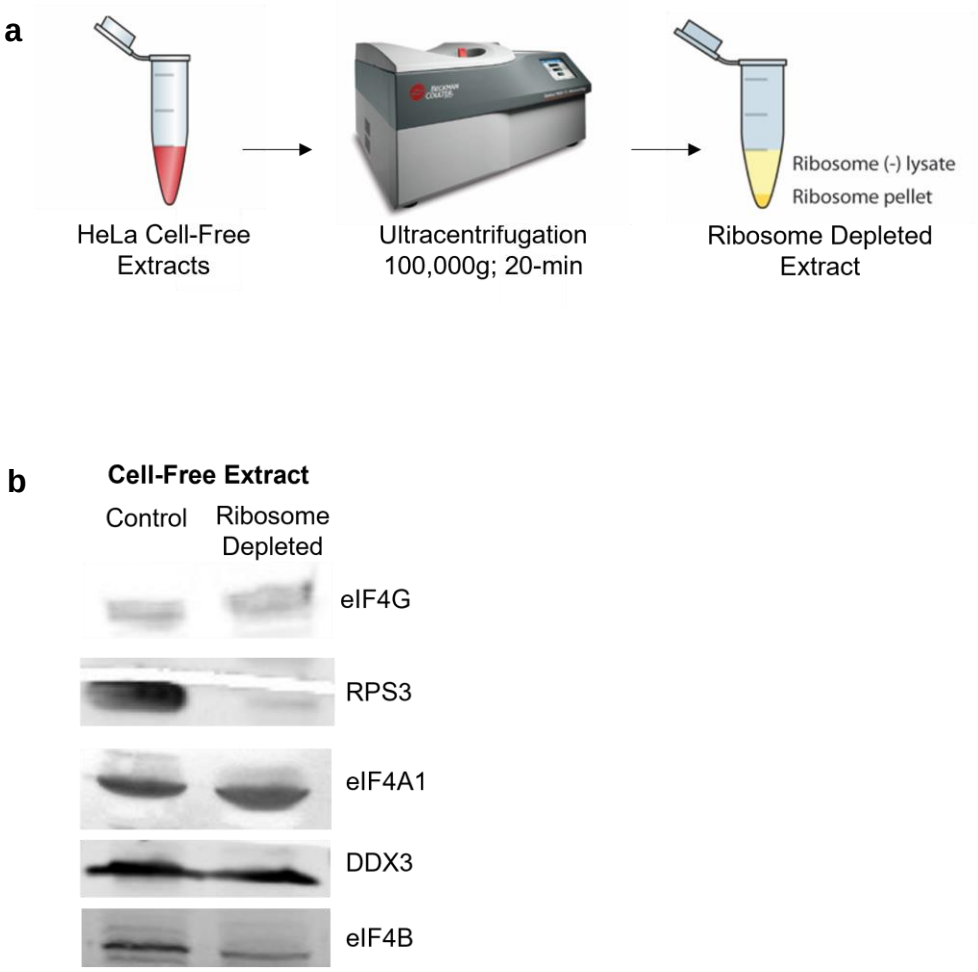

Figure 1.3. Overview of the Depletion of Ribosomes from Cell-Free Extracts

a) Schematic of method describing fractionating extract by ultracentrifugation. b) Western blot highlighting the levels of key translation factors pre- and post-ribosome depletion; 100µg of extract loaded.

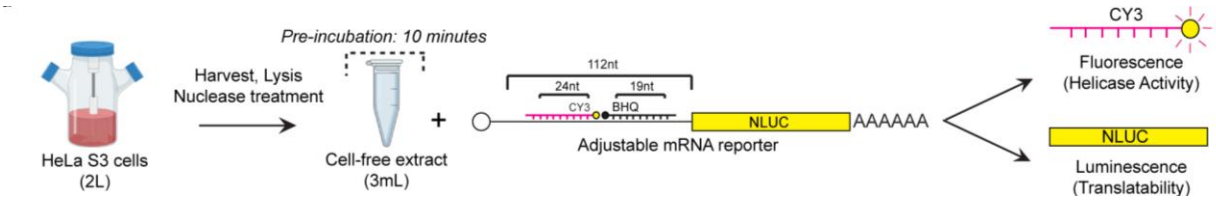

Figure 2.1 Schematic of the development of cell-free extracts for use with a novel mRNA reporter to monitor unwinding of RNA duplexes in parallel with changes in overall protein abundance.

Cell-free extracts are generated from HeLa S3 cells grown in large liquid suspension cultures (2 liters). A modular full-length mRNA reporter is used to monitor a) duplex unwinding via fluorescent beacons annealed to sites within the mRNA, and b) downstream effects on the translation of a bioluminescent gene (NanoLuc). Lysates are pre-incubated for 10 minutes at 30°C to allow any supplemented proteins or inhibitors to come to equilibrium prior to adding the mRNA reporter and taking assay measurements. Suspension cell flask depicted in this figure was created with BioRender.com

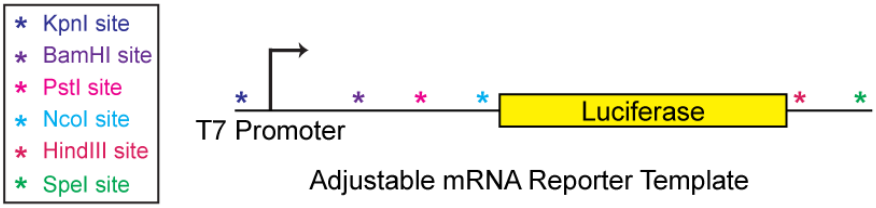

Figure 2.2 Modular mRNA Reporter Template Design

Depiction of the template used to engineer the appropriate mRNA reporter for monitoring RNA restructuring and protein synthesis of luciferase.

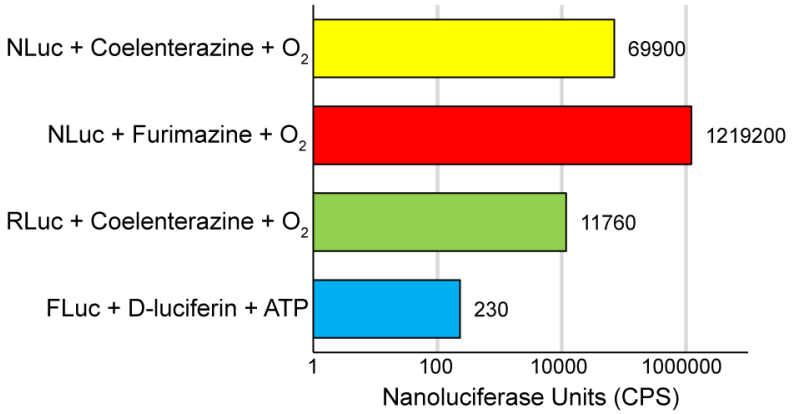

Figure 2.3 Selection of a Luciferase Reporter Gene to Monitor Protein Synthesis

Bar graph depicting luciferase translation of indicated mRNA reporter(s) with their respective substrates. Luciferase was measured after 30 minutes incubated at 30 °C with translation assay and lysate mix.

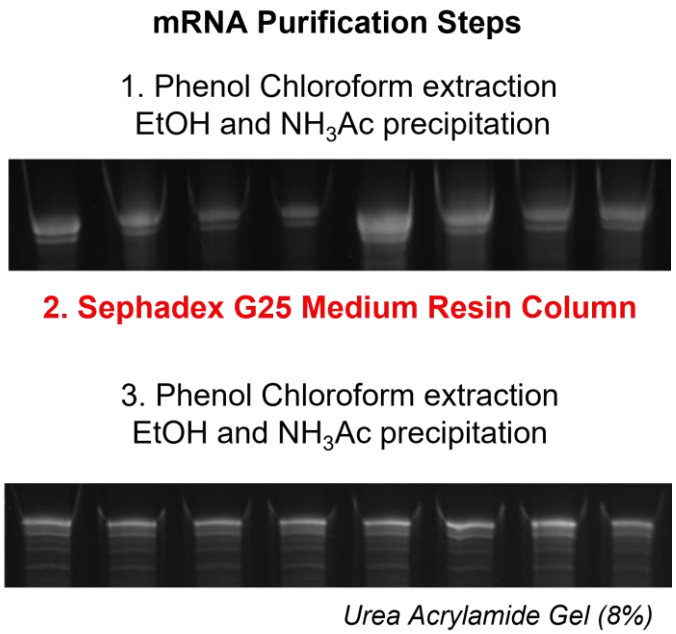

Figure 2.4 Sephadex G-25 Medium Resin is Required for Pure RNA Clean-up

The RNA transcription product is directly extracted by phenol-chloroform treatment and precipitated by ethanol and ammonium acetate. The integrity and purity of the transcription product is assayed by an 8% (wt/vol) denaturing urea-polyacrylamide gel. Free nucleotides are removed from the RNA using Sephadex G25 resin (GE Healthcare).

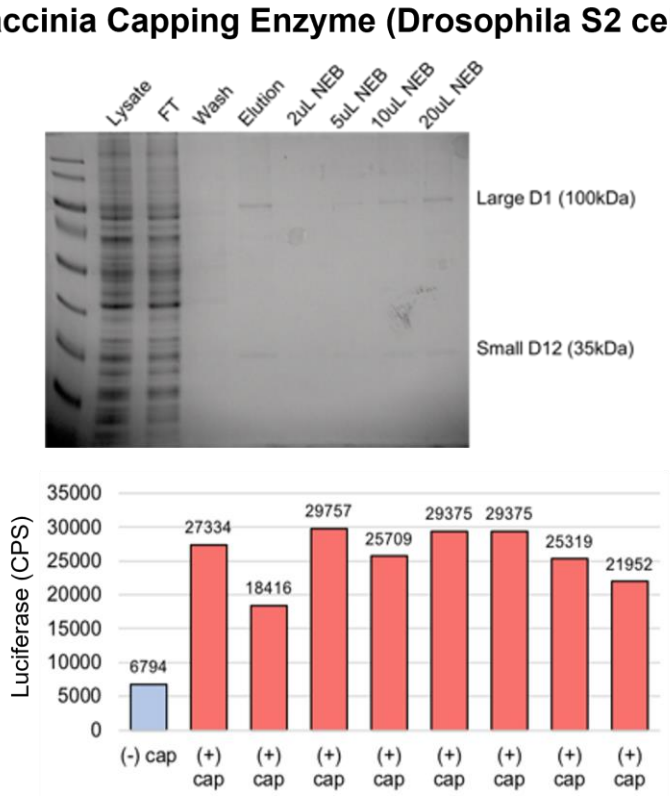

Figure 2.5 Capping Enzyme Purification Analysis

The vaccinia capping enzyme is visualized by SDS-PAGE and Coomassie stain and compared to commercial enzyme (New England Biolabs). The cap stimulates translation to a similar extent as commercial enzyme product.

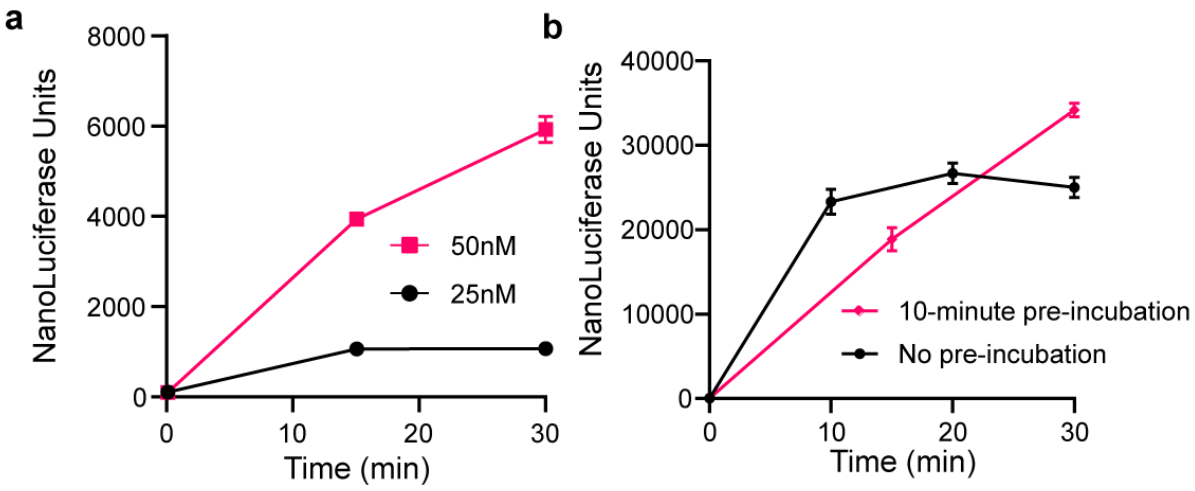

Figure 2.6 Optimization of translation conditions to ensuring linearity of protein generated over time

a) Line graph depicting luciferase translation of mRNA reporter measured over 30 min at an incubation temperature at 30 °C. *In vitro* translation reactions in lysate programmed with 25nM or 50nM mRNA reporter. b) Line graph demonstrating the importance of a 10-minute pre-incubation step prior to initiating protein synthesis. *In vitro* translation reactions in lysate programmed with 50nM reporter over a time course of 30 minutes. All data are presented as means of three independent experiments ± SEM.

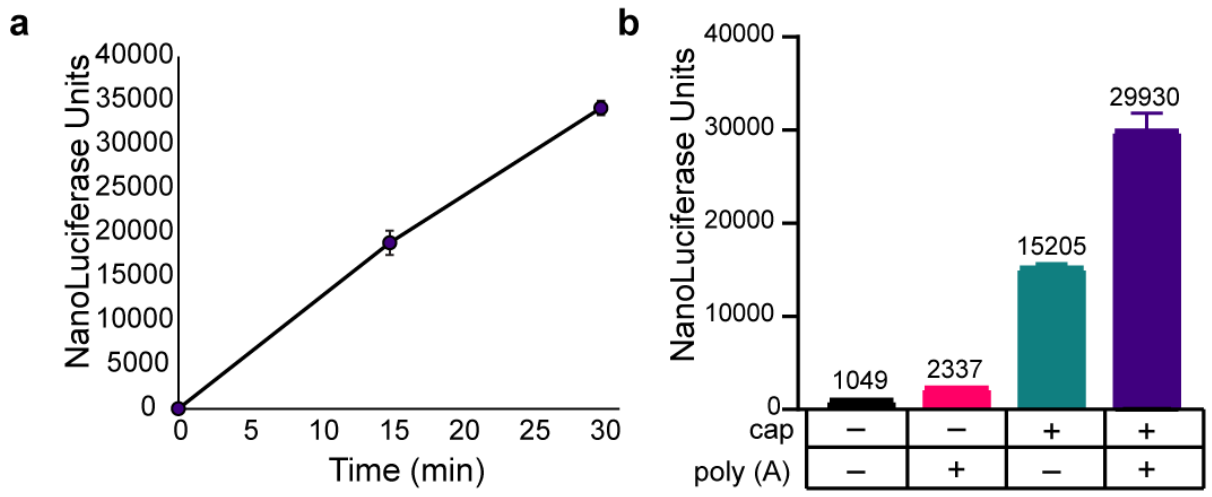

Figure 2.7 Validation of faithful translational regulation in cell-free extracts

Time course of translation in cell-free extracts using the reporter depicted in (a). Lysate and translation assay mix were pre-incubated for 10 minutes at 30°C prior to adding the appropriate mRNA (50nM) to initiate protein synthesis. The reporter and assay mix were then incubated at 30°C for the time indicated on the horizontal axis, before measuring the luciferase activity. (**c**) Bar graph depicting luciferase translation of mRNA reporter(s) with each combination of m7GTP cap and poly (A) tail modifications to the mRNA, measured after 30 minutes incubated at 30 °C. As above, lysate and translation assay mix were pre-incubated for 10 minutes at 30°C prior to adding the appropriate mRNA (50nM) to initiate protein synthesis. All data are presented as means of three independent experiments and error bars represent ± SEM.

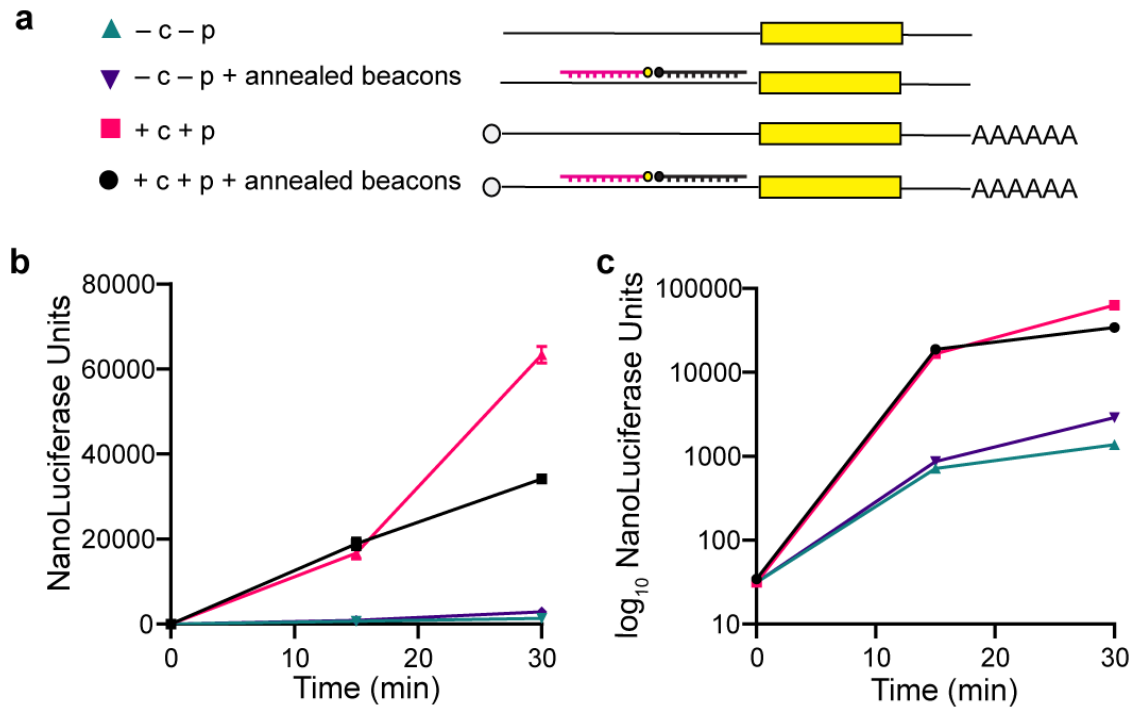

Figure 2.8 Annealed beacons to not alter the trend of protein synthesis

a) Schematic representation of the reporter constructs used in this set of experiments indicating the combination of m7G cap and poly(A) tail and fluorescent beacons annealed to the mRNA. b) Line graph depicting luciferase translation of mRNA reporter measured over 30 min at an incubation temperature at 30 °C. *In vitro* translation reactions in lysate programmed with 50nM mRNA reporter with or without m7G cap and poly(A) tail and annealed fluorescent beacons. c) Line graph using data from (b) but with the y-axis transformed to a log10 scale. All data are presented as means of three independent experiments ± SEM

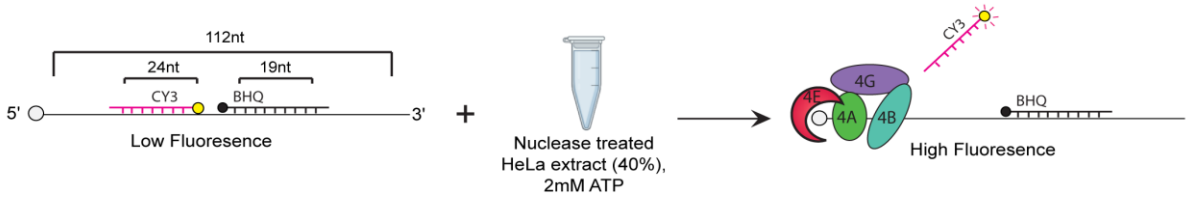

Figure 2.9 Representation of the fluorescent-based helicase assay using HeLa cell-free extract

Depiction of the mRNA reporter with annealed beacons dissociated by factors from the nuclease treated HeLa lysate.

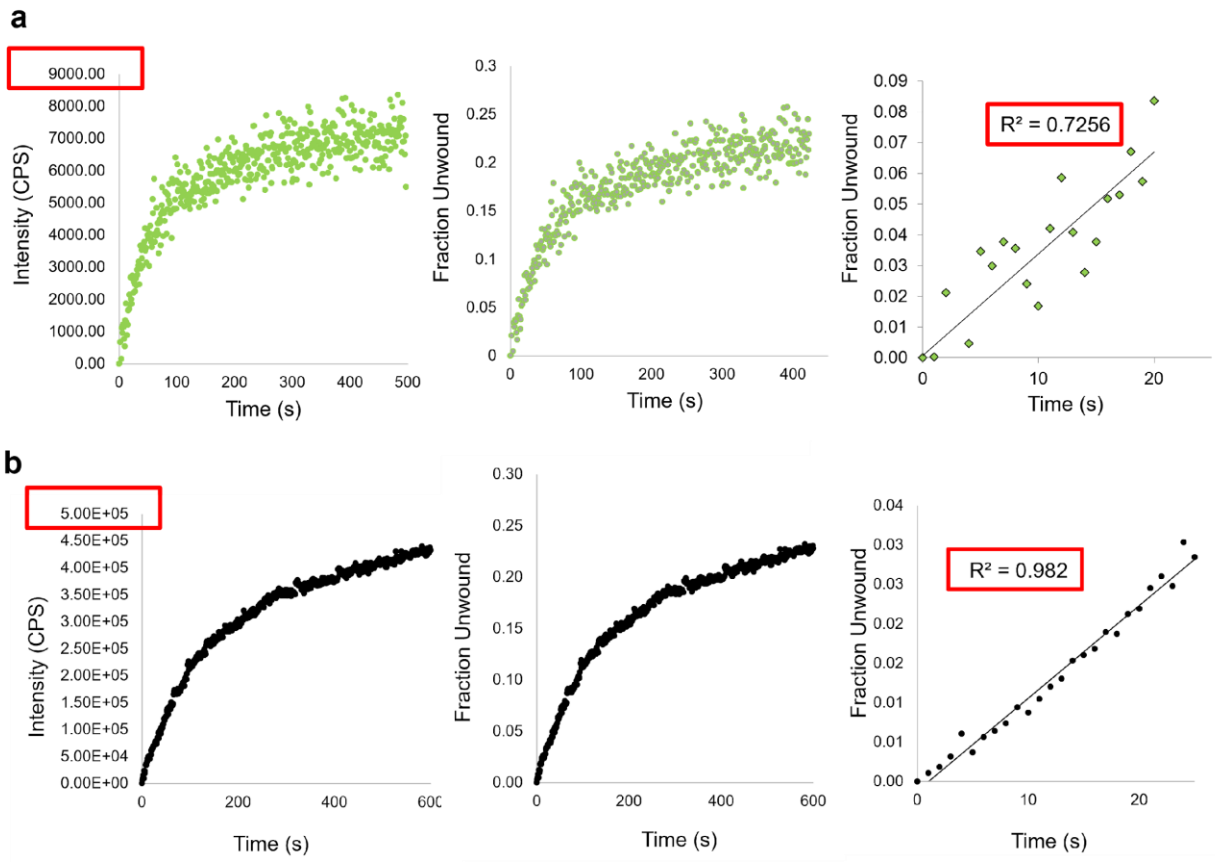

Figure 2.10 Unwinding Curves Demonstrating Optimized Fluorometer Conditions

(a) Unwinding curves prior to fluorometer optimization displaying intensity signal of 9000 (CPS) and R^2 of 0.7256, (**b)** unwinding curves after optimization displaying intensity signal of 500,000 with R^2 of 0.982.

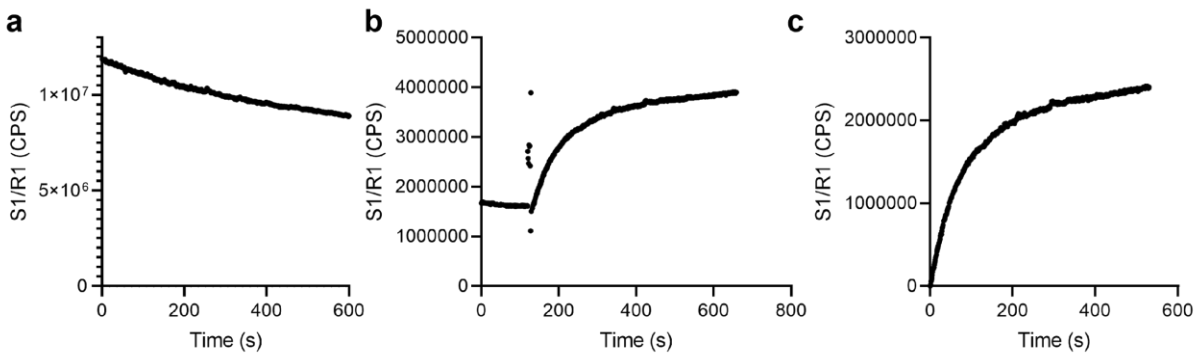

Figure 2.11 Fluorometer Data Collection of Duplex Melting in Cell-Free Extracts

(a) Maximum Cy3 fluorescence is shown for a control reaction containing 50 nM Cy3 reporter, 50 nM RNA template, 2 mM ATP, 40% cell-free extract in reaction buffer. **(b)** Data showing baseline fluorescence for unwinding reaction measured for 100 seconds prior to adding pre-incubated cell-free extract. **(c)** Data is zeroed at the time point of adding cell-free extract to convert to fraction of duplex unwound.

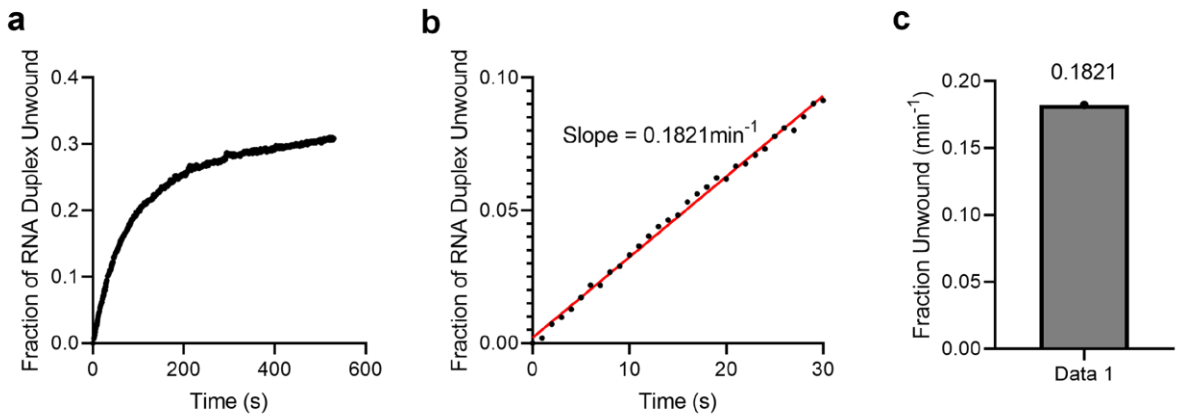

Figure 2.12 Duplex Unwinding Data Analysis

(a) Data is converted to fraction of duplex unwound per second. **(b)** Initial linear portion of the data can be fit to a linear regression line to measure the initial rate. **(c)** Initial rate converted to fraction unwound per minute and displayed as a bar graph.

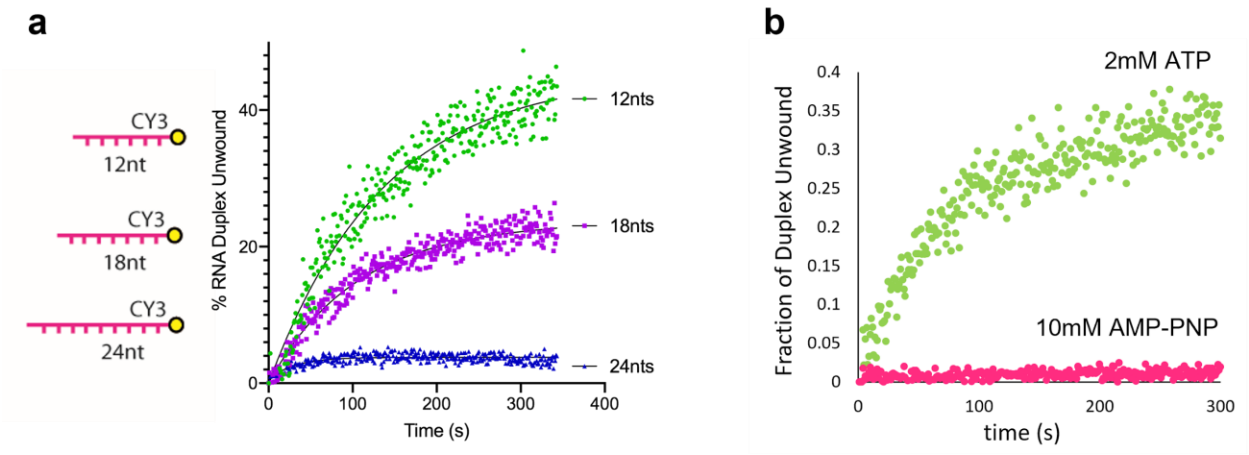

Figure 2.13 Selection of a CY3 Reporter to Monitor RNA restructuring

(a) Unwinding time course of 12nt, 18nt, and 24nt fluorescent reporter RNAs. **(b)** Unwinding time-course for the 12nt CY3 reporter in the presence of the ATP inhibitor, AMP-PNP.

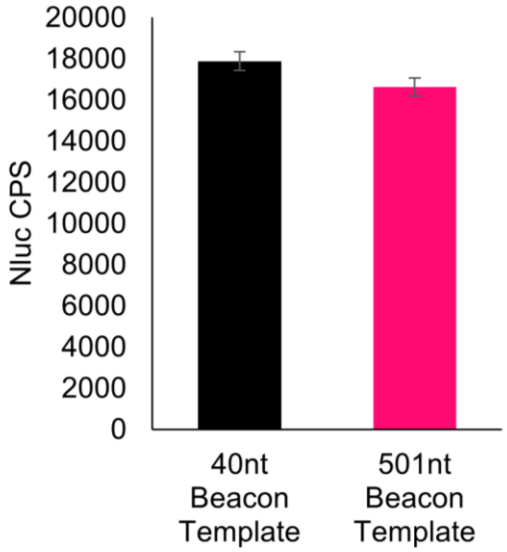

Figure 2.14 Engineering the 12nt CY3 Reporter in the middle of the luciferase gene does not disrupt translation

Bar graph depicting translation of two mRNA reporters with sites for annealing beacons at the 40nt position, and 501nt position. All data are presented as means of three independent experiments and error bars represent ± SEM.

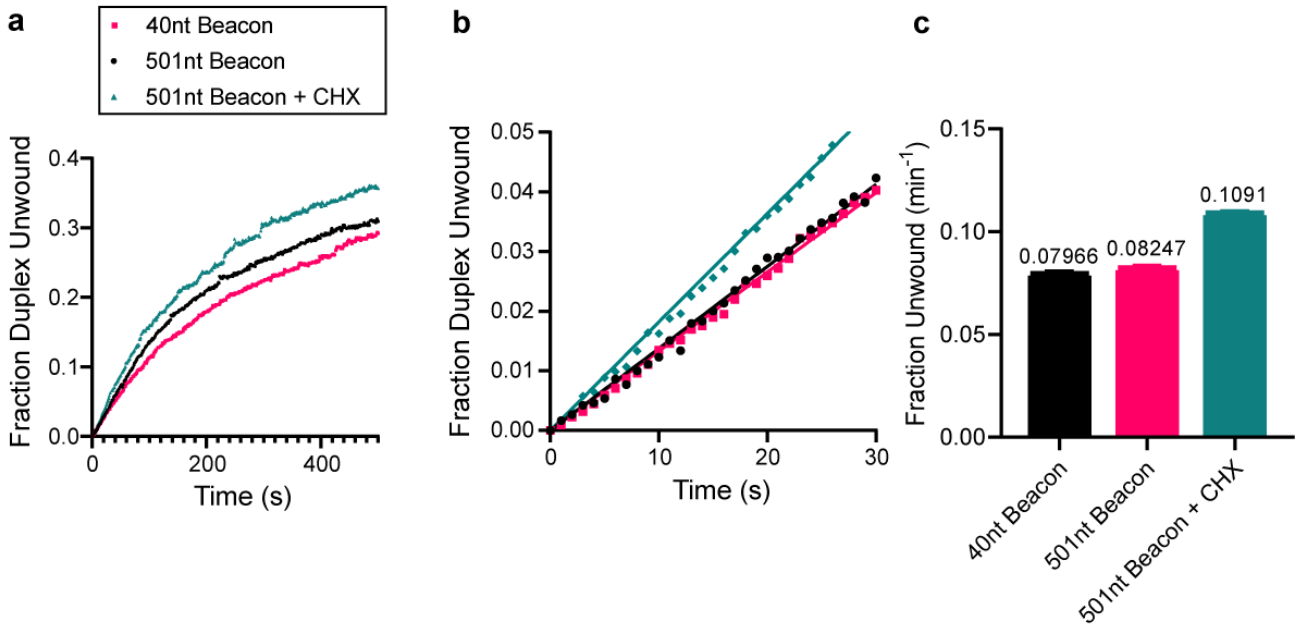

Figure 2.15 Duplex Unwinding for the 12nt CY3 Beacon Throughout the mRNA Reporter

(a) Duplex unwinding curves displayed for 40nt beacon (pink), 501nt beacon (black), and 501 nt beacon + cycloheximide (green). **(b)** Initial portion of the unwinding curves with linear fit to the data. **(c)** Bar graphs showing initial rates of unwinding per minute. All data are presented as means of three independent experiments and error bars represent ± SEM.

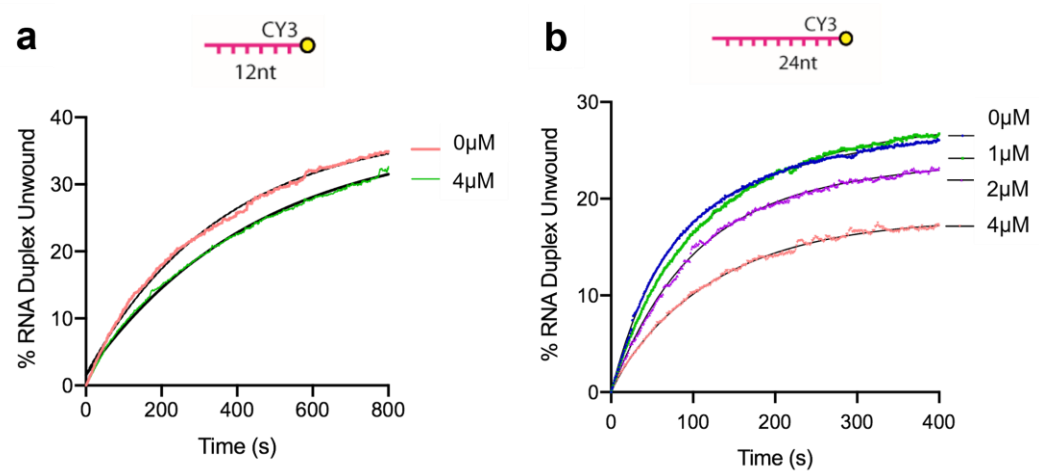

Figure 2.16 Monitoring Duplex Unwinding by 12nt and 24nt CY3 Reporters in the Presence of a Translation Inhibitor, eIF4A-R362Q

(a) 12nt CY3 duplex unwinding curves display inconsequential effect of the eIF4A inhibitor (eIF4A-R362Q) at concentration of 4μM. (b) 24nt CY3 duplex unwinding curves display a dose dependent relationship on the translational inhibitor, eIF4A-R362Q. All data are presented as means of three independent experiments.

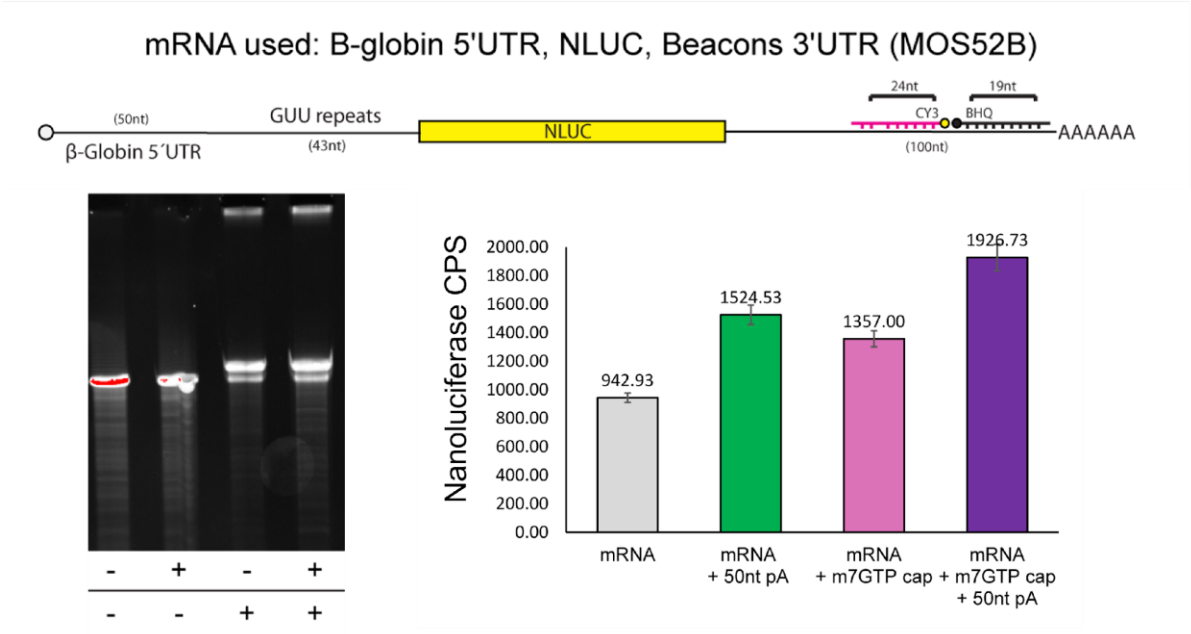

Figure 2.17 Engineering the 24nt CY3 Reporter in the 3'UTR Disrupts Synergistic Translatability of the Cap and Poly(A) tail

The construct tested is depicted with the sites for beacons present in the 3'UTR. The mRNAs were run on a 8% Urea-Acrylamide gel to confirm purity. mRNAs with combinations of cap and poly(A) did not cause a synergistic effect as demonstrated previously. All data are presented as means of three independent experiments and error bars represent ± SEM.

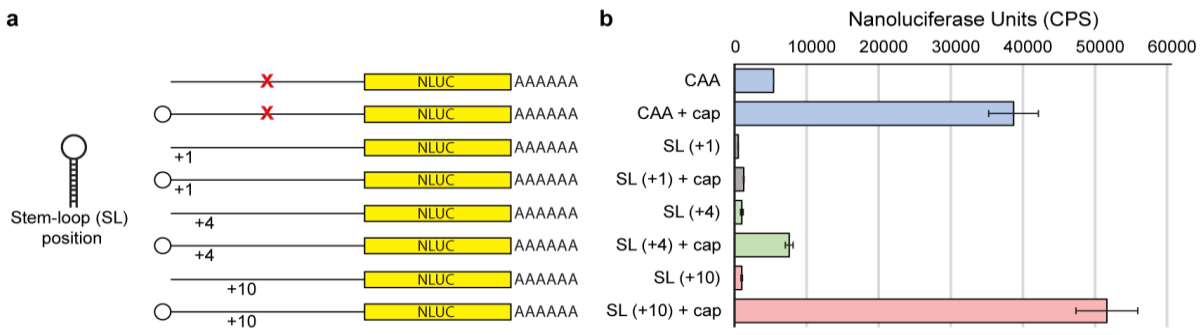

Figure 2.18 Effect of 5′ UTR length and sequence on protein synthesis

(a) Outline of reporters used to test effect of the stem-loop (SL) structure at positions +1, +4, and +10 of the 5′ UTR, using a construct with CAA repeats as a control. (**b)** Bar graph depicting luciferase translation of mRNA reporter(s) outlined in (a). Luciferase was measured after 30 minutes incubated at 30 °C with translation assay and lysate mix. All data are presented as means of three independent experiments and error bars represent ± SEM.

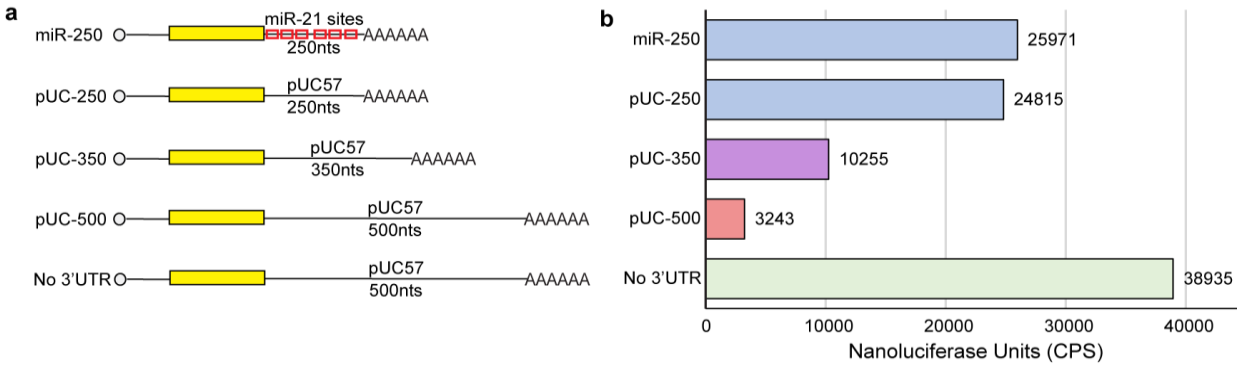

Figure 2.19 Effect of 3′ UTR length and sequence on protein synthesis

(a) Outline of reporters used to test effect of the sequence and length of different 3′ UTRs. (**b)** Bar graph depicting luciferase translation of mRNA reporter(s) outlined in (a). Luciferase was measured after 30 minutes incubated at 30 °C with translation assay and lysate mix.

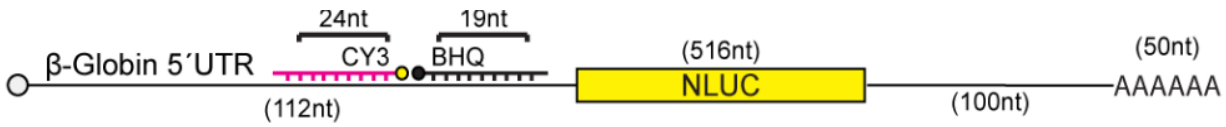

Figure 2.20 Dual-assay mRNA Reporter used for Characterization

Schematic diagram depicting capped mRNA reporter with a globin 5′ UTR, sites for annealing fluorescent beacons, a NLuc gene, a 100-nucleotide 3′ UTR sequence, and a 50-nucleotide poly (A) tail.

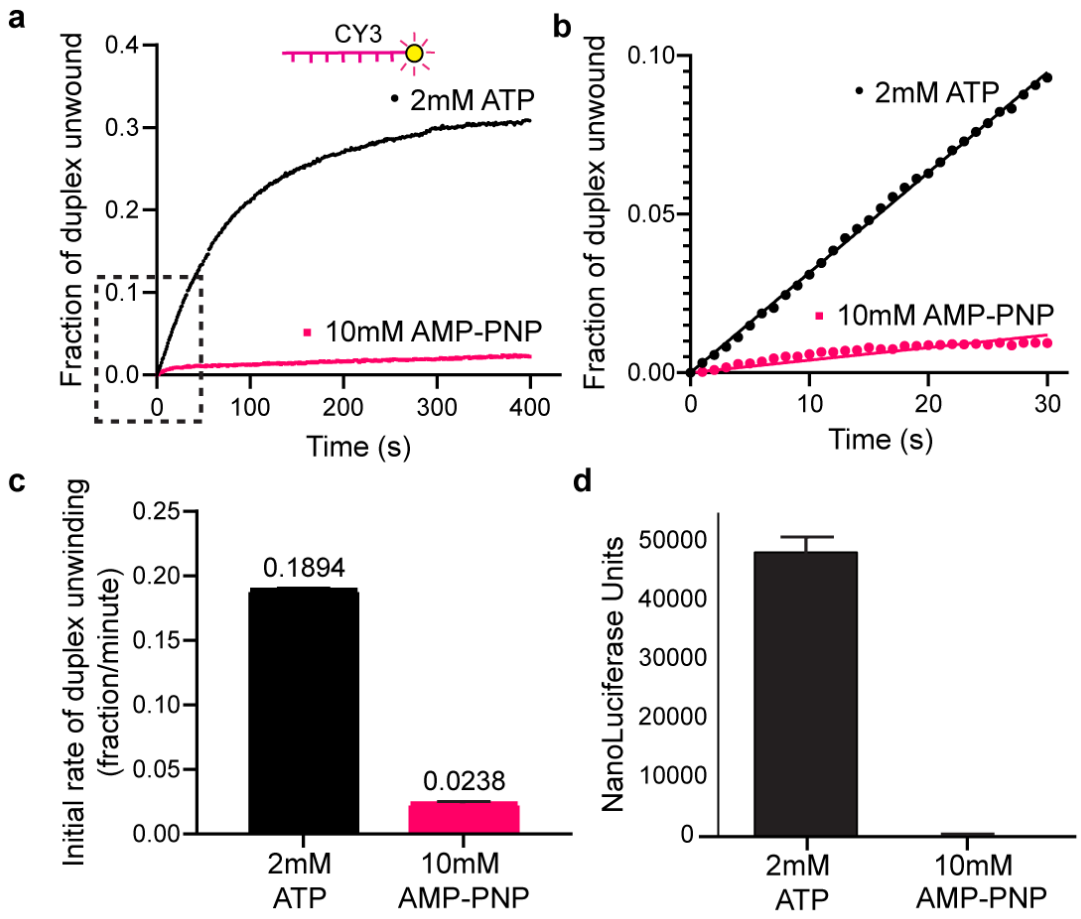

Figure 2.21 RNA duplex unwinding in nuclease-treated cell-free extracts is ATP dependent.

(a) The average of three independent time courses of the fraction of duplex unwound after 2mM ATP (black) or 10mM AMP-PNP (magenta) addition. The Cy3 fluorescence data are converted into the fraction of duplex unwound versus time after ATP addition, as described in the data analysis section. **(b)** A magnified view of the dashed region of the unwinding time course (a) is shown. Initial rates during the initial linear portion of the unwinding time course are determined by linear fits to this section of the data. **(c)** The initial rate of duplex unwinding (fraction per minute) by each dataset are shown as indicated. **(d)** NLuc translation was measured in cell-free extracts over 30 minutes. Both

the fluorescent and the luciferase assay (a-d) were conducted following a 10-minute lysate pre-incubation at 30°C. Error bars throughout represent the standard error derived from at least three separate experiments.

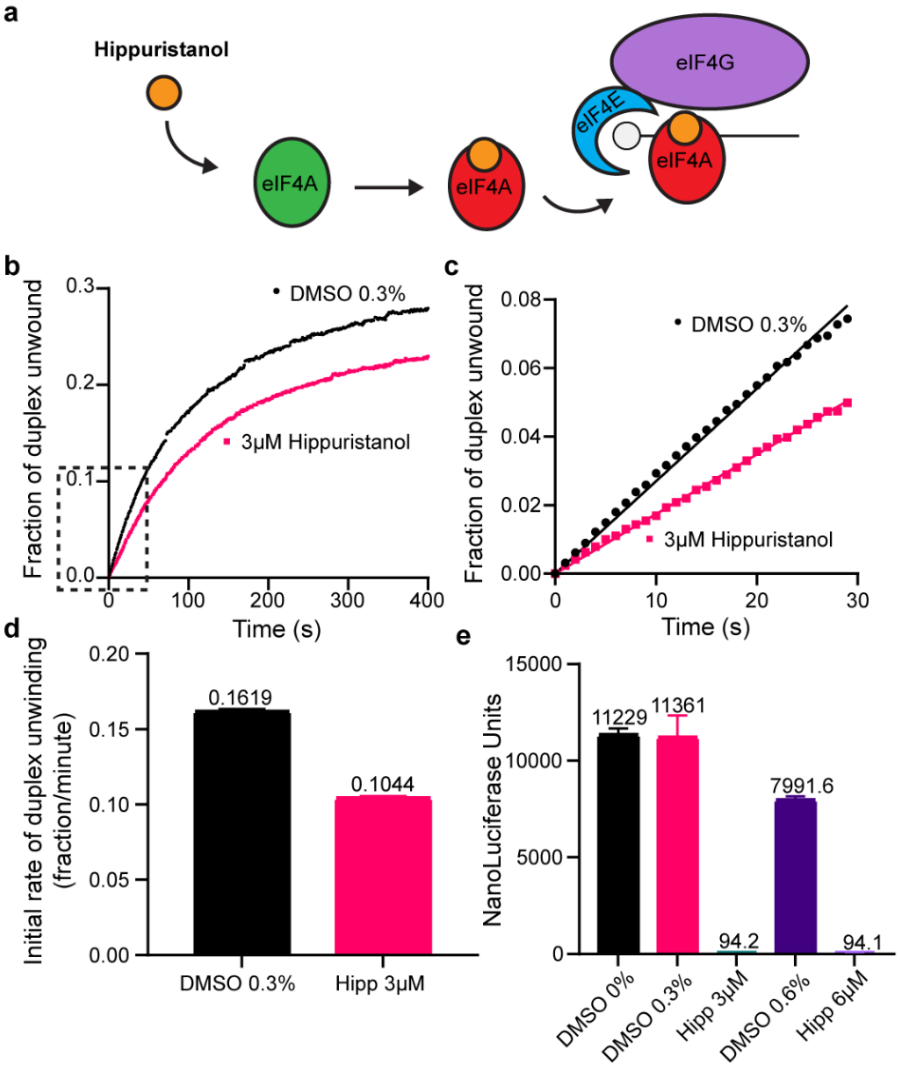
a
Hippuristanol
eIF4A
eIF4A
eIF4G
eIF4E
eIF4A
b
Fraction of duplex unwound
DMSO 0.3%
3μM Hippuristanol
Time (s)
c
Fraction of duplex unwound
DMSO 0.3%
3μM Hippuristanol
Time (s)
d
Initial rate of duplex unwinding (fraction/minute)
0.1619
0.1044
DMSO 0.3%
Hipp 3μM
e
NanoLuciferase Units
11229
11361
94.2
7991.6
94.1
DMSO 0%
DMSO 0.3%
Hipp 3μM
DMSO 0.6%
Hipp 6μM

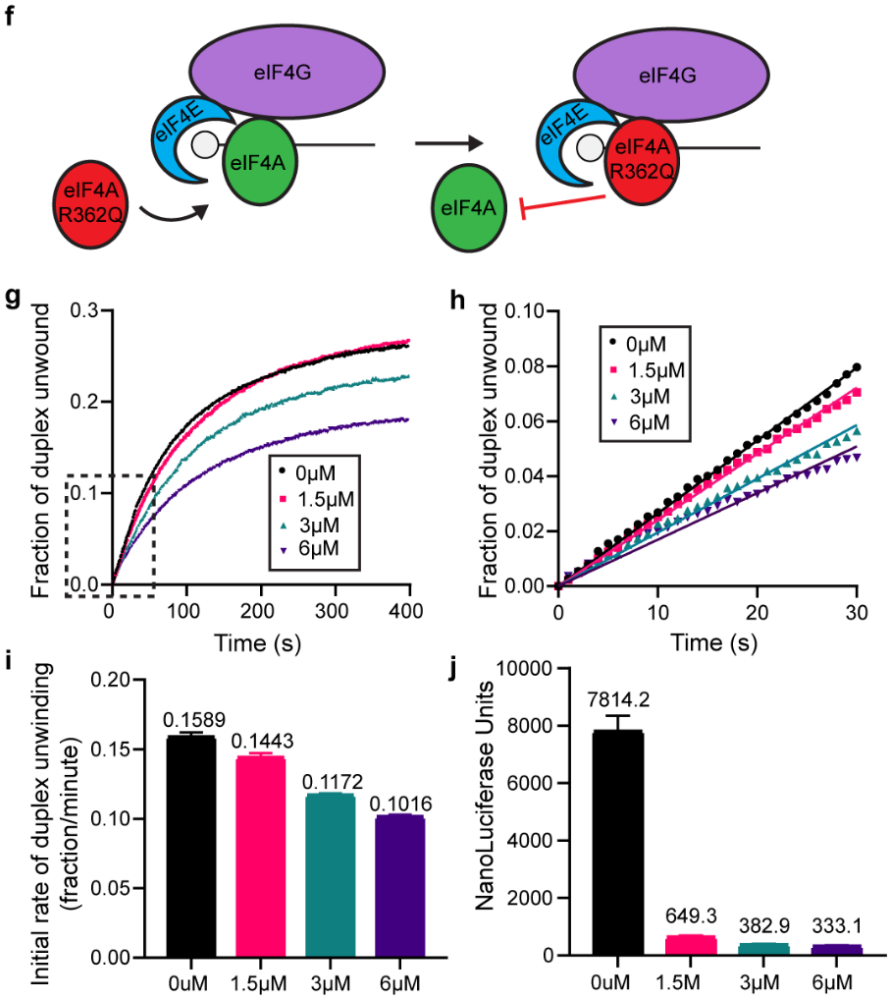

Figure 2.22. RNA duplex unwinding in nuclease-treated cell-free extracts is eIF4A-dependent.

(a) Schematic model describing the mechanism of inhibition of eIF4A by the small molecule inhibitor, hippuristanol. **(b)** The average of three independent unwinding time courses containing a titration of eIF4A R362Q: 0 μM, 1.5 μM, 3 μM or 6 μM. Lysate and protein were pre-incubated for 10 minutes at 30°C prior to adding to the cuvette with the remaining assay components. **(c)** Linear fits to the initial portion of the unwinding data in the presence of 0 μM, 1.5 μM, 3 μM or 6 μM eIF4A R362Q. **(d)** The initial rates of duplex

unwinding (fraction per minute) determined by slope of the line in (b). **(e)** Bar graph depicting luciferase translation of mRNA reporter measured after 30 min and incubated at 30 °C. *In vitro* translation reactions in lysate programmed with 50nM mRNA reporter depicted in Figure 2a, in the presence of 0 μM, 1.5 μM, 3 μM or 6 μM eIF4A R362Q. Lysate and translation assay mix were pre-incubated for 10 minutes at 30°C in the presence or absence of eIF4A R362Q prior to adding mRNA (50nM) to initiate protein synthesis. All data are presented as means of three independent experiments ± SEM. **(f)** Schematic model describing the mechanism of inhibition of the dominant negative eIF4A, eIF4A R362Q **(g)** The average of three independent unwinding time courses containing vehicle (0.3% DMSO) or 3 μM hippuristanol (in 0.3% DMSO). Lysate and protein were pre-incubated for 10 minutes at 30°C prior to adding to the cuvette with the remaining assay components. **(h)** Linear fits to the initial portion of the unwinding data in the presence of 0.3% DMSO (final concentration) ± 3 μM hippuristanol **(i)** The initial rates of duplex unwinding (fraction per minute) determined by slope of the line in (f). **(j)** Bar graph depicting luciferase translation of mRNA reporter containing a increasing concentrations of the vehicle, DMSO (0, 0.3 and 0.6%), and hippuristanol at 3 and 6 μM hippuristanol (diluted in 0.3% and 0.6% DMSO respectively). Luciferase activity was measured after the reporter had been incubated with the lysate assay mix for 30 min at 30 °C. Lysate and translation assay mix were pre-incubated for 10 minutes at 30°C in the presence or absence of DMSO and hippuristanol prior to adding mRNA (50nM) to initiate protein synthesis. All data are presented as means of three independent experiments ± SEM.

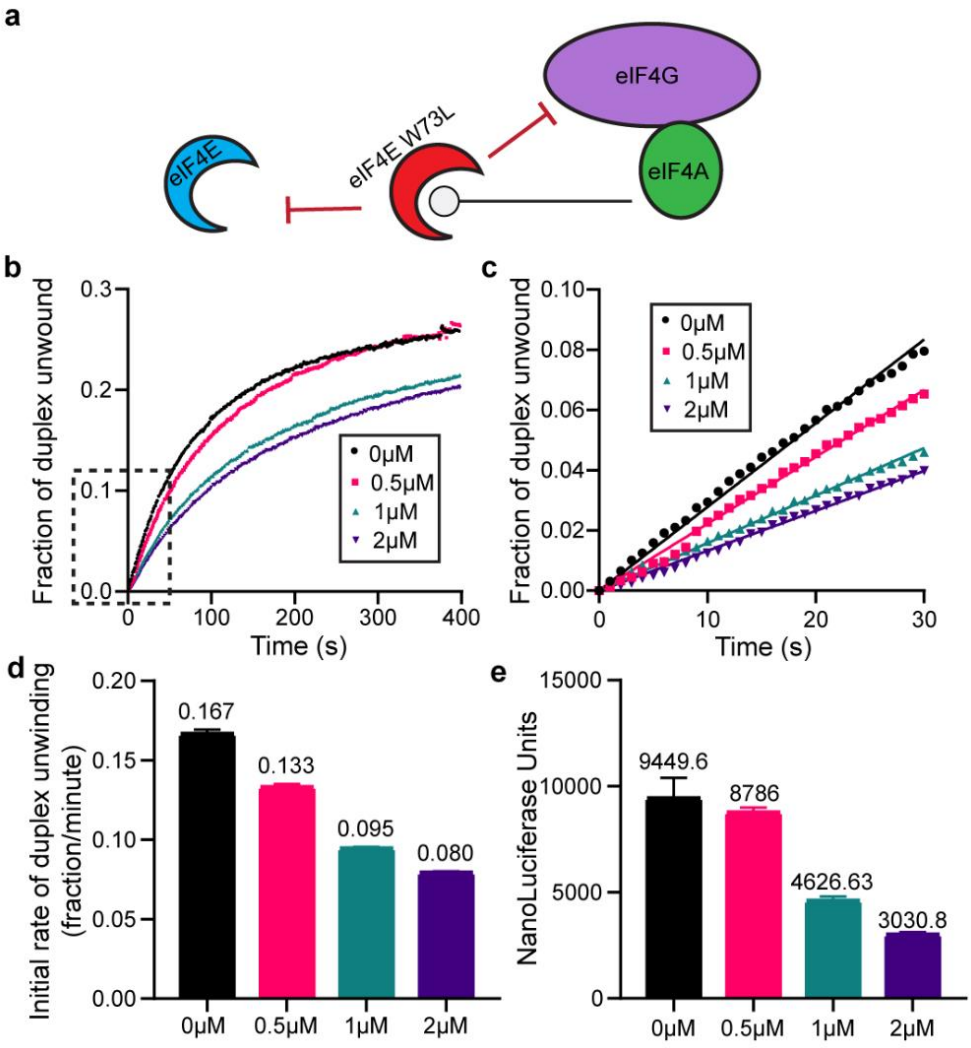

Figure 2.23. RNA duplex unwinding in nuclease-treated cell-free extracts is eIF4E-dependent.

(a) Schematic model describing the mechanism of inhibition of the dominant negative eIF4E, eIF4E W73L **(b)** The average of three independent unwinding time courses containing a titration of eIF4E W73L: 0 μM, 0.5 μM, 1 μM or 2 μM. Lysate and protein were pre-incubated for 10 minutes at 30°C prior to adding to the cuvette with the remaining assay components. **(c)** Linear fits to the initial portion of the unwinding data in the presence of 0 μM, 0.5 μM, 1 μM or 2 μM eIF4E W73L. **(d)** The initial rates of duplex unwinding (fraction per minute) determined by slope of the line in (c). **(e)** Bar graph

depicting luciferase translation of mRNA reporter measured after 30 min and incubated at 30°C. *In vitro* translation reactions in lysate programmed with 50nM mRNA reporter depicted in Figure 2a, in the presence of 0 µM, 0.5 µM, 1 µM or 2 µM eIF4E W73L. Lysate and translation assay mix were pre-incubated for 10 minutes at 30°C in the presence or absence of eIF4A R362Q prior to adding mRNA (50nM) to initiate protein synthesis. All data are presented as means of three independent experiments ± SEM

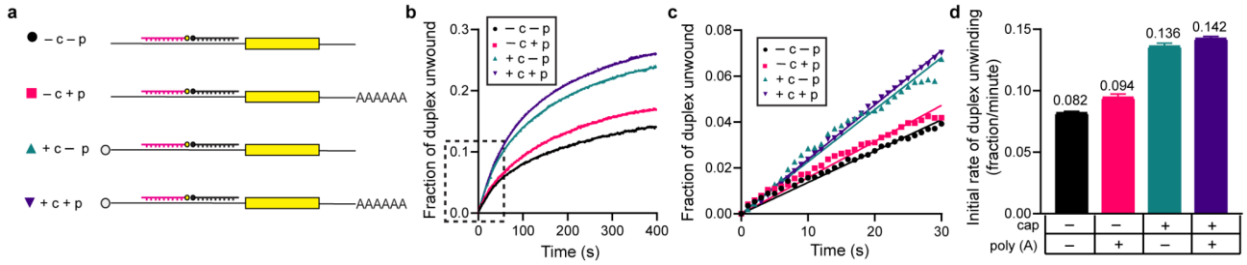

Figure 2.24. RNA duplex unwinding in nuclease-treated cell-free extracts is regulated by m7GTP cap but not poly(A) tail.

(a) Schematic representation of the reporter constructs used in this set of experiments, with each combination of the m7GTP and poly(A) tail modifications to the mRNA. **(b)** The average of three independent unwinding time courses for each mRNA reporter construct shown in (a). Lysates were pre-incubated for 10 minutes at 30°C prior to adding to the cuvette with the reporter construct and other assay components. **(c)** Linear fits to the initial portion of the unwinding data for each mRNA reporter. **(d)** The initial rates of duplex unwinding (fraction per minute) determined by slope of the line in (c). All data are presented as means of three independent experiments

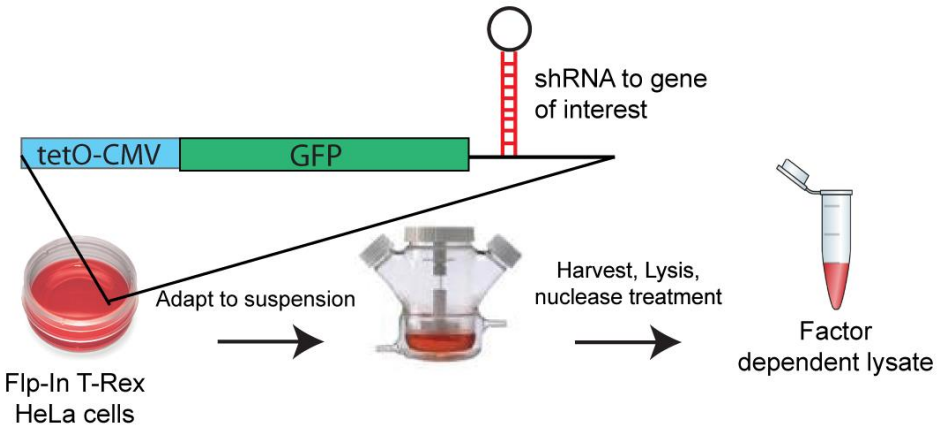

Figure 3.1. Overview of factor-dependent lysate system

HeLa R19 cells are transfected with the Flp-In T-Rex pcDNA5 vector targeting these factors using shRNAs integrated into the gene expressed by the vector. The vector is under control of a tetracycline inducible promoter enabling tight control of gene expression. The cells may be adapted to suspension culture to generate factor-depleted cell-free extracts.

(a) 3′UTR shRNA cassette design

5′ miR flanking region (Block IT): CTGGAGGCTTGCTGAAGGCTGTA
HindIII: AAGCTT
TG: Basal UG motif
KpnI: GGTACC, *KpnI twice for hairpin conservation. (BamHI can be used instead here)
CGTC: Flanking CNNC motif
CUC/GCG: mismatched GHG motif
ATGTATTGGCCTGTATTAGTT: **Specific siRNA targeting factor of interest**
TGTG: Apical UGU motif
XhoI:CTCGAG

CTGGAGGCTTGCTGAAGGCTGTAAAGCTTGGATCCCTCAGGGATGTATTGGCCTGTATTAGTTGTGCATCCAGGGAA
CTAATACAGGCCAATACATCCCCTGCGGGATCCTGATGCGTCCCACTTTTTTCTCGAG

(b) Parent Vector: MOS27 (pcDNA5 FRT TO)

AflII: CTTAAG, NcoI: CCATGG, PMOS125 Annealing site: GCGACCACATGGTGCTGCTG

CTTAAGACCATGGTGAGCAAGGGCGAGGAGCTGTTCACCGGCGTGGTCCCCATCCTGGTGGAGCTGGACG
GCGACGTGAACGGCCACAAGTTCAGCGTCTCCGGCGAGGGCGAGGGCGACGCCACCTACGGCAAGCTGAC
CCTGAAGTTCATCTGCACCACCGGCAAGCTGCCCGTCCCCTGGCCCACCCTGGTGACCACCCTGACCTAC
GGCGTGCAGTGCTTCAGCCGCTACCCCGACCACATGAAGCAGCACGACTTCTTCAAGAGCGCCATGCCCG
AGGGCTACGTGCAGGAGCGCACCATCTTCTTCAAGGACGACGGCAACTACAAGACCCGCGCCGAGGTGAA
GTTCGAGGGCGACACCCTGGTGAACCGCATCGAGCTGAAGGGCATCGACTTCAAGGAGGACGGGAACATC
CTGGGCCACAAGCTGGAGTACAACTACAACTCCCACAACGTGTACATCATGGCCGACAAGCAGAAGAACG
GCATCAAGGTCAACTTCAAGATCCGCCACAACATCGAGGACGGGTCCGTGCAGCTGGCCGACCACTACCA
GCAGAACACCCCCATCGGGGACGGCCCCGTGCTGCTCCCCGACAACCACTACCTCAGCACCCAGAGCGCC
CTGAGCAAGGACCCCAACGAGAAGCGCGACCACATGGTGCTGCTGGAATTCGTGACCGCCGCCGGCATCA
CCCTGGGCATGGACGAGCTGTACAAGTAACTGGAGGCTTGCTGAAGGCTGTAAAGCTTGAAGCTCGGTAC
CTGATGCGTCCCACTTTTTTCTCGAG

1. Determine siRNA target sequence: **AACCCATACTAGAAGTAGAAG**
2. Design final vector sequence including the shRNA target sequence with flanking regions

(c) Desired shRNA Depletion Vector Sequence

CTTAAGACCATGGTGAGCAAGGGCGAGGAGCTGTTCACCGGCGTGGTCCCCATCCTGGTGGAGCTGGACGGCGACGT
GAACGGCCACAAGTTCAGCGTCTCCGGCGAGGGCGAGGGCGACGCCACCTACGGCAAGCTGACCCTGAAGTTCATCT
GCACCACCGGCAAGCTGCCCGTCCCCTGGCCCACCCTGGTGACCACCCTGACCTACGGCGTGCAGTGCTTCAGCCGC
TACCCCGACCACATGAAGCAGCACGACTTCTTCAAGAGCGCCATGCCCGAGGGCTACGTGCAGGAGCGCACCATCTT
CTTCAAGGACGACGGCAACTACAAGACCCGCGCCGAGGTGAAGTTCGAGGGCGACACCCTGGTGAACCGCATCGAGC
TGAAGGGCATCGACTTCAAGGAGGACGGGAACATCCTGGGCCACAAGCTGGAGTACAACTACAACTCCCACAACGTG
TACATCATGGCCGACAAGCAGAAGAACGGCATCAAGGTCAACTTCAAGATCCGCCACAACATCGAGGACGGGTCCGT
GCAGCTGGCCGACCACTACCAGCAGAACACCCCCATCGGGGACGGCCCCGTGCTGCTCCCCGACAACCACTACCTCA
GCACCCAGAGCGCCCTGAGCAAGGACCCCAACGAGAAGCGCGACCACATGGTGCTGCTGGAATTCGTGACCGCCGCC
GGCATCACCCTGGGCATGGACGAGCTGTACAAGTAACTGGAGGCTTGCTGAAGGCTGTAAAGCTTGGTACCCTCAGG
GATGTATTGGCCTGTATTAGTTGTGCATCCAGGGAACTAATACAGGCCAATACATCCCCTGCGGGTACCTGATGCGT
CCCACTTTTTTCTCGAG

3. Design oligos to amplify the region between HindIII and the second KpnI restriction site

(d) Annealed Oligo Design

Primer Design for a HindIII and KpnI digest

PMOS89(F 5′-3′): AGCTTGGTACCCTCAGGG**AACCCATACTAGAAGTAGAAGT**GTGCATCCAGGG**CTTCTACTTCTAGTATGGGTT**CCCCTGCGGGTAC

PMOS90(R 3′-5′): ACCATGGGAGTCCC**TTGGGTATGATCTTCATCTTCA**CACGTAGGTCCC**GAAGATGAAGATCATACCCAA**GGGGACGCC

Primer Design for Ordering:

PMOS89(F 5′-3′): AGCTTGGTACCCTCAGGG**AACCCATACTAGAAGTAGAAGT**GTGCATCCAGGG**CTTCTACTTCTAGTATGGGTT**CCCCTGCGGGTAC

PMOS90 (R 5′-3′): CCGCAGGGGAACCCATACTAGAAGTAGAAGCCCTGGATGCACACTTCTACTTCTAGTATGGGTTCCCTGAGGGTACCA

4. Digest parent vector with HindIII and KpnI
5. Ligate parent vector with annealed oligos to create vector

Figure 3.2. Stepwise Design of Annealed Oligos for shRNA Depletion

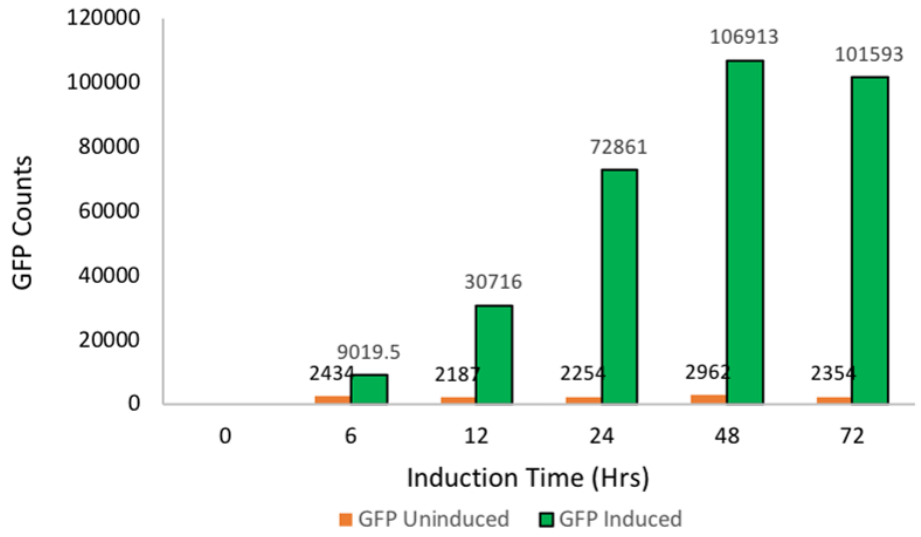

Figure 3.3. GFP Analysis of shRNA Cassette Integration

The integration of the shRNA cassette is monitored by GFP. Cells were harvested at equal density with or without tetracycline induction over time (6-72 hours). GFP fluorescence is measured using a Victor X5 Multilabel Plate Reader (Perkin-Elmer).

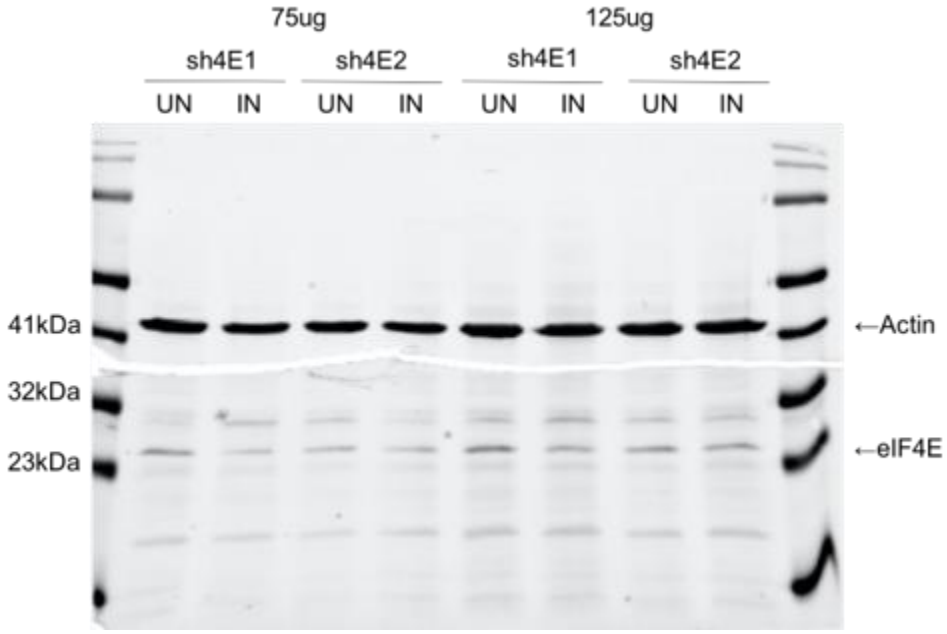

Figure 3.4. Immunoblot of eIF4E Depletion Cell Lines

The uninduced and induced cellular lysate from each depletion line (sh4E1; MOS28 and sh4E2; MOS29) were loaded at two different concentrations: 75µg and 125µg. The membrane was blotted with primary antibodies to either Actin or eIF4E.

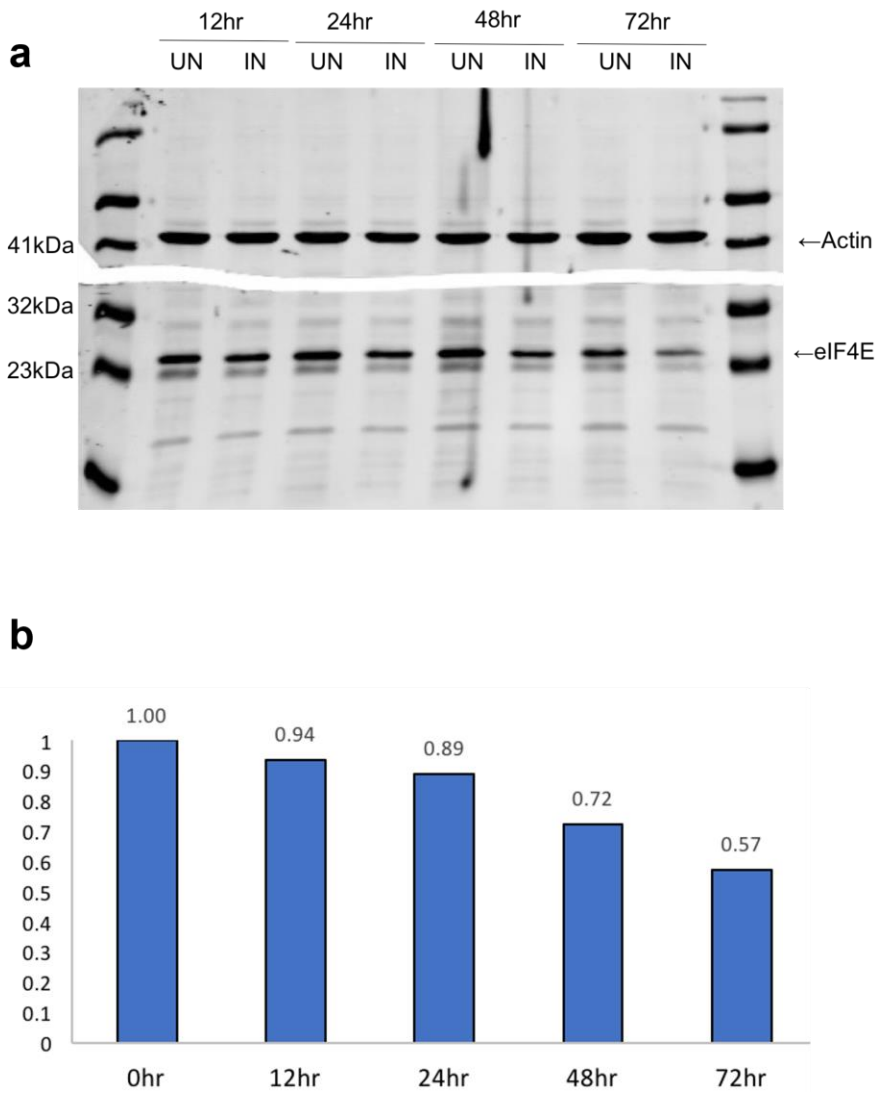

Figure 3.5. Immunoblot of eIF4E Depletion Cell-Line Tetracycline Time-Course

a) Immunoblot for eIF4E and Actin on cell lysate loaded from tetracycline induction time-course (12-72hrs). (b) Bar graph outlining the relative expression of protein bands (eIF4E/Actin) as determined by Image J analysis of the western blot.

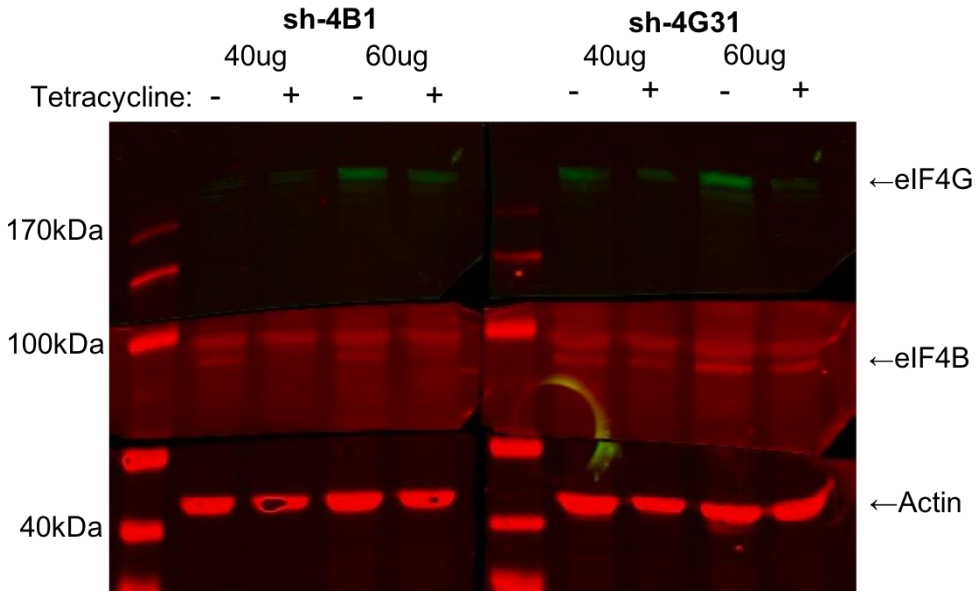

Figure 3.6. Immunoblot of eIF4G and eIF4B Depletion Cell Line

The uninduced and induced cellular lysate from each depletion line (sh4B1; MOS32 and sh4G31; MOS33) were loaded at two different concentrations: 40µg and 60µg. The membrane was blotted with primary antibodies to either Actin, eIF4G, or eIF4B.

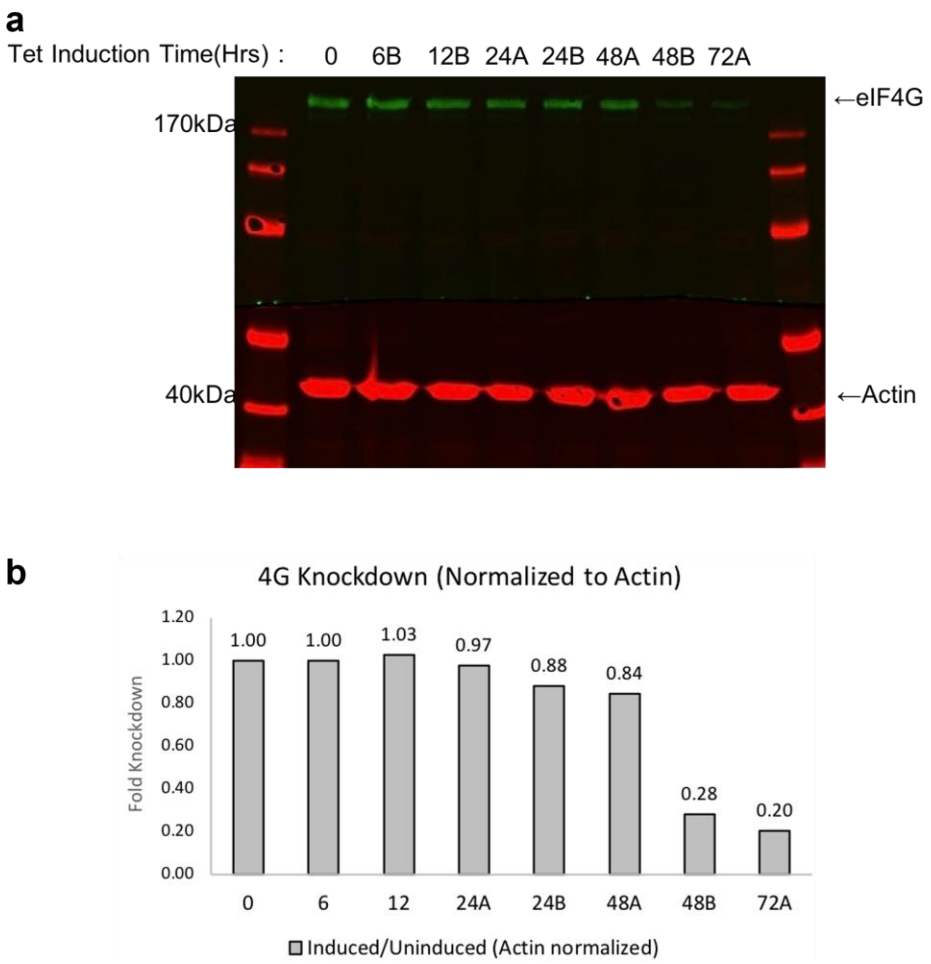

(a) Figure 3.7. Immunoblot of eIF4G Depletion Suspension Cell-Line Tetracycline Time-Coursa) Immunoblot for eIF4G and Actin on cell lysate loaded from tetracycline induction time-course (0-72hrs). (b) Bar graph outlining the relative expression of protein bands (eIF4E/Actin) as determined by Image J analysis of the western blot.

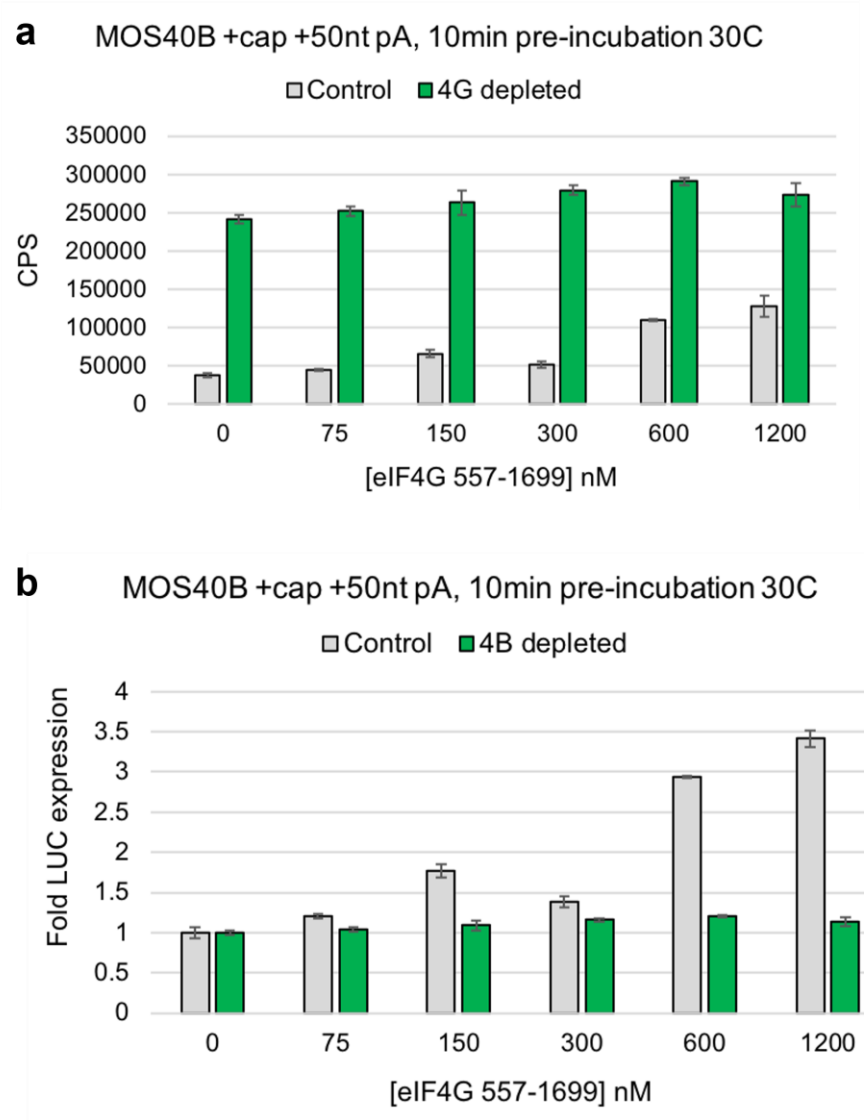

Figure 3.8. Titration of recombinant eIF4G$_{557-1699}$ to eIF4G depleted lysate

(a) Bar graph displaying the titration of recombinant eIF4G$_{557-1699}$ (75nM-1200nM) to a eIF4G depleted lysate, and a control lysate. (b) The relative amount of luciferase generated compared to a control not supplemented with recombinant protein (0nM). All data are presented as means of three independent experiments and error bars represent ± SEM.

a

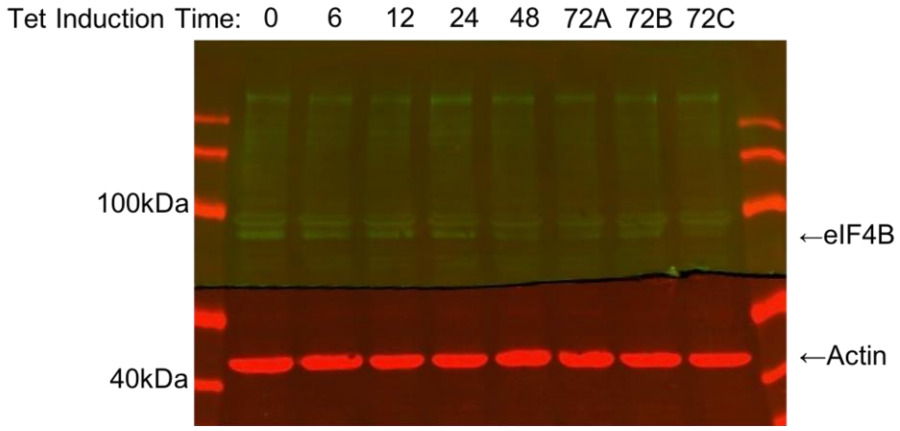

b

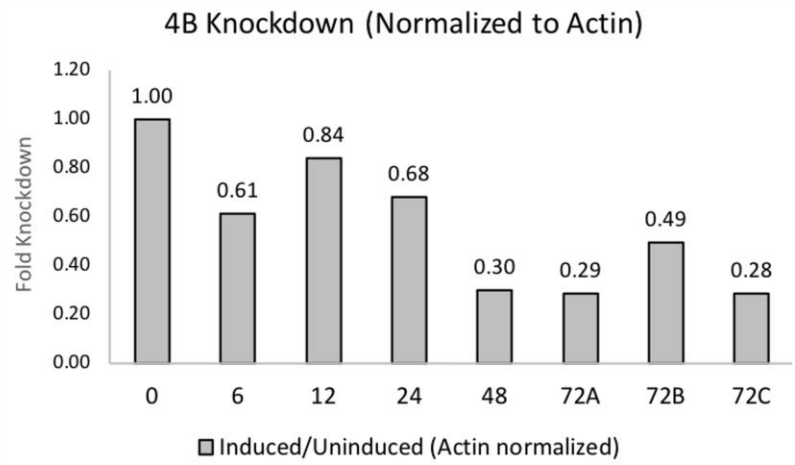

Figure 3.9. Immunoblot of eIF4B Depletion Suspension Cell-Line Tetracycline Time Course

(a) Immunoblot for eIF4B and Actin on cell lysate loaded from tetracycline induction time course (0-72hrs). **(b)** Bar graph outlining the relative expression of protein bands (eIF4E/Actin) as determined by Image J analysis of the western blot.

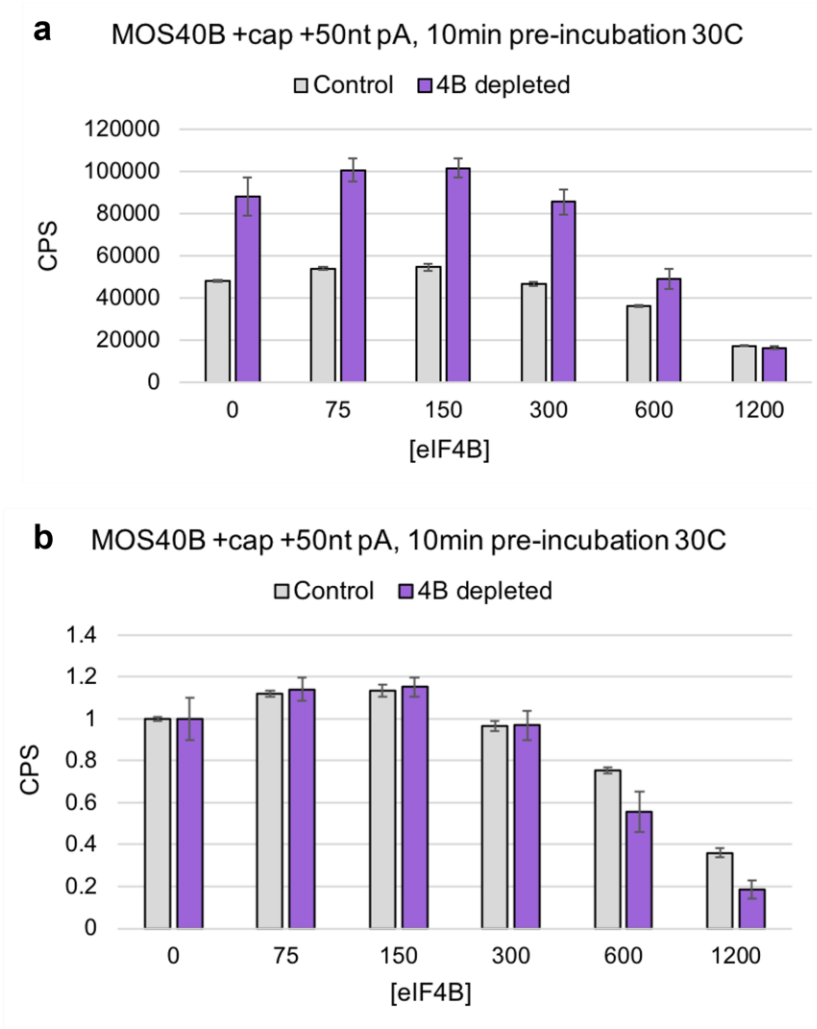

Figure 3.10 Titration of recombinant eIF4B to eIF4B depleted lysate

(a) Bar graph displaying the titration of recombinant eIF4B (75nM-1200nM) to a eIF4B depleted lysate, and a control lysate. **(b)** The relative amount of luciferase generated compared to a control not supplemented with recombinant protein (0nM). All data are presented as means of three independent experiments and error bars represent ± SEM.

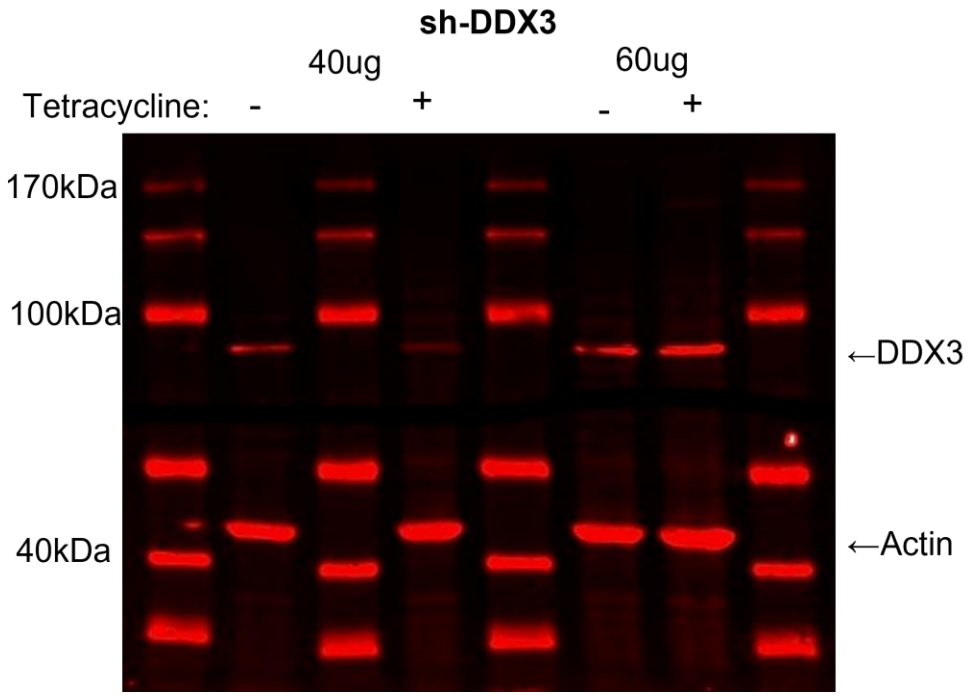

Figure 3.11. Immunoblot of DDX3 Depletion Cell Line

The uninduced and induced cellular lysate from the depletion line (shDDX3-2; MOS35) were loaded at two different concentrations: 40µg and 60µg. The membrane was blotted with primary antibodies to either Actin or DDX3.

Target	Type	Company	Catalog Number/ Species	Dilution
eIF4G	Primary	Santa Cruz	sc-11373/Rabbit	1:5000
eIF4B	Primary	John Hershey Lab	NA/Goat	1:5000
eIF4A	Primary	Thermo Scientific	PA5-17313/Rabbit	1:5000
eIF4E	Primary	BD Biosciences	61029/ Mouse	1:3000
DDX3	Primary	Santa Cruz	sc-365768/Mouse	1:5000
RPS3; 40S subunit	Primary	Santa Cruz	sc-376008/Mouse	1:5000
Actin	Primary	Santa Cruz	sc47778/Mouse	1:5000
Mouse	Secondary – DyLight 680	Invitrogen	35518/Goat	1:10,000
Rabbit	Secondary – DyLight 800	Thermo Scientific	35571/Goat	1:10,000
Goat	Secondary – DyLight 680	Invitrogen	SA5-10082/Donkey	1:10,000

Table 1. Description of primary and secondary antibodies used for western blot analysis

Reporter (Length)	Sequence	Annealing ΔG (kcal/mol)
BHQ (19-bps)	5′-GGCCCCACCGGCCCCUCCG-BHQ-3′	– 49.5
Cy3 (12-bps)	5′-Cy3-GCUUUACGGUGC–3′	– 24.2
Cy3 (18-bps)	5′-Cy3-GUUUUAGUUUUGAUUUUC–3′	– 23.9
Cy3 (24-bps)	5′-Cy3-GUUUUUUAAUUUUUUAAUUUUUUC–3′	– 24.7

Table 2. Fluorescent reporter RNA oligonucleotides lengths and sequences

HeLa extract	100%	(Final) 40%
Salt	Conc (mM)	Conc (mM)
KOAc	10	4
KCl	0	0
MgOAc	0.5	0.2

Kozak Conditions	
Salt	Conc (mM)
KOAc	90
KCl	45
MgOAc	2

Buffer (Protein/RNA)	100%	(Final) 20%
Salt	Conc (mM)	Conc (mM)
KOAc	0	0
KCl	100	20
MgOAc	2	0.4

1X Supplementary Salt Buffer (Kozak - Total)	
Salt	Conc (mM)
KOAc	86
KCl	25
MgOAc	1.4

Total Salts	
Salt	Conc (mM)
KOAc	4
KCl	20
MgOAc	0.6

10X Supplementary Salt Buffer	
Salt	Conc (mM)
KOAc	860
KCl	250
MgOAc	14

Table 3. Calculations for Supplementary Salt Buffer in Translation Assay

Reagent (Stock Concentrations)	Stock Concentration (Units in reagent column)	Final Concentration (Units in reagent column)	1X Reaction Volume (µL)	Master Mix (17X) Volume (µL)
10mM ATP-Mg	10	0.8	1.6	27.2
10mM GTP-Mg	10	0.1	0.2	3.4
5mM Spermidine	5	0.05	0.2	3.4
1M HEPES, pH=7.5	1000	16	0.32	5.44
2mM Amino Acids	2	0.06	0.6	10.2
10X supplementary salt buffer	10	1	2	34
0.5M creatine phosphate	500	20	0.8	13.6
1mg/mL Creatine Phosphokinase	1000	40	0.8	13.6
40U/uL rRNAsin	40	0.4	0.2	3.4
10X mRNA (500nM) in 1X buffer	250	25	2	0
10X supplementary protein/inhibitor in 1X buffer	10	1	2	0
100% HeLa lysate	100	40	8	136
H_2O			1.28	21.76
Total Volume			20	272
Volume of mix to add (no mRNA or protein)				56

Table 4. Translation Assay Reaction Setup Calculations

Cell Line Name	Target siRNA	Cell Type	Knockdown Efficiency (72hrs)
MOS28	si4E-1	Adherent	40-60%
MOS29	si4E-2	Adherent	10-20%
MOS32	si4B-1	Adherent	60-80%
MOS33	si4G-31	Adherent	60-80%
MOS35	siDDX3-2	Adherent	10-20%
MOS32-S	si4B-1	Suspension	60-70%
MOS33-S	si4G-31	Suspension	50-60%

Table 5. List of cell lines generated with shRNA targets integrated.

Gene	Target Sequence	ID
eIF4E	CCAAAGATAGTGATTGGTTAT	si4E1
eIF4E	CCACTCTGTAATAGTTCAGTA	si4E2
eIF4B	GACAAGTATCGAGATCGTTAT	si4B1
eIF4B	TGGTAATGACAGTGATATAAT	si4B1
DDX6	GAACATCGAAATCGTGTATTT	siDDX6-1
DDX6	GAGTATGACCACCACTATTAA	siDDX6-2
DHX29	AGTCAGACTTCCTACTAATTA	siDHX29-1
DHX29	TATTGATGGCTGGATCTATTT	siDHX29-2
DDX4	CCTTCTACCATTGATGAATAT	siDDX4-1
DDX4	GCGAGATAATACATCCACAAT	siDDX4-2
DHX9	ACGACAATGGAAGCGGATATA	siDHX9-1
DHX9	ACGACAATGGAAGCGGATATA	siDHX9-2
DDX3	GAATCAGACAAACGGTCATTT	siDDX3-1
DDX3	CCCTGCCAAACAAGCTAATAT	siDDX3-2
eIF4G si2	AAAGCTCCACAGTCCACAGGC	si4G2
eIF4G si31	AACCCATACTAGAAGTAGAAG	si4G31
eIF4A1	ACAUCAACGUGGAACGAGAtt	si4A1-1
eIF4A2	GAGCCGTGGTTTTAAGGATtt	si4A1-2
eIF4E3	caaagatagtgattggttaTT	si4E-3
NC3 (scramble)	ATGTATTGGCCTGTATTAG-TT	
GL2 (scramble)	TCGAAGTATTCCGCGTACG-TT	

Table 6. List of siRNA Sequences Generated

Primer Name	Direction (5'-3')	Target Gene	Target Sequence	Validated
PKF74	Forward	Beta actin	GAGCACAGAGCCTCGCCTT	Yes
PKF75	Reverse	Beta actin	ATCCTTCTGACCCATGCCCA	Yes
PMOS59	Forward	eIF4E	GGAGTCTCGCTTTGTCTCCC	Yes
PMOS60	Reverse	eIF4E	AAAATTAGCCGGGCATGGTG	Yes
PMOS95	Forward	eIF4GI	ACGTTACGACCGTGAGTTCC	No
PMOS96	Reverse	eIF4GI	GTCTGGGCCACAATTTATGC	No
PMOS97	Forward	eIF4B	GACTTTCTGGCTGAGGATGG	No
PMOS98	Reverse	eIF4B	GATGGAACGGTCAATTGGAG	No
PMOS109	Forward	DDX3	AGGCAACAACTGTCCTCCAC	No
PMOS110	Reverse	DDX3	CACTGGAGTTGGGCGAGTAT	No

Table 7. List of qPCR Sequences Generated

Plasmid Sequences

Dual-assay mRNA Reporter Sequences

MOS54: Dual-assay mRNA Reporter; Globin 5'UTR, 24nt CY3, Nluc gene (pUC57)

GGTACC: KpnI cut site
T7 promoter
GGATCC: BamHI cut site
B-globin 5'UTR
CCATGG: NcoI cut site
Helicase Double Reporter: 24nt Cy3 binding site, 19nt BHQ binding site
CTGCAG: PstI cut site
Nanoluciferase reporter
AAGCTT: HindIII cut site

GGTACCTAATACGACTCACTATA**G**GG**GGATCC**acatttgcttctgacacaactgtgttcactagcaacctcaaacag
acacc**CTGCAG**GAAAAAATTAAAAAATTAAAAAAC**TCGGAGGGGCCGGTGGGGCCACCATGG**TCTTCACACTCGAAG
ATTTCGTTGGGGACTGGCGACAGACAGCCGGCTACAACCTGGACCAAGTCCTTGAACAGGGAGGTGTGTCCAGTTTG
TTTCAGAATCTCGGGGTGTCCGTAACTCCGATCCAAAGGATTGTCCTGAGCGGTGAAAATGGGCTGAAGATCGACAT
CCATGTCATCATCCCGTATGAAGGTCTGAGCGGCGACCAAATGGGCCAGATCGAAAAAATTTTTAAGGTGGTGTACC
CTGTGGATGATCATCACTTTAAGGTGATCCTGCACTATGGCACACTGGTAATCGACGGGGTTACGCCGAACATGATC
GACTATTTCGGACGGCCGTATGAAGGCATCGCCGTGTTCGACGGCAAAAAGATCACTGTAACAGGGACCCTGTGGAA
CGGCAACAAAATTATCGACGAGCGCCTGATCAACCCCGACGGCTCCCTGCTGTTCCGAGTAACCATCAACGGAGTGA
CCGGCTGGCGGCTGTGCGAACGCATTCTGGCGTAA**AAGCTT**

shRNA Factor-Depletion Vectors

MOS28: si4E1 targeting eIF4E (pcDNA5/FRT/TO)

CTTAAGACC**ATG**GTGAGCAAGGGCGAGGAGCTGTTCACCGGCGTGGTCCCCATCCTGGTGGAGCTGGACGGCGACGT
GAACGGCCACAAGTTCAGCGTCTCCGGCGAGGGCGAGGGCGACGCCACCTACGGCAAGCTGACCCTGAAGTTCATCT
GCACCACCGGCAAGCTGCCCGTCCCCTGGCCCACCCTGGTGACCACCCTGACCTACGGCGTGCAGTGCTTCAGCCGC
TACCCCGACCACATGAAGCAGCACGACTTCTTCAAGAGCGCCATGCCCGAGGGCTACGTGCAGGAGCGCACCATCTT
CTTCAAGGACGACGGCAACTACAAGACCCGCGCCGAGGTGAAGTTCGAGGGCGACACCCTGGTGAACCGCATCGAGC
TGAAGGGCATCGACTTCAAGGAGGACGGGAACATCCTGGGCCACAAGCTGGAGTACAACTACAACTCCCACAACGTG
TACATCATGGCCGACAAGCAGAAGAACGGCATCAAGGTCAACTTCAAGATCCGCCACAACATCGAGGACGGGTCCGT
GCAGCTGGCCGACCACTACCAGCAGAACACCCCCATCGGGGACGGCCCCGTGCTGCTCCCCGACAACCACTACCTCA
GCACCCAGAGCGCCCTGAGCAAGGACCCCAACGAGAAGCGCGACCACATGGTGCTGCTGGAATTCGTGACCGCCGCC
GGCATCACCCTGGGCATGGACGAGCTGTACAAG**TAA**CTGGAGGCTTGCTGAAGGCTGTA**AAGCTT**GGTACCCTCAGG
G**CCAAAGATAGTGATTGGTTATGTG**CATCCAGGG**ATAACCAATCACTATCTTTGG**CCCCTGCGGGTACCTGATGCGT
CCCACTTTTTT**CTCGAG**

MOS29: si4E2 targeting eIF4E (pcDNA5/FRT/TO)

CTTAAGACC**ATG**GTGAGCAAGGGCGAGGAGCTGTTCACCGGCGTGGTCCCCATCCTGGTGGAGCTGGACGGCGACGT
GAACGGCCACAAGTTCAGCGTCTCCGGCGAGGGCGAGGGCGACGCCACCTACGGCAAGCTGACCCTGAAGTTCATCT
GCACCACCGGCAAGCTGCCCGTCCCCTGGCCCACCCTGGTGACCACCCTGACCTACGGCGTGCAGTGCTTCAGCCGC
TACCCCGACCACATGAAGCAGCACGACTTCTTCAAGAGCGCCATGCCCGAGGGCTACGTGCAGGAGCGCACCATCTT
CTTCAAGGACGACGGCAACTACAAGACCCGCGCCGAGGTGAAGTTCGAGGGCGACACCCTGGTGAACCGCATCGAGC
TGAAGGGCATCGACTTCAAGGAGGACGGGAACATCCTGGGCCACAAGCTGGAGTACAACTACAACTCCCACAACGTG
TACATCATGGCCGACAAGCAGAAGAACGGCATCAAGGTCAACTTCAAGATCCGCCACAACATCGAGGACGGGTCCGT
GCAGCTGGCCGACCACTACCAGCAGAACACCCCCATCGGGGACGGCCCCGTGCTGCTCCCCGACAACCACTACCTCA
GCACCCAGAGCGCCCTGAGCAAGGACCCCAACGAGAAGCGCGACCACATGGTGCTGCTGGAATTCGTGACCGCCGCC
GGCATCACCCTGGGCATGGACGAGCTGTACAAG**TAA**CTGGAGGCTTGCTGAAGGCTGTA**AAGCTT**GGTACCCTCAGG
G**CCACTCTGTAATAGTTCAGTATGTG**CATCCAGGG**TACTGAACTATTACAGAGTGG**CCCCTGCGGGTACCTGATGCG
TCCCACTTTTTT**CTCGAG**

MOS32: si4B1 targeting eIF4B (pcDNA5/FRT/TO)

CTTAAGACCATGGTGAGCAAGGGCGAGGAGCTGTTCACCGGCGTGGTCCCCATCCTGGTGGAGCTGGACGGCGACGT
GAACGGCCACAAGTTCAGCGTCTCCGGCGAGGGCGAGGGCGACGCCACCTACGGCAAGCTGACCCTGAAGTTCATCT
GCACCACCGGCAAGCTGCCCGTCCCCTGGCCCACCCTGGTGACCACCCTGACCTACGGCGTGCAGTGCTTCAGCCGC
TACCCCGACCACATGAAGCAGCACGACTTCTTCAAGAGCGCCATGCCCGAGGGCTACGTGCAGGAGCGCACCATCTT
CTTCAAGGACGACGGCAACTACAAGACCCGCGCCGAGGTGAAGTTCGAGGGCGACACCCTGGTGAACCGCATCGAGC
TGAAGGGCATCGACTTCAAGGAGGACGGGAACATCCTGGGCCACAAGCTGGAGTACAACTACAACTCCCACAACGTG
TACATCATGGCCGACAAGCAGAAGAACGGCATCAAGGTCAACTTCAAGATCCGCCACAACATCGAGGACGGGTCCGT
GCAGCTGGCCGACCACTACCAGCAGAACACCCCCATCGGGGACGGCCCCGTGCTGCTCCCCGACAACCACTACCTCA
GCACCCAGAGCGCCCTGAGCAAGGACCCCAACGAGAAGCGCGACCACATGGTGCTGCTGGAATTCGTGACCGCCGCC
GGCATCACCCTGGGCATGGACGAGCTGTACAAGTAACTGGAGGCTTGCTGAAGGCTGTAAAGCTTGGTACCCTCAGG
GGACAAGTATCGAGATCGTTATGTGCATCCAGGGATAACGATCTCGATACTTGTCCCCTGCGGGTACCTGATGCGT
CCCACTTTTTTCTCGAG

MOS33: si4G31 targeting eIF4G (pcDNA5/FRT/TO)

CTTAAGACCATGGTGAGCAAGGGCGAGGAGCTGTTCACCGGCGTGGTCCCCATCCTGGTGGAGCTGGACGGCGACGT
GAACGGCCACAAGTTCAGCGTCTCCGGCGAGGGCGAGGGCGACGCCACCTACGGCAAGCTGACCCTGAAGTTCATCT
GCACCACCGGCAAGCTGCCCGTCCCCTGGCCCACCCTGGTGACCACCCTGACCTACGGCGTGCAGTGCTTCAGCCGC
TACCCCGACCACATGAAGCAGCACGACTTCTTCAAGAGCGCCATGCCCGAGGGCTACGTGCAGGAGCGCACCATCTT
CTTCAAGGACGACGGCAACTACAAGACCCGCGCCGAGGTGAAGTTCGAGGGCGACACCCTGGTGAACCGCATCGAGC
TGAAGGGCATCGACTTCAAGGAGGACGGGAACATCCTGGGCCACAAGCTGGAGTACAACTACAACTCCCACAACGTG
TACATCATGGCCGACAAGCAGAAGAACGGCATCAAGGTCAACTTCAAGATCCGCCACAACATCGAGGACGGGTCCGT
GCAGCTGGCCGACCACTACCAGCAGAACACCCCCATCGGGGACGGCCCCGTGCTGCTCCCCGACAACCACTACCTCA
GCACCCAGAGCGCCCTGAGCAAGGACCCCAACGAGAAGCGCGACCACATGGTGCTGCTGGAATTCGTGACCGCCGCC
GGCATCACCCTGGGCATGGACGAGCTGTACAAGTAACTGGAGGCTTGCTGAAGGCTGTAAAGCTTGGTACCCTCAGG
GAACCCATACTAGAAGTAGAAGTGTCCATCCAGGGCTTCTACTTCTAGTATGGGTTCCCCTGCGGGTACCTGATGCG
TCCCACTTTTTTCTCGAG

MOS34: siDDX3-1 targeting DDX3 (pcDNA5/FRT/TO)

CTTAAGACCATGGTGAGCAAGGGCGAGGAGCTGTTCACCGGCGTGGTCCCCATCCTGGTGGAGCTGGACGGCGACGT
GAACGGCCACAAGTTCAGCGTCTCCGGCGAGGGCGAGGGCGACGCCACCTACGGCAAGCTGACCCTGAAGTTCATCT
GCACCACCGGCAAGCTGCCCGTCCCCTGGCCCACCCTGGTGACCACCCTGACCTACGGCGTGCAGTGCTTCAGCCGC
TACCCCGACCACATGAAGCAGCACGACTTCTTCAAGAGCGCCATGCCCGAGGGCTACGTGCAGGAGCGCACCATCTT
CTTCAAGGACGACGGCAACTACAAGACCCGCGCCGAGGTGAAGTTCGAGGGCGACACCCTGGTGAACCGCATCGAGC
TGAAGGGCATCGACTTCAAGGAGGACGGGAACATCCTGGGCCACAAGCTGGAGTACAACTACAACTCCCACAACGTG
TACATCATGGCCGACAAGCAGAAGAACGGCATCAAGGTCAACTTCAAGATCCGCCACAACATCGAGGACGGGTCCGT
GCAGCTGGCCGACCACTACCAGCAGAACACCCCCATCGGGGACGGCCCCGTGCTGCTCCCCGACAACCACTACCTCA
GCACCCAGAGCGCCCTGAGCAAGGACCCCAACGAGAAGCGCGACCACATGGTGCTGCTGGAATTCGTGACCGCCGCC
GGCATCACCCTGGGCATGGACGAGCTGTACAAGTAACTGGAGGCTTGCTGAAGGCTGTAAAGCTTGGTACCCTCAGG
GGAATCAGACAAACGGTCATTTGTGCATCCAGGGAAATGACCGTTTGTCTGATTCCCCTGCGGGTACCTGATGCGT
CCCACTTTTTTCTCGAG

MOS35: siDDX3-2 targeting DDX3 (pcDNA5/FRT/TO)

CTTAAGACCATGGTGAGCAAGGGCGAGGAGCTGTTCACCGGCGTGGTCCCCATCCTGGTGGAGCTGGACGGCGACGT
GAACGGCCACAAGTTCAGCGTCTCCGGCGAGGGCGAGGGCGACGCCACCTACGGCAAGCTGACCCTGAAGTTCATCT
GCACCACCGGCAAGCTGCCCGTCCCCTGGCCCACCCTGGTGACCACCCTGACCTACGGCGTGCAGTGCTTCAGCCGC
TACCCCGACCACATGAAGCAGCACGACTTCTTCAAGAGCGCCATGCCCGAGGGCTACGTGCAGGAGCGCACCATCTT
CTTCAAGGACGACGGCAACTACAAGACCCGCGCCGAGGTGAAGTTCGAGGGCGACACCCTGGTGAACCGCATCGAGC
TGAAGGGCATCGACTTCAAGGAGGACGGGAACATCCTGGGCCACAAGCTGGAGTACAACTACAACTCCCACAACGTG
TACATCATGGCCGACAAGCAGAAGAACGGCATCAAGGTCAACTTCAAGATCCGCCACAACATCGAGGACGGGTCCGT
GCAGCTGGCCGACCACTACCAGCAGAACACCCCCATCGGGGACGGCCCCGTGCTGCTCCCCGACAACCACTACCTCA
GCACCCAGAGCGCCCTGAGCAAGGACCCCAACGAGAAGCGCGACCACATGGTGCTGCTGGAATTCGTGACCGCCGCC
GGCATCACCCTGGGCATGGACGAGCTGTACAAGTAACTGGAGGCTTGCTGAAGGCTGTAAAGCTTGGTACCCTCAGG

GCCCTGCCAAACAAGCTAATATGTGCATCCAGGGATATTAGCTTGTTTGGCAGGGCCCCTGCGGGTACCTGATGCGT
CCCACTTTTTTCTCGAG

MOS36: si4AI-1 targeting eIF4AI (pcDNA5/FRT/TO)

CTTAAGACCATGGTGAGCAAGGGCGAGGAGCTGTTCACCGGCGTGGTCCCCATCCTGGTGGAGCTGGACGGCGACGT
GAACGGCCACAAGTTCAGCGTCTCCGGCGAGGGCGAGGGCGACGCCACCTACGGCAAGCTGACCCTGAAGTTCATCT
GCACCACCGGCAAGCTGCCCGTCCCCTGGCCCACCCTGGTGACCACCCTGACCTACGGCGTGCAGTGCTTCAGCCGC
TACCCCGACCACATGAAGCAGCACGACTTCTTCAAGAGCGCCATGCCCGAGGGCTACGTGCAGGAGCGCACCATCTT
CTTCAAGGACGACGGCAACTACAAGACCCGCGCCGAGGTGAAGTTCGAGGGCGACACCCTGGTGAACCGCATCGAGC
TGAAGGGCATCGACTTCAAGGAGGACGGGAACATCCTGGGCCACAAGCTGGAGTACAACTACAACTCCCACAACGTG
TACATCATGGCCGACAAGCAGAAGAACGGCATCAAGGTCAACTTCAAGATCCGCCACAACATCGAGGACGGGTCCGT
GCAGCTGGCCGACCACTACCAGCAGAACACCCCCATCGGGGACGGCCCCGTGCTGCTCCCCGACAACCACTACCTCA
GCACCCAGAGCGCCCTGAGCAAGGACCCCAACGAGAAGCGCGACCACATGGTGCTGCTGGAATTCGTGACCGCCGCC
GGCATCACCCTGGGCATGGACGAGCTGTACAAGTAACTGGAGGCTTGCTGAAGGCTGTAAAGCTTGGTACCCTCAGG
GCCCTGCCAAACAAGCTAATATGTGCATCCAGGGATATTAGCTTGTTTGGCAGGGCCCCTGCGGGTACCTGATGCGT
CCCACTTTTTTCTCGAG

MOS38: si4E-3 targeting eIF4E (pcDNA5/FRT/TO)

CTTAAGACCATGGTGAGCAAGGGCGAGGAGCTGTTCACCGGCGTGGTCCCCATCCTGGTGGAGCTGGACGGCGACGT
GAACGGCCACAAGTTCAGCGTCTCCGGCGAGGGCGAGGGCGACGCCACCTACGGCAAGCTGACCCTGAAGTTCATCT
GCACCACCGGCAAGCTGCCCGTCCCCTGGCCCACCCTGGTGACCACCCTGACCTACGGCGTGCAGTGCTTCAGCCGC
TACCCCGACCACATGAAGCAGCACGACTTCTTCAAGAGCGCCATGCCCGAGGGCTACGTGCAGGAGCGCACCATCTT
CTTCAAGGACGACGGCAACTACAAGACCCGCGCCGAGGTGAAGTTCGAGGGCGACACCCTGGTGAACCGCATCGAGC
TGAAGGGCATCGACTTCAAGGAGGACGGGAACATCCTGGGCCACAAGCTGGAGTACAACTACAACTCCCACAACGTG
TACATCATGGCCGACAAGCAGAAGAACGGCATCAAGGTCAACTTCAAGATCCGCCACAACATCGAGGACGGGTCCGT
GCAGCTGGCCGACCACTACCAGCAGAACACCCCCATCGGGGACGGCCCCGTGCTGCTCCCCGACAACCACTACCTCA
GCACCCAGAGCGCCCTGAGCAAGGACCCCAACGAGAAGCGCGACCACATGGTGCTGCTGGAATTCGTGACCGCCGCC
GGCATCACCCTGGGCATGGACGAGCTGTACAAGTAACTGGAGGCTTGCTGAAGGCTGTAAAGCTTGGTACCCTCAGG
GCAAAGATAGTGATTGGTTATTGTGCATCCAGGGAATAACCAATCACTATCTTTGCCCCTGCGGGTACCTGATGCGT
CCCACTTTTTTCTCGAGCTCGAGTCTAGAGGGCCCGTTTAAACCCGCTGATC